Proteolytic stability in colloidal systems

INTERACTION OF PROTEINS WITH THE SOLID-WATER INTERFACE

Marc C.L. Maste

Promotor:	dr. J. Lyklema hoogleraar in de fysische chemie, met bijzondere aandacht voor de grensvlak- en kolloïdchemie
Co-promotor:	dr. ir. W. Norde universitair hoofddocent bij de vakgroep Fysische en Kolloïdchemie

Proteolytic stability in colloidal systems

INTERACTION OF PROTEINS WITH THE SOLID-WATER INTERFACE

Marc Cornelis Ludolf Maste

Proefschrift
ter verkrijging van de graad van doctor
in de landbouw- en milieuwetenschappen
op gezag van de rector magnificus,
dr. C. M. Karssen,
in het openbaar te verdedigen
op dinsdag 9 januari 1996
des namiddags te vier uur in de Aula
van de Landbouwuniversiteit te Wageningen.

CIP-DATA, KONINKLIJKE BIBLIOTHEEK, DEN HAAG

Maste, Marc Cornelis Ludolf

Proteolytic stability in colloidal systems :
interaction of proteins with the solid-water interface /
Marc Cornelis Ludolf Maste. - [S.l. : s.n.] ;
Delft : EburonP&L [distr.]
Thesis Landbouwuniversiteit Wageningen
- With refs. - With summary in Dutch.
ISBN 90-5651-018-5
NUGI 835
Subject headings: proteolysis / adsorption.

Cover: Harry Draai.

Stellingen

1. De conformatie en/of oriëntatie van een eiwit in de geadsorbeerde toestand bepaalt of dit eiwit gevoelig is voor, of juist weerstand heeft tegen, enzymatische afbraak.

   Dit proefschrift, H. 5 en H. 6.

2. Door adsorptie op hydrofobe oppervlakken kán de hoeveelheid secundaire structuur in eiwitten toenemen, in tegenstelling tot wat vaak wordt bepaald of wordt aangenomen.

   Dit proefschrift, H. 6

3. Adsorptie-isothermen van verschillende eiwitten op éénzelfde drager laten zich goed met elkaar vergelijken als niet de massa per oppervlakte-eenheid, maar de dichtheid van de geadsorbeerde laag wordt beschouwd. De effectieve dikte van deze laag, die hiervoor bekend moet zijn, kan bijvoorbeeld bepaald worden met ellipsometrie of met dynamische lichtverstrooing. Voor bolvormige eiwitten kan hiertoe de moleculaire diameter gebruikt worden.

4. Afhankelijk van de sterkte van de bril van een onderzoeker ondergaat een eiwit onder bepaalde omstandigheden wel of geen conformatieverandering.

5. De zogenaamde 'plakkende bel' methode die ontwikkeld is door Keurentjes et al. ter bepaling van de hydrofobiciteit van poreuze membranen, heeft hooguit een semikwantitatief karakter. Een aantal ongewenste neveneffecten met betrekking tot het gebruik van methanol wordt onvoldoende onderkend. Het ware derhalve beter geweest om een goniometrische methode te ontwikkelen om direct de randhoek van een plakkende luchtbel in water te meten.

   Keurentjes, J.T.F., Harbrecht, J.G., Brinkman, D., Hanemeijer, J.H., Cohen Stuart, M.A. and van 't Riet, K., *J. Membrane Sci.*, 47, 333-344 (1989).

6. De opwinding over de bijzondere oppervlakte-eigenschappen van schimmeleiwitten (hydrofobinen) zou aanzienlijk verminderen als men zich beter bewust was van de resultaten van onderzoek van de afgelopen decennia met betrekking tot eiwit-grensvlak interacties.

naar aanleiding van artikel: "Hydrofobines veranderen aard van oppervlak", BIONieuws 8, 22 april 1995, p. 7. alsmede Wösten, H.A.B. et al., *The EMBO Journal* 13, 5848-5854, 1994.

7. Het proefschrift is niet het gepaste medium waar stellingen die geen betrekking hebben op het betreffende onderzoeksterrein, zoals deze en de hiernavolgende, geponeerd moeten worden.

reactie op artikel 2.1c van het promotiereglement Landbouwuniversiteit

8. Een welvarende economie sluit een gezond en duurzaam milieu uit.

9. Een nieuwe fonetische spelling van de Nederlandse taal is niet zinvol als je niet eerst afspreekt hoe de woorden uitgesproken moeten worden.

volgens W.J. de Haan in artikel "niet dom, maar dyslectisch", Elsevier nr. 32, 12 augustus 1995

10. De aanzienlijke omzet van produkten waarvan de werkzame stof wordt gespecificeerd als 'glucasil', 'nanosferen' of 'rechtsdraaiend melkzuur' geeft aan dat de doorgaans onwetende consument zich graag zomaar iets laat aanpraten.

11. Een sterkere arbeidsmoraal leidt tot meer werkloosheid.

12. De wet van behoud van massa gaat niet op voor zoekrakende pennen en potloden.

Stellingen
behorende bij het proefschrift

Proteolytic Stability in Colloidal Systems

door Marc C.L. Maste
in het openbaar te verdedigen
op dinsdag 9 januari 1996 om 16.00 uur
in de Aula van de Landbouwuniversiteit te Wageningen

Contents

Chapter 1 Introduction

1.1. Protein-surface interactions

The importance of interactions between proteins and surfaces is encountered in various fields such as biology, medicine, pharmaceutics, food science, biotechnology or other industrial technologies. For instance, proteins are used as stabilizers in colloidal dispersions, e.g. aerated products, cosmetics, pharmaceutics or food emulsions; enzymes are immobilized in continuous reactors for all kinds of industrial applications where a conversion process can be made more efficient [1-3]. Frequently, in those reactors, the enzyme molecule is covalently linked to the immobilizing support. A few examples which are given below may illustrate the occurrence of protein-surface interactions for the area of biomedicine. The examples have been chosen since these topics are relatively well-covered in literature.

Under healthy conditions, the luminal surface of the endothelium lining of the human cardiovascular system is non-thrombogenic. The initial event that occurs when an artificial device is implanted in the cardiovascular system is the adsorption of components from the blood on the surface of the implant material [4-6]. The adsorption of blood proteins, such as serum albumin (for transport of small molecules and ions), prothrombin and fibrinogen (involved in blood clotting at open wounds) can modify their biological activity. Also, a protein film on the implant surfaces induces adhesion of platelets, initiating a clotting cascade which eventually results in intravascular thrombosis.

Another example of proteins at interfaces is the diagnostic function of dispersed particles which are coated with immuno γ-globulin antibodies. Based on this principle, pregnancy tests are developed where adsorbed antibodies recognize the human chorionic gonadotropin antigen which is a hormone that is released via the urine of females during pregnancy. The agglutination of the particles which is initiated by the antibody-antigen binding visualizes the presence of the hormone. This example illustrates that protein-surface interactions, in contrast to the previous example, may also have desirable implications.

1.2. Definition of the problem and aim of the work

In addition to the manifold of examples where protein-surface interactions play a role, this thesis deals with the interaction between the proteolytic enzyme Savinase™‡ (or Subtilisin 309) [7] and colloidal surfaces in a liquid detergent formulation. This issue will be clarified below.

The literature on Savinase starts in 1982 where its application for silk degumming (i.e. removal of sericin from silk) has been discussed [8]. Since that time around 30 papers have been published on the characterization, modification and/or applications of this enzyme. The protein crystal structure has been fully elucidated in 1992 [7]. Apart from a few applications, such as leather tanning, removal of dental plaque or the preparation of epoxidized rubber from fresh natural rubber field latex, Savinase is mainly applied in the detergent industry. The action of the proteolytic enzyme during a washing cycle is to degrade proteinaceous stains, as occurring in e.g. blood, sweat, grass- or food, from soiled cloth. In addition to the original detergent powders, liquid detergent formulations have recently appeared on the market. This required reinvestigation of the properties of the applied enzymes, particularly because enzymes were found to be relatively unstable in these detergents. At the present time the industry makes the effort to improve the proteolytic stability such that activity is fully utilized when the detergent is applied during the washing cycle. Therefore, it is important to understand the factors that influence the stability of the enzyme.

In an ordinary aqueous solution, under relatively mild conditions, the origin of inactivation is usually autodigestion [9, 10]. As the enzyme is a protein itself, proteolytic activity is also exerted towards molecules of the same kind ("cannibalism"). In this manner fragments of the protein accumulate at the expense of its specific activity. In a liquid detergent these reactions may also occur. However, the mechanism or the rate of inactivation could be different because the enzyme may have interactions with other ingredients as well. Although many kinds of interactions may be relevant in this respect, the interaction between the enzyme and the various surfaces in the system has been chosen as the subject of study.

The surfaces to be considered are those of vesicular surfactant structures and of zeolites. The phenomenology of these surfaces in liquid detergents will be illustrated next. In an aqueous liquid detergent, various components are present, either in the dissolved or in the suspended state. Among others, the liquid contains both anionic and nonionic surfactants. Often the anionic surfactant is Na-dodecylbenzenesulphonate and the nonionic is an alcohol-polyethoxylate with a C_{12}-hydrophobic tail and a hydrophilic part that consists of 7 segments of ethylene oxide. (Fig. 1.1).

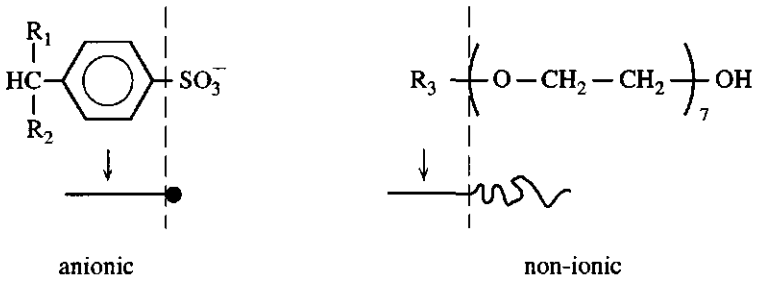

Fig. 1.1. Molecular structure and denotation of anionic and non-ionic surfactant in a liquid detergent. $R_1 \approx C_3$, $R_2 \approx C_8$, $R_3 \approx C_{12}$ (taken from ref. [11]). The hydrophilic part of the non-ionic is further denoted PEO.

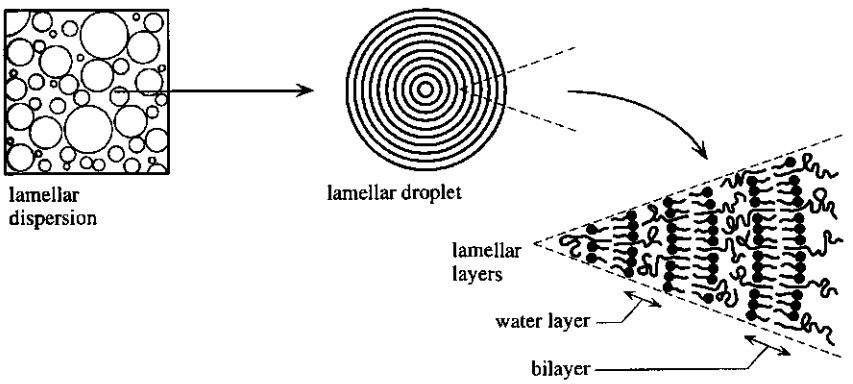

Fig. 1.2. Schematic representation of the structure of the lamellar dispersion (taken from ref. [11]). The lumen of the outer bilayer provides the surface onto which enzyme could adsorb. The overall molar ratio anionic/nonionic is about 3.5:1.

Because of the types of surfactants and the physico-chemical conditions of the detergents, the surfactant molecules are structured in a multilamellar vesicle of concentric bilayers (onion-like structure, Fig. 1.2) [11]. The polar head groups of the anionic surfactants and the hydrophilic part of the non-ionics protrude into the aqueous phase. The ethyleneoxide part of the nonionic provides a steric stabilization of the membrane layers against collapsing. As electrostatic repulsion between the anionic head groups is screened by the high electrolyte concentrations, the steric interaction contributes for a great part to the colloidal stability of the vesicle. The diameter of the lamellar droplet is 0.5 μm ($\approx$ 25 layers), while the repeating distance of one water layer + one bilayer is about 10 nm. Surfactants in a liquid detergent also occur as dispersed monomers and as micelles. These forms are in thermodynamic equilibrium with the lamellar structures.

In recent years, a crystalline silicous derivative, sodium Zeolite A, has been used to replace phosphate in detergent systems. Zeolites are crystalline aluminosilicates that have a porous structure. The zeolite lattice consists of silicon- and aluminium atoms which are both surrounded by four oxygen atoms. The negative charge near the aluminium atom in the framework is balanced by a positive sodium atom, which resides as a counterion in the framework. Spatially, the unit cell has a cubic structure in which each of the six faces of the cube has a well defined pore or window. These pores lead to a central cavity. The three-dimensional porous crystalline structure gives zeolite its properties to act as an ion exchanger (by replacing sodium for calcium) during the washing cycle. As the pore diameter is 0.4 nm, the zeolite lattice is impenetrable for protein molecules (diameter Savinase: 4.2 nm). The enzymes are only capable of contacting the outer surface of the crystal, where the oxygen atoms are organized in hydroxyl groups.

Vesicles and zeolites are abundantly present in liquid detergents (vesicles $\approx$ 65% (v/v); zeolites $\approx$ 35% (w/w)) and, although the specific surface areas of these structures are not so large, vesicles provide circa 8000 m^2 and zeolites (diameter: 2.5 μm and density: 1.5 g cm^{-3}) circa 500 m^2 of surface area in one liter of liquid detergent. Hence, they provide a large outer surface area for interaction with the enzymes (enzyme concentration $\approx$ 0.25 g l^{-1}).

1.3. Research strategy

For investigation of enzyme-surface interactions it is important that all other components that are present in a liquid detergent system, i.e. surfactants, salts, perfumes etcetera should be eliminated. Thus, a model system will be used which consists of the

enzyme in an alkaline aqueous environment (pH 8) at low ionic strength (I=0.01 M) without any "contaminants". Throughout the experiments the temperature is set at 20°C which is the assumed value during storage of the product. The absence of the large amounts of salts and/or surfactants may seem controversial. If these "contaminants" affect the adsorption characteristics they should be included in the model system. However, because they may induce inactivation as well, either directly by interaction in solution or via the adsorbed state of the protein, they have, for the time being, been excluded from the model system.

Furthermore, the use of purified vesicles for investigating the relation between adsorption and stability would introduce complexities. They involve the presence of micelles and monomolecular surfactants, which may lead to undesired additional interactions with the protein. Furthermore, as external factors, e.g. dialysis, protein addition or the absence of salt, may destabilize the bilayer structures it would be necessary to make use of polymerized vesicles [12]. Although a polymerized vesicle seems to be a workable model system, it may still disintegrate to some extent. Hence, a solid particle has been chosen which has surface characteristics that resemble those of a detergent vesicle. Because adsorption (and not absorption into the membrane) of the protein is considered, the relevant surface characteristics are the presence of negative charge and PEO-moieties at the outer surface of the vesicle. It will be assumed that a model particle, which is prepared for that purpose, i.e. a modified polystyrene latex (see chapter 4 of this thesis), has more or less the same surface characteristics. This latex is further denoted PS-B.

Unfortunately, during the course of this research, the zeolite suspension has also proven to be an inconvenient colloidal system. Although the surface is replenished with protein at the operational enzyme concentration, the affinity for adsorption is very low (data not shown). The implication is that the determination of structural properties of the fraction of protein adsorbed in such a system is very difficult. Also sedimentation of the relatively heavy zeolite particles during the timescale of particular experiments is an undesired phenomenon. A suspension of small silica particles which carry chemical groups, that are more or less identical to those on zeolite, is chosen as a model system.

Summarizing, the vesicles and the zeolite have been modelled by PS-B and silica particles, respectively. Further, hydrophobic particles like teflon and 'bare' polystyrene latex (without the PEO-group) have been introduced, in order to screen a wider range of surfaces. The academic interest can thus be expressed as to clarify the mechanism of inactivation of a proteolytic enzyme in an aqueous system containing colloidal particles, having different surface characteristics.

1.4. Outline of the thesis

The introduction of this thesis is given in chapters 1 and 2. The phenomenological aspects of the adsorption of Savinase on different surfaces from aqueous solution is reported in chapter 3. More specifically, the forces that determine adsorption of the enzyme molecule on different kinds of surfaces are investigated. Under varying physico-chemical conditions the adsorption as a function of time on a macroscopic surface has been measured by an optical technique, i.e. reflectometry.
In chapter 4 special attention is paid to the synthesis of a polystyrene latex particle carrying terminally grafted PEO-moieties (to mimic the surface of a vesicle). A number of methods for analyzing the surface structure have been practiced. For comparison, the synthesis of a polystyrene latex without the PEO-group is also regarded.
The inactivation characteristics of Savinase in the presence of the different kinds of sorbent-particles is reported in chapter 5. For those systems, where rapid inactivation is observed, a working model has been proposed. The enhanced inactivation could be due to a monomolecular denaturation or by an increased susceptibility to autodigestion when the proteins are adsorbed at the surface. The sensitivity to autodigestion may be induced by structural changes but other factors related to the adsorbed state may as well play a role. Apart from the inactivation characteristics, the proposed mechanism of inactivation will be contemplated.
Reflectometry lends itself to a certain extent to the determination of structural changes in the protein, but other optical methods provide this information in a more direct manner. This issue is addressed in chapter 6. The techniques used are fluorescence spectroscopy (both time-resolved and steady state) of the three naturally occurring tryptophans, and circular dichroism. The structure of the protein in solution and in situ on the different types of particles are determined.
The mechanism of rapid inactivation, with respect to its pathway and to the mechanism, will be further elucidated in chapter 7. On the basis of the results of chapter 5 and on the basis of additional experiments the model for rapid inactivation takes shape. In the mathematical analysis that is given it is recognized that the enzyme is inactivated by going through different stages. Consecutively, these are transport towards the interface, attachment and subsequent processes that lead to the actual inactivation.

‡ Savinase is a trademark of Novo Nordisk a/s Ltd.

References

1. Guisán, J.M., Fernandez-Lafuente, R., Rodriguez, V., Bastida, A., Blanco, R. M. and Alvaro, G. in: *Stability and Stabilization of Enzymes* (W.J.J. van den Tweel, A. Harder and R.M. Buitelaar, Eds), Proceedings of an International symposium, Maastricht, The Netherlands, p. 55-62, Elsevier Science Publishers B.V., Amsterdam, 1993.
2. Navia, M.A., St. Clair, N.L. and Griffith, J.P., in: *Stability and Stabilization of Enzymes* (W.J.J. van den Tweel, A. Harder and R.M. Buitelaar, Eds), Proceedings of an International symposium, Maastricht, The Netherlands, p. 63-73, Elsevier Science Publishers B.V., Amsterdam, 1993.
3. Weetall, H.H., in: *Immobilized Enzymes Food Process* (W.H. Pitcher, Ed), p. 175-258, CRC Press, Boca Raton, 1980.
4. Morrisey, B.W., Smith, L.E., Stromberg, R.R. and Fenstermaker, C.A., J. Colloid Interface Sci. 56, 557-563 (1976).
5. Morrisey, B.W. and Han, C.C., J. Colloid Interface Sci. 65, 423-431 (1978).
6. Brash J.L. and Horbett, T.A., *Proteins at Interfaces*, ACS Symposium Series 343, Washington D.C., 1987.
7. Betzel, C., Klupsch, G., Papaendorf, G., Hastrup, S., Branner, S., Wilson, W.S., J. Mol. Biol. 223, 427-445 (1992).
8. (Disclosed anonymously), Res. Discl., 216, 124 (1982).
9. Antonov, V.K., *Chemistry of Proteolysis*, p. 278, 2nd edn, Springer-Verlag, Berlin-Heidelberg, 1993.
10. Adler-Nissen, J., *Enzymic Hydrolysis of Food Proteins*, Elsevier Appl. Science Publ., London, 1986.
11. Pas, J.C. van de, *A study of the physical properties of lamellar liquid-crystalline dispersions*, Ph.D thesis, University of Groningen, The Netherlands.
12. Mosmuller, E.W.J., *Studies on the incorporation of lipase in synthetic polymerisable vesicles*, Ph.D thesis, Wageningen Agricultural University, The Netherlands.

Chapter 2 Biochemistry of Savinase

2.1. Classification of proteases

Proteolytic enzymes or proteases (which are enzymes acting on amide bonds in proteins or peptides, EC 3.4) contain two sets of subclasses: the peptidases (exopeptidases, EC 3.4.11-19) and the proteinases (endopeptidases, EC 3.4.21-24). Peptidases cleave peptide bonds near the amino- or carboxyl-terminal end of a substrate protein, leading to minor changes in the overall mass of the peptide substrate. However, proteinases cleave interior peptide bonds, giving rise to a large size reduction of the attacked protein. Studies on the several hundreds of known proteinases indicate that there may be only four major types of catalytic mechanisms and that serine proteinases are predominant. According to Enzyme Nomenclature, endopeptidases are divided into four sub-classes on the basis of the catalytic mechanism.

3.4.21. serine proteinases, having a serine, histidine and aspartate in their active centre;
3.4.22. cysteine proteinases, having a cysteine residue in the active centre;
3.4.23. aspartic proteinases, acting at a pH optimum below 5, with a negatively charged residue in the active centre;
3.4.24. metalloproteinases, using a metal ion in catalysis;

The chemistry of proteolysis in general and the action of each type of proteinase in particular has been thoroughly reviewed by Antonov [1]. The substrate specificity observed in cleavage of many protein- and peptide substrates for all recognized endopeptidases has been surveyed by Keil [2]. Proteinases are very abundant in nature, occurring in virtually all living organisms, from viruses to humans. Because the study described in this thesis, is concerned with a serine proteinase, attention will be focussed on this type of enzyme.
Serine proteinases can be divided into four subgroups: (1) proteinases of the trypsin superfamily, among which pancreatic trypsin, chymotrypsin and elastase. These digestive enzymes are produced as zymogens, which are activated by the action of trypsin; (2) enzymes of the blood, like plasmin or thrombin, which convert fibrinogen into fibrin in blood clotting; (3) enzymes of invertebrates, like carboxypeptidase,

cathepsin or acrosin; (4) microbial serine proteinases (EC 3.4.21.14), such as the subtilase superfamily. The enzyme Savinase is a synonym for Subtilisin 309 which belongs to this family.

The enzymes isolated from different sources (e.g. bovine and porcine trypsin) generally have minimum variations in structural features. In case of remote species (e.g. trypsins of mammals and sharks) the differences in homology are larger. As can be expected for enzymes belonging to different subgroups (e.g. thrombin and enzymes of the pancreas), the variations are even larger. Despite a dramatic difference in amino acid sequences in animal and microbial proteinases, these enzymes are similar as referred to the spatial structure of the catalytically significant regions.

2.2. Catalysis

2.2.1. Active site

The events taking place in catalysis occur in a region called the active site. The active site can be defined as a set of amino acids of the enzyme involved in bonding and chemical conversion of a substrate. Peptide- and synthetic ester substrates are hydrolyzed by a serine proteinase according to the so called acylenzyme mechanism, as depicted below.

In the first step an enzyme-substrate complex (I) is produced, which is held together by non-covalent attractive forces. Next a tetrahedral intermediate (II) is formed by the

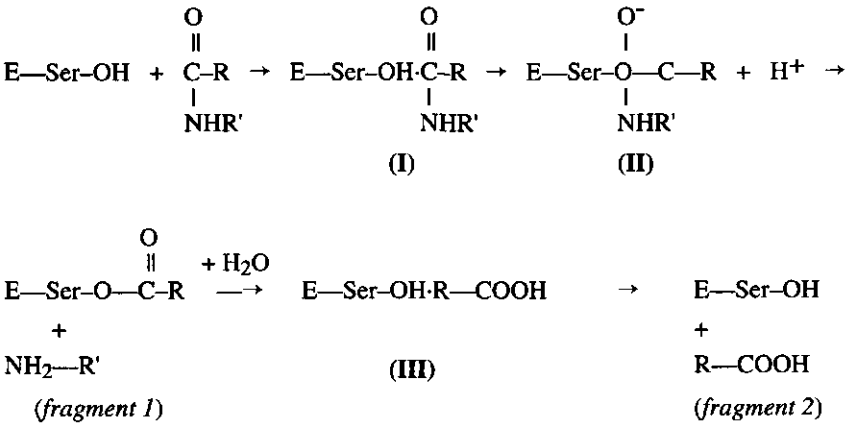

attack of the nucleophilic hydroxyl group of Ser-221 on the carbonyl carbon atom of the cleavable substrate group. The decomposition of intermediate (II) starts by the release of the amine (fragment 1) and the acylenzyme intermediate. The acylenzyme then hydrolyzes to give the enzyme-product complex (III). By dissociation of this complex fragment 2 is released [3].

In 1969 an explanation regarding the abnormally high reactivity of the serine hydroxyl in chymotrypsin was put forward [4]. An analogous theory has been postulated for other serine proteinases. According to this theory the chemical transformation of a substrate by Savinase (and other Subtilisins as well) is achieved by a concerted action of three functional groups in the active site: Ser-221, His-64 and Asp-32 (the numbering is based on the homology with Subtilisin BPN' [5]; the absolute positions are 216, 64 and 32, respectively, counted from the N-terminal amino acid). These active site residues are closely located in the enzyme spatial structure (Fig. 2.1). The catalytic triad thus forms a so-called charge-relay network linked by hydrogen bonds. Since Asp-32 is screened from the solvent and resides in a relatively hydrophobic environment (apart from His-64 and Ser-221 the nearest neighbours of Asp-32 in Savinase are Val-30, Thr-33 and Val-68), its pK_a is proposed to be abnormally high. Hence, the carboxylate of Asp-32 polarizes the imidazole group of His-64, which enhances the capacity of His-64 to accept a proton from Ser-221. Therefore, the bond network can be isomerized. The deprotonated Ser-221 is rendered extremely nucleophilic, which would explain the high reactivity. Subtilisin 309 displays optimal activity at pH 9-11 and at a temperature of 55°C.

2.2.2. Binding site

Besides the catalytic site which interacts with the cleavable substrate group, a binding cleft exists. This region consists of a series of subsites (*S*) across the surface of the enzyme where attachment of the substrate groups (*P*) other than the reactive one, occurs. According to Schechter and Berger [6] the amino acid residues of a substrate peptide which are involved in binding are designated as P_1, P_2, P_3, P_4 etcetera going towards the *N*-terminal direction from the bond to be cleaved (Fig. 2.2, on left of the sequence) and P'_1, P'_2, P'_3, P'_4 etcetera in the *C*-terminal direction (on right of the sequence). The corresponding positions in the enzyme are designated as S_x and S'_x, in which the subscript x refers to the number of the position.

A study into the catalytic properties of Savinase towards small synthetic substrates [7, 8] shows that the enzyme has broad substrate specificity, although the enzyme has a preference for hydrophobic amino acid residues in positions P_1 and P_4. A similar study,

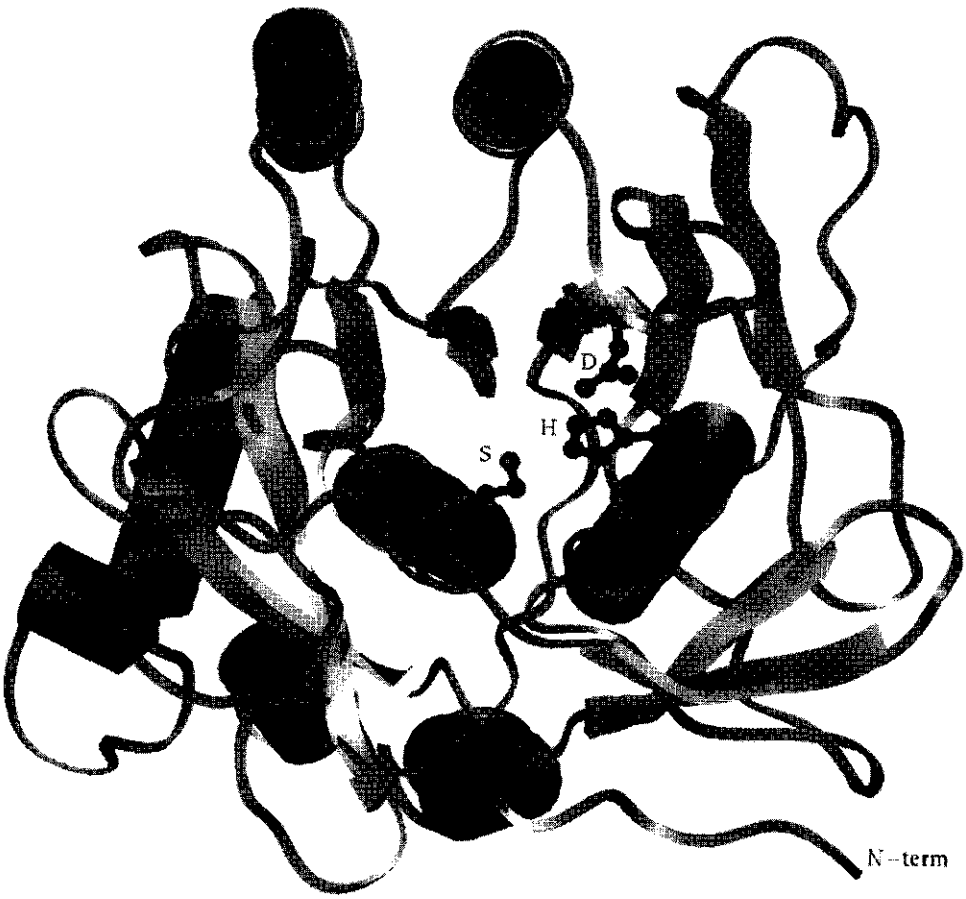

Fig. 2.1. Molecular model of Savinase. The active site consists of Ser-221 (S), His-64 (H) and Asp-32 (D). Secondary structure elements, α-helices and β-sheets, are represented by cylinders and arrows, respectively.

which has recently been carried out at the Unilever Research Laboratory (Vlaardingen, The Netherlands) reveals more or less the same features. In that study, the fragments from an autolysate of Savinase in solution were collected by HPLC-reverse phase chromatography. From N-terminal sequence analysis of the different fragments the statistics on the occurrence at positions around cleavage sites were tabulated. Again, Savinase shows broad substrate specificity, although aliphatic amino acids (Ala, Val, Leu, Ile) are preferred on position P_4. Further, there is a tendency to dislike charged amino acids whatever their position.

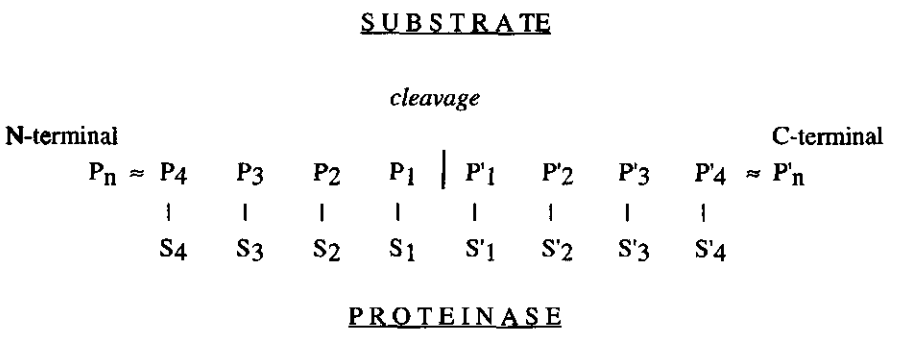

Fig. 2.2 Schematic representation of the enzyme-substrate complex with eight residues in the binding site.

The serine amide hydrolase is sensitive to specific inhibitors interacting with the active serine residue [9, 10]. They are diisopropylfluorophosphate (DIP), phenylmethanesulfonylfluoride (PMSF) and some protein inhibitors of microbial-, animal- and plant origin. The DIP and PMSF molecules are covalently bound to the serine residue and act as irreversible inhibitors, while protein inhibitors are mainly substrates that remain strongly bound even after cleavage. For a couple of experiments that are described in chapters 3 and 6 of this thesis Savinase has been inhibited with PMSF. A schematic representation of the inhibition with PMSF is given in Fig. 2.3. Under neutral conditions the small uncharged PMSF molecule reacts with Ser-221 of Savinase by nucleophilic substitution of the hydroxyl proton. Unfortunately, the Protein Data Bank [Brookhaven] does not contain any information on the crystallographic structure of the PMSF-inhibited form of a serine proteinase. Nevertheless, it is expected that the adsorptive and structural properties and the extent of possible structural alterations upon adsorption of the PMSF-inhibited Savinase are not significantly altered as compared to the active Savinase [11-13].

Phenylmethane-sulfonyl fluoride | Ser-221 of Savinase | 'PMS - Savinase'

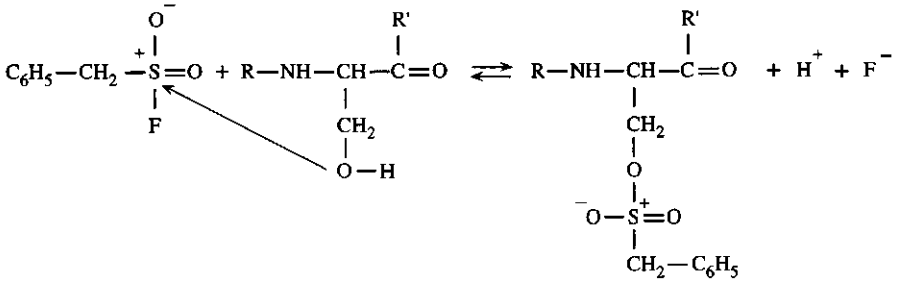

Fig. 2.3. Molecular representation of active site inhibition of Savinase. Phenylmethanesulfonylfluoride binds irreversibly with Ser-221.

2.3. Autocatalysis

Enzymatic autolytic cleavage in solution is a characteristic phenomenon for proteases, particularly for those with broad substrate specificity. Several authors have reported on the pathway that is followed by a proteolytic enzyme to become inactivated by autoproteolysis [14-17]. It is generally believed that the protein molecule must unfold prior to autodigestion. Once a primary cleavage site has been hydrolyzed, the protein conformation changes and interior residues will become available allowing further degradation. For a given protein, unfolding occurs in flexible regions of the protein that are exposed to a denaturing aqueous solvent [18-22]. The tightly folded structures in a globular protein are generally more resistant to proteolytic attack than more extended structures like in fibrous proteins [14, 16, 23-25].

The structure of Savinase [26] demonstrates that for autodigestion a change of the protein conformation is required to make it accessible to interaction with the attacking enzyme [1, 15, 16, 27, 28]. Attempts to reduce autodigestion may involve the search for cleavage sites. As a next step, controlled enzyme engineering may be used to design mutant proteases in order to alter the amino acids close to the primary cleavage site. Of course, it is important to maintain the structure that is necessary for enzyme activity whereas autodigestion itself is prevented.

A change in structure is achieved by, for example, a change in temperature-, media or pH. None of these parameters, however, have been varied in the investigations described in this thesis. The conditions in solution have been chosen such that changes

in the conformational state of the enzyme in aqueous solution are minimized. Perturbations in the protein molecular structure are merely achieved by the adsorption of the protein on a solid-water interface. The extent of a conformational change on a surface depends on the type of protein, the type of sorbent surface and the physicochemical conditions [29, 30].

Studies on proteolysis in an aqueous system that contains an adsorbing surface have been carried out before [31, 32]. Although the proteolysis described in these references did not involve autocatalysis, but attack of a different protein adsorbate, the results support the idea of a structural change of the substrate protein. True autodigestion in the presence of adsorbing particles [33-35] is only marginally studied.

2.4. Structural properties of Savinase in aqueous solution

The Subtilisin 309 molecule (M_w=28 kDa) consists of 269 amino acid residues which are folded into a tight globular structure with a diameter of 4.2 nm. The derived secondary structure, based on the Kabsch & Sanders algorithm [5, 26, 36], demonstrates the occurrence of 9 α-helices (83 residues ≈ 31%) and 9 β-pleated sheets (50 residues ≈ 19%). A schematic representation of the secondary structure elements is given in Fig. 2.1. The amino acid composition and the sequence of the residues are given in Tables 2.1 and 2.2, respectively.

Table 2.1. Amino-acid composition of Savinase (three-letter and one-letter codes are used)

Ala (A)	40	Gln (Q)	10	Leu (L)	19	Ser (S)	34
Arg (R)	8	Glu (E)	5	Lys (K)	5	Thr (T)	17
Asn (N)	22	Gly (G)	35	Met (M)	3	Trp (W)	3
Asp (D)	5	His (H)	7	Phe (F)	2	Tyr (Y)	7
Cys (C)	0	Ile (I)	9	Pro (P)	13	Val (V)	25

The residues that are involved in the surface charge are (the supposed pK_a of the side group is put between brackets): Arg (12.5), Asp (3.9), Glu (4.3), His (6.0), Lys (10.5), Tyr (10.1), the *N*-terminal amino- (7.9) and *C*-terminal carboxylic acid (3.5). Hence, the iso-electric point (IEP) of a protein is the pH value at which the protein does not migrate in an electric field. The electrophoretic mobility is determined by the surface charge on the protein together with the specifically bound charge (usually anions). The

electrokinetic charge is positive for pH < IEP and negative for pH > IEP. The charge on the Savinase molecule as a function of pH has been calculated [13] according to equations given by Tanford and Kirkwood [37]. The result is presented in Fig. 2.4. It can be inferred that the point of zero charge is at pH 10.0 (including one stabilizing Ca^{2+}-ion in the high affinity calcium binding site). At pH 10 the positive charges originate from Arg, Lys and the *N*-terminal amino acid, which are more or less compensated (depending on the amount of bound anions) by negative charges from Asp, Glu and Tyr.

Table 2.2. Primary structure of Savinase on the basis of homology with Subtilisin BPN' (the numbering starts from the *N*-terminal amino acid):

1																								25
A	Q	S	V	R	W	G	I	S	R	V	Q	A	P	A	A	H	N	R	G	L	T	G	S	G
V	K	V	A	V	L	D	T	G	I	-	S	T	H	P	D	L	N	I	R	G	G	A	S	P
V	P	G	E	-	P	S	T	Q	D	G	N	G	H	G	T	H	V	A	G	T	I	A	A	L
N	N	S	I	G	V	L	G	V	A	P	S	A	E	L	Y	A	V	K	V	L	G	A	S	G
S	G	S	V	S	S	I	A	Q	G	L	E	W	A	G	N	N	G	M	H	V	A	N	L	S
L	G	S	P	S	P	S	A	T	L	E	Q	A	V	N	S	A	T	S	R	G	V	L	V	V
A	A	S	G	N	S	G	A	-	G	S	I	S	-	-	-	Y	P	A	R	Y	A	N	A	M
A	V	G	A	T	D	Q	N	N	N	R	A	S	F	S	Q	Y	G	A	G	L	D	I	V	A
P	G	V	N	V	Q	S	T	Y	P	G	S	T	Y	A	S	L	N	G	T	S	M	A	T	P
H	V	A	G	A	A	A	L	V	K	Q	K	N	P	S	W	S	N	V	Q	I	R	N	H	L
K	N	T	A	T	S	L	G	S	T	N	L	Y	G	S	G	L	V	N	A	E	A	A	T	R
																								275

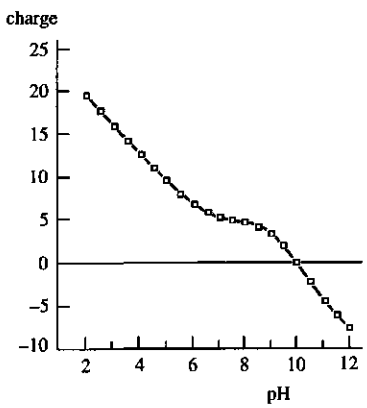

Fig. 2.4. Calculated titration curve of Savinase at I=0.01 M (taken from ref. [13])

The hydrophobic effect is recognized as the dominant force in protein folding [38-41]. Hydrophobic residues tend to attract each other across water and enrich in the core of a protein molecule. A relative scale for residual hydrophobicity is usually derived from the Gibbs energy of transfer of the amino acid residue from an aqueous to a nonpolar environment as compared to the energy of transfer of glycine [42, 43]. The amino acids that are thus identified as hydrophobic are Ala, Val, Leu, Ile, Phe (arranged in order of increasing accessible surface area of the side group). Also Thr, His, Met, Tyr and Trp (arranged in the same way) can be considered hydrophobic, although each of these contains an electronegative oxygen-, nitrogen- or sulfur atom in its side chain.

Considering the above-mentioned criterion for hydrophobicity, hydrophobic amino acid residues make up 49% of the Savinase molecule. The inner core of the protein molecule is relatively hydrophobic, although many hydrophobic residues (57 residues = 43 %) contact the surrounding aqueous environment. This number is more or less comparable to that for other proteins, such as RNase, lysozyme and myoglobin [44]. By molecular graphics analysis it is inferred that the hydrophobic surface residues of Savinase are more or less evenly distributed over the surface.

The hydrophobic residues (set to 100%) are distributed among the different structure elements: α-helix (39%), β-sheet (27%) and remainder (34%), which means that hydrophobic residues tend to accumulate in secondary structure elements (β-turn not considered). However, the hydrophobic residues Tyr and His are hardly found in the α-helix- and β-sheet structures of Savinase respectively. This is in line with general observations on the protein secondary structures, since these residues are so-called breakers of the respective structures [45].

References

1. Antonov, V.K., *Chemistry of Proteolysis*, 2nd edn, Springer-Verlag, Berlin-Heidelberg, 1993.
2. Keil, B., *Specificity of Proteolysis*, Springer-Verlag, Berlin-Heidelberg, 1992.
3. Fersht, A., *Enzyme Structure and Mechanism*, 2nd ed., pp. 27-28, W. H. Freeman and Company, NY, 1985.
4. Blow, D.M., Birktoft, J.J. and Hartley, B.S., Nature 221, 337-340 (1969).
5. Siezen, R.J., Vos, W.M. de, Leunissen, J.A.M. and Dijkstra, B.W., Protein Engineering 4, 719-737 (1991).
6. Schechter, I. and Berger, A., Biochem. Biophys. Res. Commun. 27, 157-162 (1967).
7. H. Grön and Breddam, K., Biochemistry 31, 8967-8971 (1992).
8. Bech, L.M., Sörensen, S.B. and Breddam, K., Biochem. 32, 2845-2852 (1993).
9. Markland, F.S. and Smith, E.L., in: *The enzymes*, 3rd ed, pp 561-608 (Subtilisins: Primary structure, Chemical and physical properties), P. D. Boyer (Ed), Acad. press, NY and London, 1971.
10. Ottesen, M. and Svendsen, I., in: *Methods in Enzymology*, Volume XIX, pp 199-215, Perlmann G.E. and Lorand, L. (eds), Acad. Press, NY and London, 1970.

11. Uemitsu, N., Sugiyama, M. and Matsumiya, H., Biochim. Biophys. Acta 258, 562-565 (1972).
12. Gold, A.M. and Fahrney, D., Biochem. 3, 783-791 (1964).
13. Duinhoven, S., *Enzyme Adsorption at Interfaces*, Ph.D thesis, Wageningen Agricultural University, The Netherlands, 1992.
14. Beynon, R.J. and Bond, J.S., *Proteolytic enzymes*, A practical approach, IRL press, Oxford, England, 1985.
15. Eijsink, V.G.H., Dijkstra, B.W., Vriend, G., Zee, R. van der, Veltman, O.R., Vinne B. van der, Burg, B. van der, Kempe, S. and Venema, G., Protein Eng. 5, 421-426 (1992).
16. Adler-Nissen, J., *Enzymic Hydrolysis of Food Proteins*, Elsevier Appl. Science Publ., London, 1986.
17. Tombs, M.P., J. of Appl. Biochem. 7, 3-24 (1985).
18. Voordouw, G., Milo, C. and Roche, R.S., Biochemistry 15, 3716-3724 (1976).
19. Fassina, G., Vita, C., Dalzoppo, D., Zamai, M., Zambonin, M. and Fontana, A., Eur. J. Biochem., 156, 221-228 (1986).
20. Burg, B. van den, *Engineering the thermostability of Bacillus neutral proteases*, Ph.D thesis, University of Groningen, The Netherlands, 1991.
21. Fontana, A., Fassina, G., Dalzoppo, Zamai, M. and Zambonin, M., Biochemistry 25, 1847-1851 (1986).
22. Fontana, A., Biophys. Chem. 29, 181-193 (1988).
23. Daniel, R.M., Cowan, D.A., Morgan, H.W. and Curran, M.P., Biochem. J. 207, 641-644 (1982).
24. Ogasahara, K., Tsunasawa, S., Yutani, K. and Sugino, Y., Eur. J. Biochem. 150, 17-21 (1985).
25. Parsell, D.A. and Sauer, R.T.., J. Biol. Chem. 264, 7590-7595 (1989).
26. Betzel, C., Klupsch, G., Papaendorf, G., Hastrup, S., Branner, S. and Wilson, W.S., J. Mol. Biol. 223, 427-445 (1992).
27. Kumar, S., Biochem. 9, 291-297 (1970).
28. Sakai, T., Suzumura, M. and Nohara, D., Chem. Pharma. Bull. 36, 2750-2758 (1988).
29. Andrade, J.D., *Surface and Interfacial Aspects of Biomedical Polymers*, vol. 2, Plenum Press, NY, 1985.
30. Norde, W., Adv. Colloid Interface Sci. 25, 267-340 (1986).
31. Wikström, M.B., Elwing, H. and Möller, A.J.R., Enzyme Microb. Technol. 4, 265 (1982).
32. Welin-Klintström, S., Wikström, M., Askendal, A., Elwing, H., Lundstrom, I., Karlsson, J. and Renvert, S., Colloids Surfaces 44, 51 (1990).
33. Johnson, P. and Whateley, T.L., Biochem. J. 193, 285-294 (1981).
34. Lewis, D. and Whateley, T.L., Biomaterials 9, 71-75 (1988).
35. Brode, P.F. III, Erwin, C.R, Rauch, D.S., Lucas and Rubingh, D.N., J. Biol. Chem. 269, 23538-23543 (1994).
36. Kabsch, W. and Sanders, C., Biopolymers 22, 2577- (1983).
37. Tanford, C. and Kirkwood, J.G., J. Am. Chem. Soc. 79, 5333 (1957).
38. Tanford, C., *The hydrophobic effect*, 2nd edition. Wiley, NY, 1980.
39. Doig, A.J. and Williams, D.H., J. Mol. Biol. 217, 389-398 (1991).
40. Dill, K.A., Biochemistry 29, 7133-7155 (1990).
41. Lim, W.A. and Sauer, R.T., Nature 339, 31-36 (1989).
42. Cantor, C.R. and Schimmel, P.R., *Biophysical Chemistry Part I*: The conformation of biological macromolecules, p 52, Freeman and Company, San Francisco, 1980.
43. Creighton, T.E., *Proteins*, p 7 and pp 145-152, Freemand and Company, NY, 1983.
44. Lee, B. and Richards, F.M., J. Mol. Biol. 55, 379 (1971).
45. Chou, P.Y. and Fasman, G.D., Biochemistry 13, 22 (1974).

Chapter 3

The adsorption mechanism of Savinase

a reflectometry study of protein adsorption on macroscopic surfaces

Abstract

The mechanism of adsorption of Savinase from aqueous solution on a hydrophilic silica and a hydrophobic methylated silica surface were studied. In order to prevent autodigestion during the experiments, a small competitive inhibitor was bound to the active site of the enzyme. The adsorption experiments were performed by combining stagnation point flow towards a macroscopic surface and reflectometry. The adsorbed amount was monitored continuously as a function of time. The experimental variables were the amphipathicity of the solid surface (i.e., silica or hydrophobized silica), pH, ionic strength, the type of monovalent ions used and the protein concentration.

For hydrophilic silica it was observed that the charge contrast between protein and sorbent surface, the extent of charge screening and the protein concentration determine the rate of adsorption and the final adsorbed amount. It is concluded that electrostatic interactions play a decisive role in the adsorption of Savinase on hydrophilic silica and that unfolding of the protein molecule does not take place. On the other hand, for the hydrophobic surface, variation of pH, ionic strength or protein concentration hardly affected the adsorption. Hence, adsorption was achieved through other factors that were directly related with the sorbent hydrophobicity. At elevated salt concentrations, the adsorption curve for the hydrophobic surface was characterized by overshoot and spontaneous re-adsorption. The exact shape of the curve depended on the type of salt used. It is concluded that unfolding of the protein structure and hydrophobic dehydration probably dominate the adsorption on a hydrophobic surface.

3.1. Introduction

The mechanism and phenomenology of the adsorption of proteins onto surfaces has been extensively studied over the last decades. Several reviews [1-8] cover this topic to a varying degree. Gradually, systematic information has become available, which has up to now provided a fair understanding of the factors that are involved. Nevertheless, the field of proteins at interfaces seems to be boundless since the various types of proteins exhibit their own peculiarities. For each specific protein-surface combination several aspects may be the object of study, viz. adsorption kinetics, the type of interactions, the conformational state, the orientation of the adsorbed protein molecules, the thickness of the adsorbed layer, translational and rotational diffusion, reversibility of adsorption and biological activity. Each aspect could be examined by several analytical techniques. The (changes in) structural state, for example, could be investigated by infrared- or fluorescence spectroscopy, circular dichroism, optical rotation dispersion, microcalorimetry, proton titrations and other more indirect methods. The diversity of the physico-chemical conditions also provides a wealth of variables, in particular when other components are present in the system.
The basic question that should be considered is for what reasons the protein would prefer the interface. At constant temperature and pressure, the decisive factor is always the change in Gibbs energy of the system upon adsorption ($\Delta_{ads}G$), which is defined as the amount of work (excluding expansion work) that is performed by the system in a reversible process (Eq. 3.1).

$$\Delta_{ads}G = \Delta_{ads}H - T\Delta_{ads}S \qquad (3.1)$$

where H and S are the enthalpy and the entropy, respectively, and T is the absolute temperature. For protein adsorption to occur spontaneously $\Delta_{ads}G$ must be negative. Hence, the driving forces for protein adsorption are those that decrease $\Delta_{ads}H$ and/or increase $T\Delta_{ads}S$. At the present time there is more or less agreement on the driving forces for protein adsorption. The major ones are *electrostatic attraction, unfolding of secondary structure elements* and *hydrophobic dehydration* [6]. Electrostatic attraction lowers $\Delta_{ads}H$, while the latter two forces increase $\Delta_{ads}S$. In addition, there appear to be other intrinsic protein properties that determine the surface activity. These include, for example, the size, the solubility and the quarternary structure of the protein [5]. An obvious counteracting force for adsorption of any molecule is the decrease in the rotational and translational freedom

upon adsorption. Altogether, most proteins appear to adsorb on many interfaces.
The contribution of hydrophobic dehydration is yet a controversial issue, since the notion is not always well defined or determined. Moreover, there is dispute about the question whether this type of interaction is of entropic nature or also contains enthalpic contributions from hydrogen bonds and from van der Waals interactions [9-11]. The various driving forces, mentioned above, will be treated in more detail below. Then, the experiments aim at elucidating the mechanism of the adsorption of Savinase at hydrophilic and hydrophobic surfaces.

3.2. Factors determining protein adsorption

3.2.1. Electrostatic interactions

When a charged protein molecule and a charged surface come into close proximity their diffuse layers overlap, causing interaction. The net charge of the protein depends on the pH, as was explained in section 2.4. The charge of the sorbent surface may originate from dissociation or association of protons with surface groups, including carboxyl, sulphate, sulphonate, hydroxyl, amino or imidazole groups.
In general, electrostatic *attraction* occurs when the charges on the confronting surfaces have opposite signs, while the interaction is *repulsive* for like-charged surfaces. For like-charged surfaces, the interaction may become attractive when charges on the exterior of the protein molecule are inhomogeneously distributed and/or when additional ions are incorporated to prevent high elecrostatic potentials. Incorporation of ions between protein and sorbent involves a change in both a chemical and an electric potential. Because of the less-aqueous nature of the adsorbed layer the chemical term is positive and opposes protein adsorption. The electrical term of ion pair formation in the low dielectric region of the adsorbed layer usually has a negative value because of strong enthalpic contributions and, hence, it promotes adsorption [12, 13].
Electrostatic attraction always leads to a certain extent of protein adsorption. The adsorption may be reduced by strong hydrophilic hydration of the protein- and/or the sorbent surface, for example when the charge density or the polarity of these surfaces are high.
Electrostatic interactions are screened at relatively high ionic strength. When more salt is

present in the bulk solution, the range of the potential of both protein and sorbent surface becomes smaller. When the protein is electrostatically attracted by the surface, the affinity decreases upon salt addition. Usually this leads to a smaller adsorbed amount. On the other hand, when the protein is electrostatically repelled by the surface, the adsorbed amount may increase when salt is added.

An additional electrostatic effect emerges when the sorbent surface is covered with protein molecules up to the level where the adsorbed molecules start to interact laterally. When the net protein charge is zero it may lead to attraction between positively charged residues of the one molecule and negatively charged residues of the other. Far outside their isoelectric region, the adsorbed molecules are highly charged and they will repel each other laterally [14]. At an ionic strength of e.g. 10 mM, the Debye length (κ^{-1}) is 3.2 nm which would, given the diameter of 4.2 nm of the enzyme, significantly oppose completion of a monolayer.

3.2.2. Unfolding of the protein structure

Unfolding of the protein structure may also contribute to adsorption. In general the extent of a conformational change is, among other things, dependent on the internal coherence of the protein [14], the sorbent surface occupation [7, 15-18], the charge density of protein and sorbent [13, 19, 20] and the sorbent hydrophobicity [4, 21, 22].

Unfolding of secondary structure elements such as α-helices or β-sheets leads to an increased probability of attaining different random states of the polypeptide backbone and hence to an increase in the conformational entropy. As a result $\Delta_{ads}G$ becomes more negative and hence unfolding can be a driving force for protein adsorption. The conformational change may occur rapidly (within a timescale of seconds to minutes), about as fast as attachment to the surface or it may occur on longer time scales (minutes to hours) when the molecule optimizes its interaction with the sorbent surface [5]. Conformational changes may not always be entropically favourable; in some cases specific parts of the protein structure may become more folded upon adsorption. The protein may be forced into a specific structure when electrostatic attractions and/or hydrophobic interactions dominate the adsorption process.

Experimental evidence for unfolding has been found for the adsorption of human serum albumin (HSA) at pH > IEP on negatively charged and hydrophilic silica or hematite surfaces [13, 15, 23]. The argument for protein unfolding stems from the observation that

adsorption takes place under electrostatic repulsion and in the absence of hydrophobic dehydration. In addition, for silica, circular dichroism revealed that the α-helix content of HSA (74%) has been reduced by a factor of 2 upon adsorption. For hematite it has been demonstrated that, under certain conditions, the adsorption of HSA is endothermic ($\Delta_{ads}H>0$). This implies that a positive entropy of adsorption, probably stemming from the unfolding of the protein structure, outweighs the negative enthalpy. Endothermic effects have also been measured for proteins on polystyrene surfaces [7, 24] but in those cases the entropic contribution could as well be due to hydrophobic dehydration.

Proteins that have a relatively low structural stability in the native state, such as HSA, are relatively sensitive to structural rearrangements upon adsorption. This has been demonstrated by the effect of the charge density of HSA on the amount adsorbed at different pH on various surfaces [13, 19]. At pH $\approx$ IEP the amount was at a maximum value. Outside the iso-electric region the adsorbed amount decreased and it has been reasoned that this effect is mainly due to a larger extent of unfolding away from the IEP. The intramolecular electrostatic repulsion reduces the structural stability of the protein and, hence, renders it more sensitive to extrinsic factors. The intramolecular repulsion may be reduced at higher electrolyte concentrations.

On the other hand, proteins that have a relatively strong internal coherence, so called 'hard proteins', will hardly adsorb under conditions of electrostatic repulsion on a hydrophilic surface. This has been illustrated for e.g. lysozyme (LSZ) and ribonuclease (RNase) at pH < IEP on a positively charged and hydrophilic hematite surface [13, 23].

Finally, more extended unfolding reactions may occur at a lower surface occupation. This has been inferred from CD data for the adsorption of LSZ and HSA on silica particles [15] and for the adsorption of bovine serum albumin (BSA) on polystyrene particles [17]. Although the CD-measurements may be somewhat obscured by light scattering (certainly for ref. [17], see also chapter 6) the trends do indicate that the amount of α-helix is reduced at a lower surface coverage. This suggests that the protein molecule spreads more readily on the surface when space is available.

3.2.3. Hydrophobic dehydration

Hydrophobic dehydration refers to the release of water molecules from non-polar matter. The traditional view of hydrophobic dehydration is that water molecules cannot interact with the apolar component like they can with a polar or charged entity. Consequently, the

adjacent water molecules form a maximum number of hydrogen bonds between each other [25]. The interaction between two apolar species in aqueous solution, is believed to originate from a gain in entropy when water molecules are released from the interacting species. Thus, the association of two hydrophobic species is denoted hydrophobic interaction (HI). Although the concept of an ice-like water structure near the apolar surface helps in understanding the hydrophobic interaction, this view has been argued by several workers [11, 26, 27]. Nevertheless, it is generally accepted that a region of specially structured water is present around an apolar species.

In the experimental part of this chapter we have attempted to learn about the occurrence of hydrophobic dehydration of the protein and sorbent surface. As the protein exterior contains 57 hydrophobic residues, a contribution from hydrophobic dehydration upon adsorption on a hydrophobic interface could be expected. To this end, the effect of different types of monovalent salts on the adsorption characteristics has been investigated. Specifically, it is believed that the hydration state of small ions may somehow affect the degree of hydration of hydrophobic areas. However, examining the literature about the effect of salt on hydrophobic interaction [25, 26, 28] it appears that a well-established relationship is lacking: there is even controversy about the qualitative effect of salt on HI. Some authors reported that HI is strengthened upon salt addition [26], while others state that HI can only be reduced by the salt addition [28]. Considering the more subtle effect of the action of individual ions on HI, there is even greater lack of experimental and theoretical consistency. These problems encountered can be reduced to the incomplete understanding of HI. This is further illustrated by the disparate criteria invoked in making a gradation of the effect of different salts on HI, viz. on the basis of the entropy of hydration or heat capacity [25], the Gibbs free energy of HI [26] or, more empirically, the rate of coalescence of air bubbles [28].

There has not yet been a paper in which the effect of hydrophobic dehydration on protein adsorption is explicitly discriminated from electrostatics and unfolding. Nevertheless, in a few studies attempts have been made [29-32] or its contribution to protein adsorption has been rationalized [7, 24, 33]. The obvious problem is that the adsorption of proteins on hydrophobic surfaces under conditions of electrostatic repulsion could be driven by other factors as well. For soft proteins the assumption of structural changes is common, but the so-called hard proteins may also change their structure on a hydrophobic surface ([7] and see chapter 6). Alternatively, from the calorimetric data for the adsorption of LSZ and RNase (pH < IEP) on positively charged polystyrene latex [23], it could be inferred that the

co-adsorption of ions may be fully responsible for protein adsorption. Obviously, the relevance of hydrophobic dehydration as a driving force can only be established when adsorption isotherms, calorimetric and circular dichroism data are combined. Then, the occurrence of dehydration can reasonably be concluded from a positive value for ΔH upon adsorption on a hydrophobic particle and an unchanged secondary structure, but this has not yet been observed.

A final note is made on the effect of salt on the stability of the protein structure in solution. The presence of salt may have its consequences for hydrophobic and/or electrostatic interactions between amino acid residues that are positioned in the periphery of the protein molecule. Both destabilization [34, 35] and stabilization [36] of proteins at high salt concentrations have been reported. These effects should be recognized when studying hydrophobic dehydration in protein adsórption.

As from above, the salt experiments as described in this chapter do not yet have a consistent theoretical basis. However, we tend to think that any difference in adsorption characteristics that is observed upon variation of salt type is mainly due to a difference in dehydration of hydrophobic areas. Hence, the adsorption of Savinase on a hydrophobic surface is studied for several types of salts under conditions where electrostatic interactions are screened (i.e., at I=0.2 M).

3.3. Adsorption kinetics and equilibrium

The interaction between a protein and a sorbent surface as such is at best studied at a low surface occupation, where lateral interactions between the adsorbed proteins are absent. When a protein-sorbent system at low surface coverage has attained equilibrium, the amount of adsorbed protein relative to the amount of protein remaining in solution reflects the true affinity of the protein for the surface. High affinity adsorption is found when the equilibrium protein concentration in solution attains significant values not until the surface has been almost saturated. A low affinity isotherm is characterized by an increase of surface coverage concomitant with a significant and analytically detectable increase of the solution concentration. The various properties of the protein-sorbent system, involving the affinity and the plateau value, are reflected in an adsorption isotherm (see chapter 5 and 7).

Another aspect of protein adsorption are the kinetics, i.e. its rate towards equilibrium. The maximum rate of adsorption is the rate of transport towards the interfacial layer. For

reflectometry, which merely detects the adsorbed mass, this statement is true. Rate-limiting factors during attachment involve, for example, reorientation of the molecule or rearrangements of the structure prior to adsorption or the existence of an electrostatic energy barrier for adsorption. At high protein concentration in solution attachment becomes rate-limiting; then, surface processes could be revealed.
The remainder of this chapter deals with the kinetics and equilibrium aspects of the adsorption of Savinase on hydrophilic and hydrophobic surfaces. To this end, an optical technique called reflectometry has been applied.

3.4. Principles of reflectometry

Reflectometry is a technique with which the adsorbed mass of protein on a solid-liquid interface can be established fairly accurately and continuously as a function of time. The mass transport of protein towards the surface is controlled by stagnation point flow of the protein solution [37], while the adsorbed molecules are detected by the change of polarization of a reflected light beam. The principles of this method have been discussed by Dijt [37] and by Oldenzeel [38]. The experimental set-up is schematically shown in Fig. 3.1a. A linearly polarized He/Ne laser beam (1) enters the cell through a glass prism (2). The light beam reflects on a macroscopic silicon wafer that is covered with a silica (=oxidized silicon) layer (3). After reflection the beam again passes a glass prism (4) and is divided into its parallel (p) and perpendicular (s) components by a polarizing beam splitter (5). The reflected intensities I_p and I_s of the parallel and perpendicularly polarized light, respectively, are detected by photodiodes (6) and combined by the detection electronics (7) to yield the output signal S:

$$S = I_p/I_s = f R_p/R_s \tag{3.1}$$

where f accounts for intensity losses of the light in the system. The quantities R_p and R_s are the so-called reflectivities for parallel and perpendicularly polarized light, respectively. In order to calculate the adsorbed amount Γ, it is necessary to establish a mathematical relationship between Γ and S. To that end, use has been made of an optical model where the silica covering and the adsorbed protein molecules are considered to be homogeneous layers which are fully characterized by their respective refractive indices, n_f and n_p and by

their respective layer thicknesses, d_f and d_p [39]. The computation is based on the exact matrix formalism of Abeles [40]. Further, use is made of a straightforward equation where Γ and d_p are related:

$$n_p = n_s + (dn/dc)\,(\Gamma/d_p) \tag{3.2}$$

where n_s is the refractive index of the solvent and dn/dc is the refractive index increment of the protein solution. Hence, the value for n_p is estimated from assumed values for Γ and d_p. For the calculation of R_p and R_s, a set of parameters should be known. These are the angle of incidence θ_i (with respect to the normal of the surface), the wavelength λ of the light beam, n_{Si} of the silicon, n_f, n_p, n_s and d_f. The adsorption of molecules will cause a change in signal according to:

$$\Delta S = f\,\{(R_p/R_s)_\Gamma - (R_p/R_s)_0\} \tag{3.3}$$

where the subscripts Γ and 0 denote the situations after and before adsorption, respectively. The essence of the computational method of Abeles is that a virtually linear relationship is obtained between R_p/R_s and Γ. This can be verified by calculating Γ by Eq. 3.2 and R_p/R_s by the optical model on changing d_p (assuming a constant n_p). Hence, the first term between brackets in Eq. 3.3 is equal to $\Gamma\, d(R_p/R_s)/d\Gamma$. The relationship between Γ and S is then obtained by combination of Eqs. 3.1 and 3.2 when we consider that f is calculated from S_0 and $(R_p/R_s)_0$ (before adsorption) of a wafer with known d_f. Hence,

$$\Gamma = Q\,\Delta S/S_0 \tag{3.4}$$

where Q is written as:

$$Q = (R_p/R_s)_0/\{d(R_p/R_s)/d\Gamma\} \tag{3.5}$$

The thickness of the silica layer d_f is yet an unknown parameter, but it can be determined by calibration. Since we know R_p/R_s from the apparatus constant f and the experimentally determined value for S, we read the value for d_f from a curve of R_p/R_s as a function of d_f that can be obtained from the optical model.

It has been demonstrated how R_p and R_s depend on θ_i and d_f [37]. It appears that changes

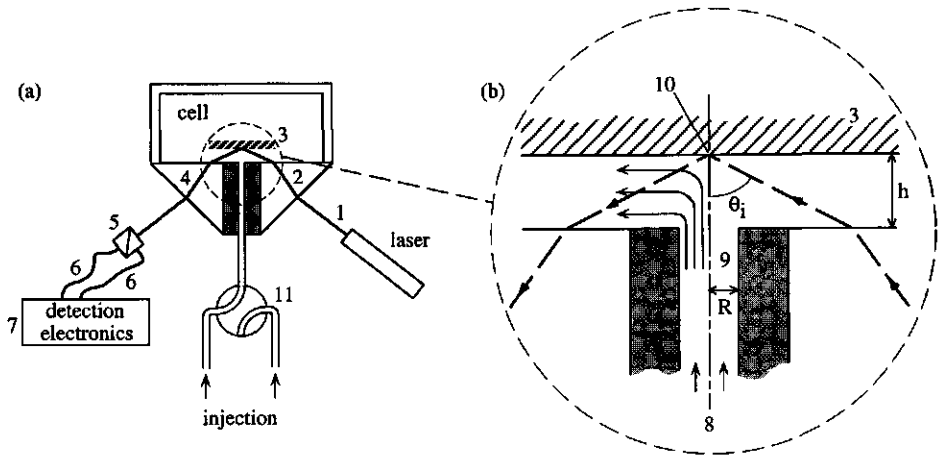

Fig. 3.1. (a) Schematic diagram of the experimental setup. (b) Stagnation point region. The dashed line represents the light beam. The solid arrows indicate the direction of the liquid flow. For explanation of the numbers, see text. For all experiments: h=1.1 mm, R=0.9 mm, $\theta_i=\theta_b=71°$ (taken from ref. [37]).

in R_p/R_s upon adsorption are most pronounced around the Brewster angle θ_b, which is 71° for the water/silicon interface. Because at the Brewster angle the reflectivity for parallel light is much lower than that for perpendicular light, the polarization angle of the incident beam is adjusted such that $I_p/I_s\approx1$. As R_p and R_s vary periodically (out of phase) upon variation of d_f, a change in R_p/R_s is most pronounced at a certain thickness of the silica layer ($d_f\approx100$ nm).

3.5. Stagnation point flow

The transport of a protein towards a surface in a reflectometry setup is well-controlled when use is made of stagnation point flow [37]. The principle is demonstrated in Fig. 3.1b. The solvent or protein solution (8) is forced into the cell through a cylindrical conduit (of radius R) (9) at a constant flow rate. The liquid is supplied from a stock and it enters the cell by the gravitational force. The channel is positioned perpendicularly to the adsorbing wafer, and the intersection of its symmetry axis with the silica-solution interface is the stagnation point (10). After the cell has been replenished with liquid, the superfluous liquid is removed by a simple overflow system. The laser beam is positioned such that it coincides with the stagnation point and such that $\theta_i=\theta_b$. However, the cross-section of the light beam

is larger than the area where stagnation flow is realized. As a result, the level of adsorption will be somewhat overestimated at prolonged times when proteins are adsorbed outside the stagnation point as well. This small deviation is further neglected. With the aid of a two-way valve (11), as depicted in Fig. 3.1a, it is possible to switch from solvent to solution (for adsorption studies) or vice versa (for e.g. desorption studies).
When surface processes are rate-limiting the probability of sticking becomes lower than unity. This is observed as a decrease with respect to the maximum adsorption rate during the initial stage of adsorption. Dabros and Van de Ven [41] derived a theoretical equation for the mass transfer rate J of particles (e.g. protein molecules) at the stagnation point. Because of convective transport towards the surface, the diffusion layer has a constant thickness (see also chapter 7). Due to the mode of the experimental set-up, depletion of the bulk is zero. Hence, J is a constant. Under a set of conditions, the following relation holds [42]:

$$J \equiv m c_p = 0.287\, \nu^{-1/3} \Phi^{2/3} R^{-5/3} D^{2/3} c_p \qquad (3.6)$$

where m is the mass transfer coefficient, ν is the kinematic viscosity of the solution, Φ the volume flux, R the radius of the cylindrical conduit, D the diffusion coefficient of the dissolved protein and c_p the protein concentration in bulk solution.

3.6. Experimental

3.6.1. Purification and inhibiton of Savinase

The enzyme studied in this chapter is a wild-type (WT) alkalophilic serine proteinase secreted by *Bacillus lentus* (subtilisin 309: E.C 3.4.21.14), which is commercially named Savinase™. The enzyme was isolated from a commercial preparation (ex NOVO-Nordisk) at the Unilever Research Laboratory (Vlaardingen, The Netherlands) and desalted on a NAP-5 column (Pharmacia), prior to use. The concentration was established using an experimentally determined extinction coefficient $\varepsilon_{280}^{0.15\%} = 1.03\ \mathrm{l\ g^{-1}\ cm^{-1}}$.
Prior to the adsorption experiments the enzyme was irreversibly inhibited by reaction of the active site with phenylmethanesulfonylfluoride (PMSF). The reaction of PMSF (dissolved in 2-propanol) with a diluted Savinase sample ($\approx$ 1 μM) was carried out in 0.05 M

phosphate buffer at pH 7.0 at a molar ratio of 1000 to 1, respectively, for 1 h at 5°C. The mixture was then concentrated to 20 μM by 24 h filtering through a YM-10 filter (Amicon) at a pressure of 3 atm. at pH 6.5. After removal of the redundant PMSF-crystals the protein solution was dialyzed against deionized water for 7 h and finally filtered through a 0.2 μm Acrodisc filter (Gelman Sciences). The protein solution was frozen in liquid nitrogen and subsequently stored at -70°C.

The purity of both active- and inhibited enzyme was checked by the ratio of A_{280}/A_{250} ($\geq$3.0) and by HPLC-reversed-phase (HPLC-RP) chromatography with subsequent detection at 214 nm. The column specifications and the eluent gradient are described in the legend to Fig. 5.5. It was established that the solution of the PMSF-inhibited enzyme is free of both fragments and non-bound PMSF (not shown). The remaining activity of Savinase after inhibition was 0.1%, as will be demonstrated in section 5.2.2. The protein molecule is further denoted PMS-Savinase.

3.6.2. Sorbent surfaces

The sorbent surfaces were either hydrophilic or hydrophobic. The hydrophilic surface was a macroscopic oxidized silicon wafer. The surface contains -OH groups, it has a point of zero charge around pH 2-3 [43]. This implies that in the alkaline region the surface is always negatively charged. The silicon wafers were oxidized by heat treatment in an oven (at T≈1000°C) for one hour. Next, strips were cut from this wafer and subsequently cleaned by a combined treatment with UV and ozon. The (advancing) contact angle of a sessile drop of water (volume 15 μl) on the oxidized strip as measured by a goniometric device was always < 5° which confirms the hydrophilic nature of the surface. In order to obtain a hydrophobic surface, the silica surface was methylated by dimethyldichlorosilane (DDS) [44]. A clean silica strip was placed in 0.50% DDS in trichloroethane for 30 min after which it was rinsed with ethanol and water, in that order. The water contact angle on the silanized surface was found to be >90°, which confirms the hydrophobic nature of the methylated surface. An attempt was made to establish the charge on the methylated surface by streaming potential experiments (data not shown). However, the results were not representative because of the inherent conduction through the silicon layer. However, the methylated surface was found to be negatively charged which must be due to the presence of free -OH groups that have not reacted with DDS. As the methylsilane molecule is very small, it was neglected as a distinct layer in the optical model.

3.6.3. Solution conditions

In all experiments the temperature was 20°C. For controlling the pH, a $Na_2B_4O_7$-buffer was used. The buffering action originates from hydrolysis of $B_4O_7^{2-}$ into a HBO_2/BO_2^- couple (pK_a=9.2). The assumption of hydrolysis seems valid as pH≈pK_a after dissolving the solid borate. The pH of the borate solution was adjusted to pH 8.0 with HCl or NaOH. The buffer ionic strength was set at 10 mM for all pH values. The total ionic strength I was varied by the addition of NaCl in the range between 10 and 200 mM. The range was extended to I=1 mM for the determination of the adsorption of PMS-Savinase at pH 11 on the hydrophilic silica surface as a function of salt concentration. For the investigation of possible hydrophobic dehydration the effect of a series of salts on protein adsorption was investigated at 200 mM. Besides NaCl, these salts were $NaClO_4$, NaF, CsCl and LiCl.

Before the protein solution was dispensed, establishment of a constant value for S_0 was awaited during the flow of solvent. Usually, temperature fluctuations contribute significantly to fluctuations in S_0. The protein concentration was maintained at 5.8 or 7.5 g m^{-3} or it is varied between 2.5 and 20 g m^{-3}. The maximum protein flux was calculated, using the following data: ν=10^{-6} m^2 s^{-1}, Φ=2.0 10^{-8} m^3 s^{-1}, R=9 10^{-4} m and D= 10^{-10} m^2 s^{-1} (D is calculated from the Stokes-Einstein relation, using a protein radius of 2.1 nm). Hence, for e.g. c_p=5.8 g m^{-3}, J ≈ 1.9 mg m^{-2} min^{-1}.
For the calculation of Q, to be used in Eq. 3.4, the following values were taken: $\theta_i \approx \theta_b$=71°, λ=632.8 nm, n_{Si}=3.84, n_f=1.46, n_s=1.33, dn/dc=0.185 10^{-6} m^3 g^{-1} [38] and n_p=1.44 (assuming Γ=2.5 10^{-3} g m^{-2} when d_p=4.2 10^{-9} m); d_f was calculated from calibration as described before.
All experiments were performed at least in duplicate. Unless otherwise stated, the results were reproducible.

3.7. Results and Discussion

3.7.1. Electrostatic interactions

When adsorption barriers, e.g. electrostatic repulsion, dehydration or reorientation are absent, the initial rate of adsorption, $d\Gamma/dt$, should follow the rate of transport J, according to Eq. 3.6. This assumption is validated for $2.5 \leq c_p \leq 12.5$ g m^{-3} under electrostatic attractive conditions at pH 8.0 and I=0.01 M on both a silica and a silane surface, see Fig. 3.2. Apparently, diffusion is rate-limiting over this c_p-range, which implies that under these conditions, surface processes cannot be revealed from the initial part. Therefore, the observation that $d\Gamma/dt$ on silica is slightly lower than that on silane cannot have a physical meaning. First, we consider the effect of electrostatic interactions on the adsorption behaviour.

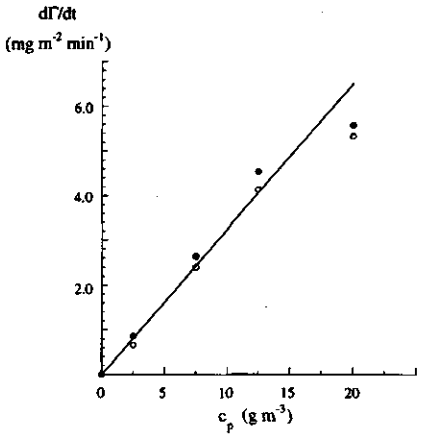

Fig. 3.2. Observed rate of adsorption on silica (○) and on silane (●) versus protein concentration. The straight line corresponds with the theoretical flux (from Eq. 3.6).

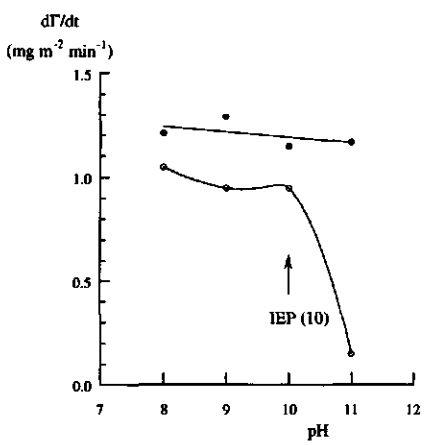

Fig. 3.3a. Initial rate of adsorption, $d\Gamma/dt$, on silica (○) and on silane (●) versus pH; I=0.01 M; c_p=5.8 g m^{-3}.

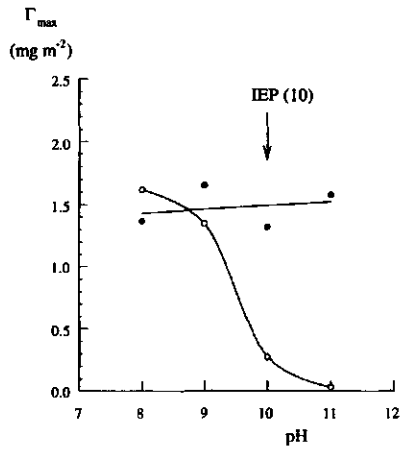

Fig. 3.3b. Maximum adsorbed amount, Γ_{max}, on silica (○) and on silane (●) versus pH; I=0.01 M; c_p=5.8 g m^{-3}.

The values for the initial $d\Gamma/dt$ and the maximum adsorbed amount, Γ_{max}, at different pH values (I=0.01 M) are given in Figs. 3.3a and b. Variation in protein adsorption (cf. Figs. 3.2. and 3.3a) is observed throughout the investigations between experiments that were done at different time periods by different workers. Hence, conclusions will not be drawn from comparison to other experiments, but from within a set of experiments. As from Fig. 3.3, above the IEP of the protein, the rate of adsorption on silica is virtually zero. Apparently, at and below the IEP, the amount of positive charges on the exterior of the protein is sufficient to become attached which leads to high values for $(d\Gamma/dt)_{t\to 0}$. However, the final adsorbed amount at pH 10 does not exceed 0.3 mg m^{-2}. At an increasing charge contrast between PMS-Savinase and silica, i.e. at pH 8 and 9, the surface can accomodate more proteins. The similarity of the adsorption values for pH 8 and 9 could be due to the fact that amino acid residues are not titrated in this region (see Fig. 2.4). The results exhibit a marked effect of electrostatic contributions to the adsorption process on silica. The relatively high surface concentration below the IEP demonstrates the insignificance of lateral repulsions between the adsorbed species. This is also inferred from the low adsorption at pH 10. If lateral interactions on the surface were significant they would have increased the adsorbed amount, due to the attraction of iso-electric protein molecules.

The low surface activity (i.e, low Γ_{max}) of PMS-Savinase at the IEP is remarkable since this is seldomly found for other proteins around their IEP. For e.g. Serum-albumin and Immunoglobulin on a hydrophilic surface (SiO_2 or α-Fe_2O_3) the amount adsorbed is usually at its highest value at the pH where the protein is most resilient against unfolding. It appears that, depending on the charge sign of the sorbent surface, a maximum in adsorption occurs just below or above the IEP [45, 46]. For more rigid molecules, such as RNase, the adsorption around the IEP (9.2) on negatively

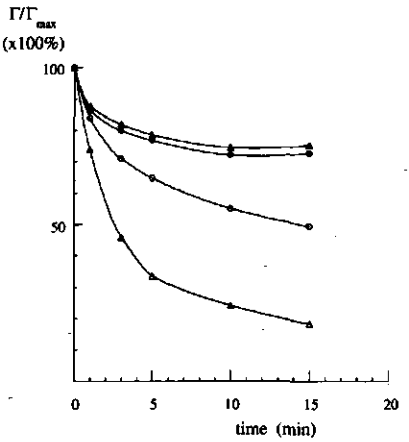

Fig. 3.4. Desorption of protein into buffer at pH 8 (circles) and pH 9 (triangles) from silica (○, △) and silane (●, ▲) at I=0.01 M. Before t=0 the protein had been equilibrated with the surface for 10 min. Thus, the adsorbed amount during desorption in this figure has been normalized with respect to the final value of the adsorbed amount after 10 min of adsorption as can, for example, be read from Fig. 3.5a for silica and silane at pH 8.

charged α-Fe_2O_3 is reported to be 1.0 mg m^{-2}. This confirms the high surface activity of RNase, because a complete monolayer coverage with this protein would yield an adsorbed amount of circa 1.5 mg m^{-2}. The low adsorption of PMS-Savinase at pH 10 will be discussed in a forthcoming paragraph. Generally, the results confirm the contribution to the adsorption process of electrostatic interactions between protein and silica.

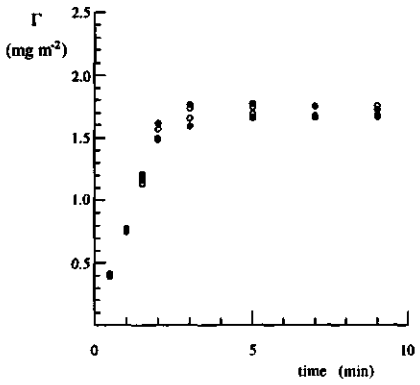

Fig. 3.5a. Time dependence of the adsorption on silica (O) and on silane (●); pH 8; I=0.01M; c_p=5.8 g m^{-3}.

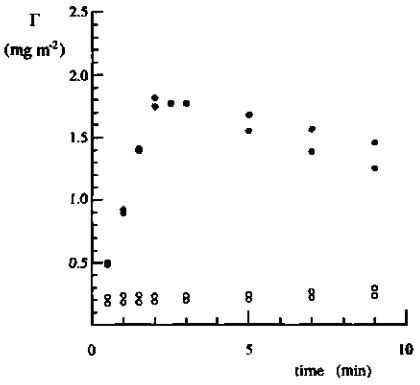

Fig. 3.5b. As Fig. 3.5a; I=0.05M (NaCl).

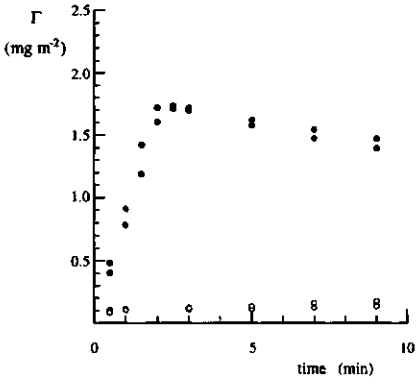

Fig. 3.5c. As Fig. 3.5a; I=0.10M (NaCl).

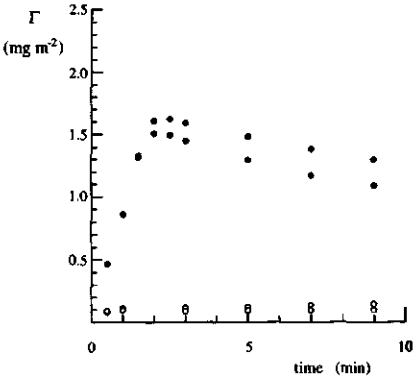

Fig. 3.5d. As Fig. 3.5a; I=0.20M (NaCl).

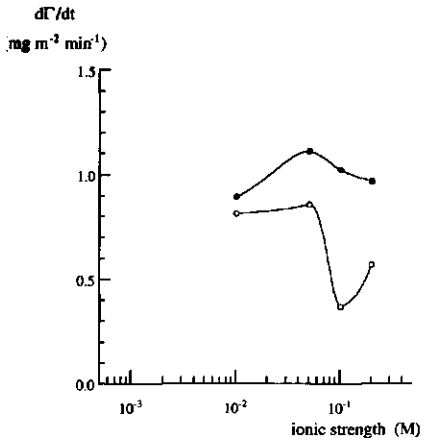

Fig. 3.6a. Initial rate of adsorption, $d\Gamma/dt$, versus ionic strength on silica (○) and on silane (●) at pH 8. Salt type is NaCl; c_p=5.8 g m^{-3}.

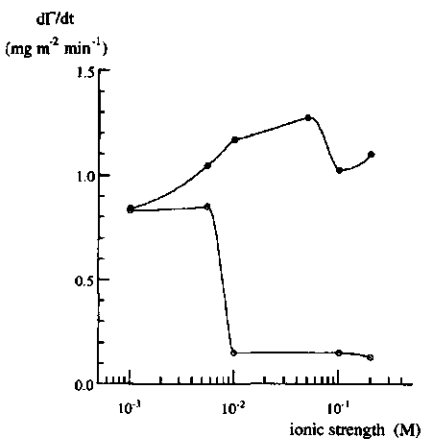

Fig. 3.6b. As Fig. 3.6a. pH 11.

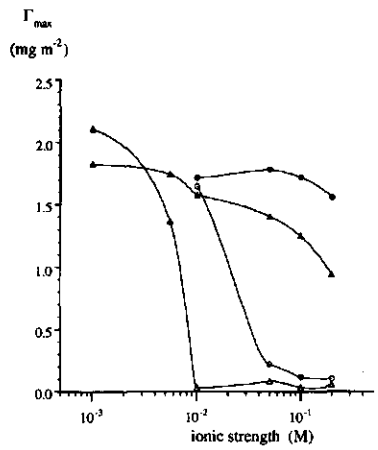

Fig. 3.6c. Equilibrium adsorbed amount, Γ_{max}, on silica (open symbols) and silane (closed symbols) versus ionic strength at pH 8 (○, ●) and pH 11 (Δ, ▲); I=0.01 M; c_p=5.8 g m^{-3}.

Fig. 3.3 further demonstrates that on the silane surface $d\Gamma/dt$ and Γ_{max} are independent of pH, viz. the charge of the protein. Moreover, below the IEP, Γ_{max} has more or less the same value as for silica. Furthermore, from the two types of surfaces the protein is desorbed into its solvent to a different extent (Fig. 3.4). Hence, it is reasoned that the forces that keep the protein adsorbed are probably different for silica and for silane.

As far as the electrostatic contributions to the adsorption are concerned we arrive at similar conclusions upon varying the ionic strength. In addition, other features are also observed. Fig. 3.5a-d show the adsorption curves at pH 8.0 on silica and on silane at different salt concentrations. It is observed that at $I \geq 0.05$ M the amount adsorbed on silica is practically reduced to zero, while on silane the accumulation of protein is only slightly dependent on ionic strength. It is also observed that at $I \geq 0.05$ M the adsorption on silane reaches an optimum whereafter the amount adsorbed gradually decreases. This overshoot-effect will be discussed in a forthcoming paragraph. The effect of salt has also been investigated at pH 11 and similar trends are observed. The combined results on $d\Gamma/dt$ and the maximum amount adsorbed, Γ_{max}, given in Figs. 3.6a, b and c, confirm this conclusion. Moreover, also from these experiments, lateral repulsion between adsorbed PMS-Savinase molecules away from the IEP can be considered to play a minor role since, if they were significant, would give rise to an *increased* adsorption upon an increase of ionic strength.

Reconsidering the low value for Γ_{max} at pH 10 on silica it now may become clear why the isoelectric PMS-Savinase has a low affinity for the silica-water interface. At pH 11 and $I \leq 0.0055$M it is observed from Fig. 3.6c that the protein is considerably surface active, although the charge signs of the protein and the surface are similar. Perhaps, under these conditions, the positive charges on the protein (mainly from Arg and to a small extent from Lys) are barely screened and enable the protein to adsorb. The low surface activity at pH 10 and I=0.01 M could be due to a relatively strong binding of anions on cationic groups of the protein molecule. Hence, the sorbent charge cannot sufficiently be compensated which gives rise to low protein adsorption.

The experimental results on the adsorption of PMS-Savinase on polystyrene latex particles in the work of Duinhoven et al. [47] seem intermediate between the results shown in Figs. 3.3b and 3.6b of this chapter. The adsorption of PMS-Savinase on negatively charged polystyrene latices *gradually* decreases upon increasing salt concentration and increasing pH. Hence, the discrepancies between our results and those of the work of Duinhoven et al. could be explained by the fact that the polystyrene particles used contain both hydrophilic and hydrophobic patches. Consequently, this type of particle does not lend itself for a

systematic study into the mechanism of protein adsorption.

The adsorption curves in Fig. 3.5 show that at $I \geq 0.05$ M and pH 8 the adsorbed amount on silane decreases after passing through an optimum. The rate of this decrease at $I \geq 0.05$ M is independent of the ionic strength. A similar effect is found at pH 11, but the rate of overshoot is lower and it only occurs at $I \geq 0.10$ M (data not shown). The relatively strong overshoot-effect is difficult to understand, but it may be explained as follows. It is noted that at pH 8 the effect appears when electrostatic attractions, if any, are screened, i.e. at $I \geq 0.05$ M. Possibly, the protein adsorbs in a different way when other than electrostatic interactions dominate adsorption. It could mean that, upon first contact, the protein adsorbs relatively patchwise on silane, e.g. through hydrophobic dehydration. The adsorbed protein molecules could then rearrange their structure, thereby expelling neighbouring molecules from the surface. Hence, the overshoot-effect is interpreted as caused by a structural change that occurs on longer time scales. Adsorbed proteins slowly increase their area of contact. The remaining vacant sites would be replenished after the protein islands have formed and so overshoot and further adsorption take place simultaneously. The reason that the overshoot occurs to a lesser extent at pH 11 could be that PMS-Savinase in solution has less internal coherence. This idea stems from the observation that Savinase is more sensitive to alkaline than to acid denaturation. Hence, a high rate of denaturation above the IEP on the interface could preclude its detection.

3.7.2. Unfolding of the protein structure

So far, the dominant force for adsorption on hydrophobic silane has been considered to be of a non-electrostatic origin, for instance unfolding of the protein or hydrophobic dehydration or both. Conformational changes have been invoked to explain the overshoot at elevated salt concentrations. In order to detect possible structural changes at pH 8.0 and I=0.01 M, c_p is varied for adsorption on both silane and silica under these conditions. Since diffusion is rate-limiting over the c_p-range studied (see Fig. 3.2) it could be expected that possible conformational changes that occur over a longer timescale are observed by reflectometry as overshoot of the adsorbed amount. Specifically, the adsorbed protein may expel other adsorbed proteins from the surface when it changes its conformation. The results are given in Figs. 3.7a and b. Overshoot is absent at low c_p on silane and it is marginal at high c_p. This could mean that the sensitivity to conformational changes is smaller at lower ionic strength. It could also mean that the sensitivity is equally large, but

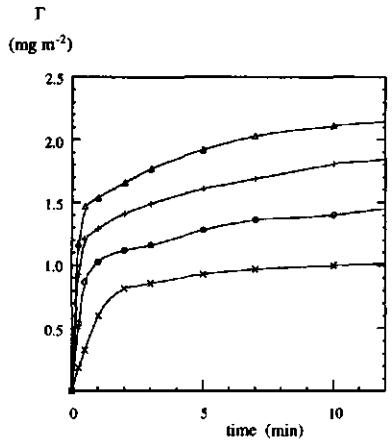

Fig. 3.7a. Adsorption in time on silica as a function of c_p at pH 8, I=0.01 M; c_p=2.5 (X), 7.5 (O), 12.5 (+) and 20 g m^{-3} (Δ). The initial rates of these curves versus c_p were plotted in Fig. 3.2.

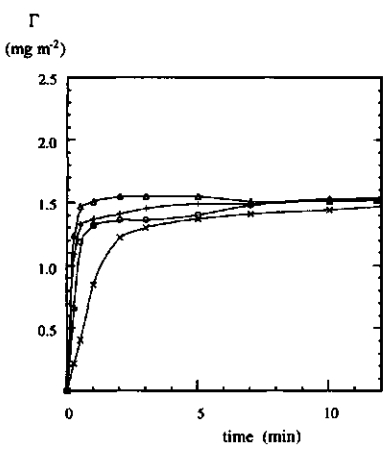

Fig. 3.7b. As Fig. 3.7a. Adsorption on silane

that the spatial distribution of proteins over the surface is more homogeneous at low c_p and hence the lateral distance between adsorbed proteins would be too large to cause any overshoot. Further scrutinizing the curves in Fig. 3.7b, it is noticeable that Γ_{max} has the same value at all c_p. For silica, the adsorbed amount continuously increases as time proceeds. This happens at all values of c_p. Moreover, at high c_p, Γ_{max} is also higher. The effects on silane could be explained by again referring to conformational changes. Apparently, the structurally changed adsorbed layer on silane requires space, i.e. ≈0.67 m^2 mg^{-1}. As such, conformational changes do not take place on silica, as overshoot is absent and the occupation increases up to the level of a saturated monolayer of native molecules, i.e. circa 2.5 mg m^{-2}. The same phenomena have been observed with an inhibited T71A-mutant of Savinase. The mutant is characterized by a lower temperature for denaturation (see chapter 6). It was expected that a possible larger sensitivity to structural changes upon adsorption would lead to a stronger effect on the adsorption, if it were determined by structural rearrangements.

Concluding this section, the protein seems to adapt its structure on a hydrophobic surface, whereas the structure seems to remain intact on a hydrophilic surface.

3.7.3. Hydrophobic dehydration

The final point to consider is the occurrence of hydrophobic dehydration as a driving force for protein adsorption. It is not yet clear what characteristics of the adsorption curve are influenced by hydrophobic dehydration. For example, it could be argued that the initial rate of adsorption is dependent on hydrophobic dehydration since dehydration is a process that enhances the sticking probability and could thus be involved in the initial attachment. For investigation of this effect, this would require the rate of adsorption to be limited by surface processes. Alternatively, or in addition, it could be that the equilibrium adsorbed amount is indicative for dehydration, since the overall dehydration capacity of the protein and sorbent surfaces would influence the extent of occupation. Thus, the difference in the level of adsorption between silica and silane at c_p=2.5 g m^{-3} (Figs. 3.7a and b) may be an indication for this.

Another aspect that has been studied was the influence of the type of electrolyte for the adsorption on silane. The salts are composed of monovalent ions which do not have chemical interactions with other charges, like e.g. Ca^{2+} often has. Hence, one may assume that any difference in the adsorption behaviour upon alteration of the type of salt is due to a difference in HI between the protein and sorbent surface. However, the salt may also exert its influence on hydrophobic interactions between amino acid residues of the protein that maintain the tertiary structure. This effect should be recognized when interpreting the results.

It appears that Γ_{max} tends to decrease when either the positive or the negative ion increases in size (data not shown). For example, when comparing the adsorption from LiCl to that from CsCl-solution, Γ_{max} decreases from 1.45 to 1.25 mg m^{-2}. A similar trend was observed upon variation of the negative ion (Γ_{max} with $NaClO_4$ was 1.1 mg m^{-2}). The maximum was, unfortunately, not well enough reproducible in the presence of NaF and NaCl. The results suggest that HI between protein and sorbent is weaker for larger ions. Alternatively, it could be argued that larger ions *enhances* HI between protein and sorbent, thereby triggering the molecule to unfold at a faster rate which, in turn, leads to a decreased adsorbed amount.

The adsorption curves for the different salts are given in Figs. 3.8a and b, where the initial part has been left out. The adsorption values have been normalized with respect to the maximum amount adsorbed. Thus, the curve starts at the maximum adsorption value at t>0. The curves are characterized by the succession of overshoot during at least 5 min, spontaneous re-adsorption (but not when Li^+ or F^- are present) and desorption of the

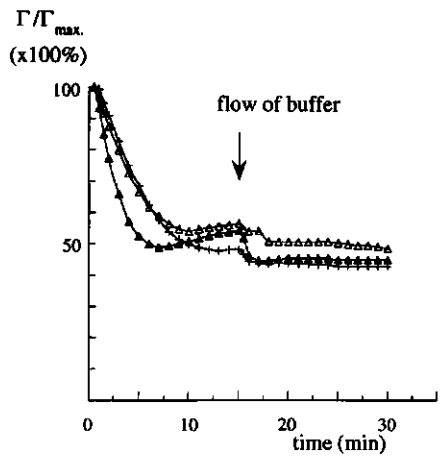

Fig. 3.8a. Time-dependence of the adsorption of protein on silane at c_p=7.5 g m^{-3}, pH 8, I=0.20 M; LiCl (+), NaCl(Δ), CsCl (▲). The initial part has been omitted. Adsorbed amounts, Γ, have been normalized with respect to the optimal amount adsorbed, Γ_{max}. After circa 15 min from t=0 of adsorption, the protein solution was replaced by buffer.

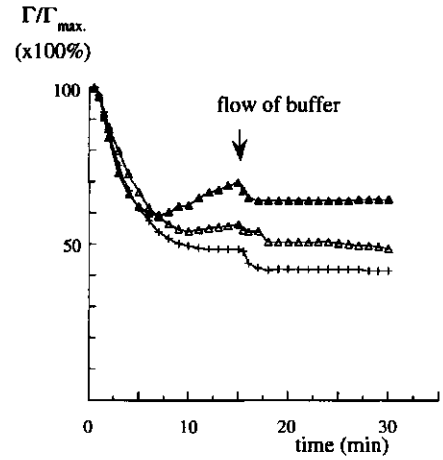

Fig. 3.8b. As Fig. 3.8a. NaF (+), NaCl (Δ), $NaClO_4$ (▲).

protein into its buffer after 15 min. The data in Fig. 3.8 demonstrate that —with the exception of Cs^+— the rate of overshoot is similar for all types of ions.

A remarkable feature in the curves are the different rates of re-adsorption for the different salts used. The rate of re-adsorption increases upon an increase of the size of the positive or negative ion. Presumably, the rate of adsorption is not diffusion-limited anymore at this stage and has now become dependent on surface processes. This could mean that HI between protein and sorbent is stronger for larger ions, thereby increasing the rate of re-adsorption.

The extent of desorption from the hydrophobic surface into buffer is only small and more or less the same for all ions. Hence, it could suggest that other than dehydration forces contribute to adsorption as well.

Altogether, differences in protein adsorption are observed between the various salts. Although the differences can not be explained in a straightforward manner, they could suggest that dehydration and hence HI, plays a role in protein adsorption.

3.8 Conclusions

The adsorption of PMS-Savinase on a hydrophilic silica surface is driven by electrostatic interactions only. The rate of adsorption and the equilibrium adsorbed amount are dependent on the charge interactions between the protein and sorbent surface. Thus, pH and ionic strength are important variables. Lateral electrostatic interactions between adsorbed proteins play a minor role. The adsorption on hydrophobic silane surfaces is not determined by electrostatic interactions. The important determinants are probably unfolding of the protein structure and hydrophobic dehydration.

Acknowledgements

We are indebted to Esther van de Plasse, Ivon van den Dries, Eveline Bollen, Carline Brands and Toine Overbeeke for the performance and the reporting of the reflectometry experiments. The useful suggestions of Maarten Egmond (Unilever Research Laboratory, Vlaardingen) are appreciated.

List of symbols

c or c_p	concentration of protein in solution	[mol m^{-3}] or [g m^{-3}]
Γ	adsorbed amount	[mg m^{-2}]
d_f	thickness of the adsorbed layer	[m]
d_p	thickness of the adsorbed layer	[m]
D	diffusion coefficient	[m^2 s^{-1}]
f	coefficient that accounts for intensity losses	
θ_b	Brewster angle	
θ_i	angle of incidence of light	
I_p	reflected intensity of parallel polarized light	
I_s	reflected intensity of perpendicularly polarized light	
I	ionic strength	[M]
J	flux of protein towards the surface	[mg m^{-2} s^{-1}]
λ	wavelength	
S	output signal	
R_p	reflectivity for parallel polarized light	
R_s	reflectivity for perpendicularly polarized light	
m	mass transfer coefficient	[m s^{-1}]
n_p	refraction index of the adsorbed protein layer	
n_s	refraction index of the solution	
n_f	refraction index of the silica layer	
ν	kinematic viscosity of the solution	[m^2 s^{-1}]
Q	coefficient of output signal for calculation of the adsorbed amount	
R	radius of the cylindrical conduit	[m]
T	temperature	
t	time	
Φ	volume flux	[m^3 s^{-1}]

References

1. James, L.K. and Augenstein, L.G., Adv. Enzymology 28, 1-40 (1966).
2. Miller, I.R. and Bach, D., in: *Surface and Colloid Science*, Vol. 6 (E. Matijevic, Ed.), p. 185-260, John Wiley & Sons, NY, 1973.
3. Andrade, J.D., *Surface and Interfacial Aspects of Biomedical Polymers*, vol. 2, Plenum Press, NY, 1985.
4. Norde, W., Adv. Colloid Interface Sci. 25, 267-340 (1986).
5. Brash J.L. and Horbett, T.A., *Proteins at Interfaces*, ACS Symposium Series 343, Washington D.C., 1987.
6. Norde, W.and Lyklema, J. J. Biomater. Sci. Polymer Edn. 2, 183-202 (1991).
7. Haynes, C.A. and Norde, W., Colloids and Surfaces 2, 517-566 (1994).
8. Ivarsson, B. and Lundström, I., CRC Critical Reviews in Biocompatibility, Vol. 2, p.1, 1986.
9. Privalov, P.L. and Gill, S.G., Adv. Protein Chem. 39, 191-234 (1988).
10. Roth, C.M., Johnson, C.A. and Lenhoff, A.M., The role of structural details in models of electrostatic and van der Waals contributions to protein adsorption, oral presentation on the 68th Annual Colloid and Surface Science Symposium, Stanford University, Stanford, California, June, 19-22, 1994.
11. Blokzijl, W. and Engberts, J.B.F.N., Angew. Chem. Int. Ed. Engl. 32, 1545-1579 (1993).
12. Norde, W., Colloids Surfaces 10, 21-31 (1984).
13. Dulm, P. van, Norde, W. and Lyklema, J., J. Colloid Interface Sci. 82, 77-82 (1981).
14. Koutsoukos, P.G., Norde, W. and Lyklema, J., J. Colloid Interface Sci. 95, 385-397 (1983).
15. Norde, W. and Favier, J.P., Colloids Surfaces 64, 87-93 (1992).
16. Jönsson, U., Lundström, I. and Rönnberg, I., J. Colloid Interface Sci. 117, 127- (1986).
17. Kondo, A., Murakami, F. and Higashitani, K., Biotechn. Bioeng. 40, 889-894 (1992).
18. Galisteo, F. and Norde, W., J. Colloid Interface Sci. 172, 502-509 (1995).
19. Norde, W. and Lyklema, J., J. Colloid Interface Sci. 66, 257-265 (1978).
20. Morrisey, B.W., Smith, L.E., Stromberg, R.R. and Fenstermaker, C.A., J. Colloid Interface Sci. 56, 557- 563 (1986).
21. Steadmann, B.L., Thompson, K.C., Middaugh, C.R., Matsuno, K., Vrona, S., Lawson, E.Q. and Lewis, R.V., Biotechn. Bioeng. 40, 8- (1991).
22. Kondo, A., Oku, S. and Higashitani, K., Biotechn. Bioeng. 37, 537-543 (1991).
23. Arai, T. and Norde, W., Colloids Surfaces 51, 1-15 (1990).
24. Norde, W. and Lyklema, J., J. Colloid Interface Sci. 66, 295-302 (1978).
25. Lyklema, J., *Fundamentals of Interface and Colloid Science*, Vol. 1, section 5.3-5.4, Academic Press, London, 1991.
26. Ben-Naim, A., *Hydrophobic Interactions*, p. 65 and p. 222, Plenum Press, NY, 1981.
27. Besseling, N.A.M. and Lyklema, J., Pure Appl. Chem. 67, 881- (1995).
28. Craig, V.S.J., Ninham, B.W. and Pashley, R.M., J. Phys. Chem. 97, 10192-10197 (1993).
29. Shibata, C.T. and Lenhoff, A.M., J. Colloid Interface Sci. 148, 468- (1992).
30. Shibata, C.T. and Lenhoff, A.M., J. Colloid Interface Sci. 148, 485- (1992).
31. Mizutani, T., J. Colloid Interface Sci. 82, 162-166 (1981).
32. Duinhoven, S., *Enzyme adsorption at solid-liquid interfaces*, Ph.D thesis, Wageningen Agricultural University, The Netherlands, 1992.
33. Norde, W., J. Dispersion Sci. Techn. 13, 363-377 (1992).
34. Villa, A., Zecca, L., Fusi, P., Colombo, S., Tedeschi, G. and Tortora, P., Biochem. J. 295, 827- (1993)
35. Dale, B.E. and White, D.H., Enzyme Microb. Technol. 5, 227-229 (1983).
36. Mihalyi, E., *Application of proteolytic enzymes to protein structure studies*, p. 148, CRC Press, 1972.
37. Dijt, J.C., *Kinetics of polymer adsorption, desorption and exchange*, Ph.D thesis, Wageningen Agricultural University, The Netherlands.
38. Oldenzeel, M., *Reflectometric studies of protein interactions at solid-liquid interfaces*, Ph.D thesis, University Twente, The Netherlands.
39. Hansen, W.N., J. Optical Soc. Am. 58, 380-390 (1968).
40. Born, M., Wolf, E., In: *Principle of Optics*, 5th ed. Pergamon Press, Oxford, 1975.
41. Dabros, T. and Van de Ven, T.G.M., Colloid Polym. Sci. 261, 694- (1983).

42. Norde, W., Arai, T., Shirahama, H., Biofouling 4, 37-51 (1991).
43. Bousse, L., Mostarshed, S., Shoot, B. van der, Rooij, P. de, Gimmel, P. and Göbel, W., J. Colloid Interface Sci. 147, 22- (1991).
44. Penners, G., Priel, Z. and Silberberg, A., J. Colloid Interface Sci. 80, 437- (1981).
45. Norde, W., MacRitchie, F., Nowicka, G. and Lyklema, J., J. Colloid Interface Sci. 112, 447-456 (1986).
46. Buijs, J.A.G., Berg, P. van den, Lichtenbelt, J.W.Th., Norde, W., Lyklema, J., Colloids Surfaces, acc. (1995).
47. Duinhoven, S., Poort, R., Voet, G. van der, Agterof, W.G.M., Norde, W. and Lyklema, J., J. Colloid Interface Sci. 170, 340-350 (1995).

Chapter 4

Synthesis and characterization of a short-haired poly(ethylene oxide)-grafted polystyrene latex

Abstract

A preparation method is developed to prepare charge-stabilized polystyrene latex particles, carrying terminally grafted short PEO-chains. The latices had relatively large particles (480 nm), a surface charge and possessed on the surface a PEO-350/methacrylate molecule. The surface properties of this latex were compared to those of a similar latex but without the PEO-surface group.

The presence of the PEO-moiety on the particle surface could be established by the colloidal stability against salt, complexation with molybdatophosphoric acid and proton NMR. From the molybdatophosphoric acid- and ^1H NMR-results it followed that the average surface coverage of PEO-350 is roughly one molecule per 2.5 square nanometre.

This chapter has been published in Colloids and Surfaces A: Physicochemical and Engineering Aspects. Maste, M.C.L., Velthoven, A.P.C.M. van, Norde, W. and Lyklema J., Colloids Surfaces 83, 255-260 (1994).

4.1. Introduction

In the extensive literature on the synthesis of colloidal dispersions, several authors have reported on the preparation of polystyrene latices that are sterically stabilized by methoxy poly(ethylene oxide) methacrylate-moieties (further denoted PEO), which are covalently grafted on the surface of the particles [1-3].
For some applications it is desirable to have grafted relatively short PEO molecules. For large particles that have relatively strong van der Waals attractions, however, the short PEO molecules do not provide enough steric stability. In these cases additional charge must be introduced, for example, by using a charged initiator. The van der Waals attraction will then be overcome by a small steric repulsion from the PEO and a larger electrostatic repulsion. This chapter deals with the preparation of such a colloid, and discusses several methods by which the presence of the covalently bound PEO can be demonstrated.

4.2. Characterization of the latices

Two kinds of (emulsifier free) latices have been synthesized by suspension polymerization [4]. The first latex only carried sulphate groups (originating from the initiator used) and sulphonate groups (from vinylsulphonic acid); this latex is denoted as polystyrene A (PS-A). The second latex also carried these surface groups as well as methoxy poly (ethylene oxide) methacrylate residues. The latter molecule contains eight monomers of ethyleneoxide and is denoted PEO-350 (supplied by ICI Paints Division), the number referring to the average molecular mass of the ethylene oxide part. This latex is called polystyrene B (PS-B). For comparison a polystyrene latex sterically stabilized by PEO-2000 moieties [3] (further denoted PS-C; 25% (w/w); diameter, d=892 nm) has also been examined (PS-C; kindly supplied by ICI. Agrochemicals).
The latices were characterized using three different methods, i.e. coagulation, complexation with molybdatophosphoric acid and ^{1}H NMR spectrometry. The first two methods will be discussed in more detail.

4.2.1. Dispersion stability

The dispersion stability against salt-induced aggregation is the quantity in terms of which the difference between PS-A and PS-B is established. The method is based on

the determination of the colloidal stability ratio $W = k^f/k$, which is the ratio between the rates of fast and slow coagulation at different salt-concentrations. In our experiments the rate constant is related to the fast aggregation rate constant in the case of PS-A. The value of k^f may be different from the theoretical value and may differ between the different latices [5, 6]. Another quantity that is determined is the critical coagulation concentration (*CCC*), which is the salt concentration above which W=1. It is expected that in the PS-B case the *CCC* is larger because of the additional steric barrier.

4.2.2. Molybdatophosphoric acid method

The concept of this experiment has been put forward by Nuysink and Koopal [7]. These workers have demonstrated a quantitative complexation between molybdatophosphoric acid and free poly (ethylene oxide) polymer in aqueous solution. Molybdatophosphoric acid absorbs light around 218 nm. Depletion of this molecule from solution by complexation with ethylene oxide segments at the particle surface is expected to lead to a decrease in absorbance.

4.2.3. ^{1}H NMR

As can be seen from Fig. 4.1, the PEO-350 molecule contains 8 monomers of ethyleneoxide. The vinyl bond in the methacrylate group on the left hand side is the polymerizable bond. The assignments of peaks in a ^{1}H NMR spectrum of this molecule dissolved in $CDCl_3$ is in correspondence with the integrated peak area. The spectrum is given as below:

PEO-350/methacrylate: δ 1.89 (t, 3H, CH_3), 3.33 (s, 3H, OCH_3), 3.50 (m, 2H, -OCH_2), 3.60 (m, 26H, -OCH_2), 3.72 (m, 2H, -OCH_2), 4.23 (m, 2H, -OCH_2), 5.52 + 6.12 (m, 2H, =CH_2) [s=singlet, t=triplet, m=multiplet].

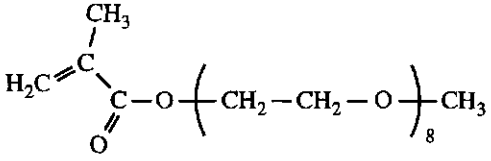

Fig. 4.1. Molecular structure of methoxy poly(ethylene oxide) methacrylate, where $n \approx 8$ for PEO-350.

The main feature of this spectrum is the high peak area at δ of 3.6 ppm. This specific peak is from the H-atoms of the middle part of the ethylene oxide chain and is used as a characteristic for the presence of PEO-350 in the PS-B system.

4.3. Experimental

4.3.1. Preparation of the polystyrene latices

Initially, the preparation was carried out according to Goodwin et al. [4], but a few modifications were made regarding the introduction of surface groups. The two polymerization reactions were carried out in a 1.5 l five-necked reaction vessel. The first three inlets were used for the glass stirrer, a water-cooled reflux condenser and the nitrogen gas supply, respectively. A thermometer which is connected to a recorder, was placed in the fourth inlet. The experimental conditions were chosen such that, according to an empirical formula given by Goodwin et al. [4] that relates the amount of styrene ([*S*]) and potassium persulphate ([*P*], initiator), the ionic strength *I* and the temperature *T* to the final particle size, the diameter should become 440 nm. In the procedure followed, [*S*]= 0.9 M (Baker grade and freshly distilled under reduced pressure at 44°C prior to use), [*P*]=2 mM; *I*=16 mM (adjusted by an additional amount of 10 mM $KHCO_3$), *T*=85°C and the total volume was about 1.2 l (supplemented with deionized water).

The moment of addition of the PEO monomers and vinylsulphonic acid (VSO_3) (=$C_2H_3NaO_3S$; Fluka Chemika) is crucial for the success of copolymerization. These groups will be mainly located at the surface when the reagents are added in the final stage of polymerization [8, 9]. This final stage can be traced by following the temperature inside the reaction vessel. At some stage during the reaction the temperature starts to increase by about 1 to 2 degrees (over 15 min) whereafter it decreases and remains constant at 85°C. The temperature increase is rationalized by an increase of the polymerization rate at the end of the suspension polymerization. Because of diffusion limitation of the termination reaction within relatively large polymeric particles, the average amount $\bar{n}$ of radicals inside the large polystyrene particle increases ($\bar{n}$>1) and, hence, the rate of polymerization [10].

The PEO-350 and the VSO_3 were added under their expected starved conditions. After 3 h from the start of the reaction (i.e. from the moment of addition of initiator) a VSO_3 solution (0.88 M in methanol/water (1:1)) and a PEO-350 solution (0.36 M in distilled styrene) were added at a constant rate of 0.32 mmol min^{-1} and 0.08 mmol min^{-1},

respectively. This was performed continuously during 50 minutes using two independent automatic burettes. After these 50 min (i.e. 3.8 h after the initiator addition) the temperature was, as expected, at its highest value (about 87°C). The VSO_3 and PEO solutions were administered through the fifth inlet which was always thoroughly sealed when not in use.

After 20 h from the start of the reaction the latex was allowed to cool and subsequently freed from the coagulum. From the high pH of the latex after polymerization (pH 9.2) it was concluded that generation and incorporation of $OH^{\bullet-}$ radicals (taking place at pH values below 4; [11, 12]) did not occur during the period of polymerization.

The latex was then thoroughly cleaned with deionized water by diafiltration according to a method described by Labib and Robertson [13]. The filtration was performed with use of an Amicon stirred cell and reservoir device at an operating liquid pressure of 0.5 bar. The filter used had a pore size of 0.2 μm. The progress of cleaning is monitored by measuring the conductance of the permeate. For both latices the conductance decreased from 17 mS cm^{-1} to 25 μS cm^{-1} (the value for deionized water is about 2 μS cm^{-1}) after a volume throughput of 10 times the volume of latex in the cell. Hereafter the latex is considered to be almost free of disturbing substances. After filtration the pH was 5.5. During this procedure about 25% of the initial added amount of styrene has disappeared by both the coagulation of the particles in the vessel and the removal of unpolymerized styrene by filtration.

Single particle optical sizing [14], dynamic light scattering and electron microscopy (see also appendix chapter 5) showed that latices A and B were both highly homodisperse, while the average particle diameter is 490 nm for latex A and 480 nm for latex B, which is in fairly good agreement with those predicted by Goodwin et al. [4].

4.3.2. Characterization

Dispersion stability. The volume fraction θ of the polystyrene particles in the system was set at $\theta = 6.10^{-5}$ which corresponds to approximately 10^9 particles per cm^3. The latex suspensions were always sonicated prior to use. Coagulation took place in the cuvette. A volume of 0.2 ml of a properly diluted latex suspension was added to 2.8 ml of a KNO_3 solution. The stirring conditions were kept constant. The increase in turbidity of the coagulating latex suspensions was measured at 600 nm in the presence of monovalent inert salt ([KNO_3]=0.2-2.0 M). The PS-C latex was not suitable for such a coagulation experiment because the large particle size of this latex would preclude a significant increase in absorbance when coagulating [15].

Molybdatophosphoric acid method. For our experiments it was necessary to modify the method described by Nuysink and Koopal [7]. The molybdatophosphoric acid reagent was prepared by mixing the following ingredients: (0.25 g $20MoO_3 \cdot 2H_3PO_4 \cdot 48H_2O$ + 0.50 g $BaCl_2 \cdot 2H_2O$ +1.5 ml HCl (32%), supplemented with water to a total volume of 250 ml. In the assay used, 1.0 ml of this reagent was added to 2.5 ml of the polystyrene suspension (PS-A, PS-B: three times diluted prior to sampling; PS-C: 0.5%) in a centrifuge tube. The incubation was carried out for 20 min, after which the complex was centrifuged for 30 min at 25000 *g*. A volume of 1.0 ml of the clear supernatant was then diluted 25 times and the absorbance at 218 nm (A_{218}) of this solution was measured.

The latices were cleaned thoroughly in order make certain that the decrease in absorbance in the PS-B case was due to complexation with PEO-surface groups and not with unreacted PEO in solution. To this end, during filtration, samples of the permeate were taken and also analyzed for the presence of PEO. In this case the above-mentioned 2.5 ml latex should be read as 2.5 ml of permeate. After extensive filtration the absorbance of the permeate should be the same as that for water (and the same as for PS-A).

A calibration was performed by treating both water (2.5 ml) and a known amount of a monomeric PEO-350 solution with the reagent (0-60 mg PEO-350 dissolved in 50 ml methanol, then diluted ten times in methanol, of which 2.5 ml were taken for the assay). Thus, the molybdatophosphoric acid reagent was not exhausted and a linear relationship was obtained between the amount of PEO-350 and A_{218}.

4.4. Results and discussion

From the log *W*-log *C* plots (where *C* is the concentration of KNO_3) in Fig. 4.2 it is seen that there is a significant difference between the stability ratios of PS-A and PS-B over the whole concentration range, although it is difficult to locate the respective *CCC*'s.

It is assumed that the outer surface of both types of particles are 'hairy' in nature, although the PS-B particle is stabilized by an extra steric factor from PEO moieties. The presence of steric interactions generally eliminates aggregation into the deep primary minimum; only loose, reversible aggregation at relatively large separation distances is observed in the shallow secondary minimum. The aggregates formed by coagulation are transient and back-dissociation into single particles occurs. For the latex particles of type A the energy minimum is probably deeper and hence the stability ratio is smaller than that of the particles of type B.

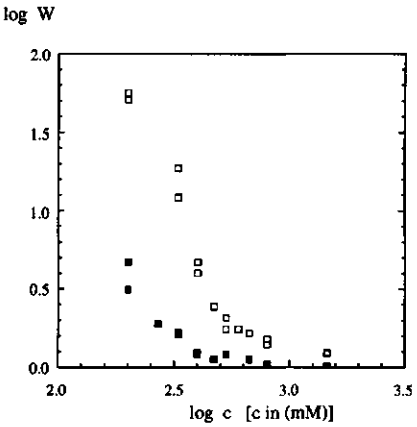

Fig. 4.2. Stability ratio of PS-A (■) and PS-B (□).

From the absorbance-values in Table 4.1 (the values for PS-A and PS-B are tabulated on a 8.50% (w/w) basis) it is evident that monomeric PEO-350, PS-B and PS-C form a complex with molybdatophosphoric acid. After filtration the PS-B system in the retentate still showed a lower absorbance (A=0.20) than water (A=0.42). The removal of unpolymerized PEO can be regarded as complete (A_{218} shifts from 0.25 to 0.43) The PS-C system (as supplied) also showed a decrease (A=0.19), as expected. The PS-A system has the same A_{218}-value as water, so polystyrene by itself and the surface groups other than PEO behave as though they were inert in this method.

Table 4.1. The absorbance A_{218} of different samples treated according to the molybdatophosphoric acid method.

Sample		A_{218}
Water		0.42
Monomeric PEO-350		0.12
Permeate from filtration of	PS-A after 0 h	0.42
	PS-B after 0 h	0.25
	PS-B after 2 h	0.27
	PS-B after 4 h	0.40
	PS-B after 15 h	0.43
PS-A		0.42
PS-B		0.20
PS-C		0.19

Assuming equal reactivities of surface-bound PEO and free PEO-350, a PEO-distribution in the PS-B system can be roughly estimated (Table 4.2). Departing from the calibration data and using the absorbance values of PS-B before filtration (A_{218}=0.16), PS-B after filtration and the permeate of PS-B (from which the amount of PEO is derived from integration over filtration time), the estimated amounts can be expressed as a percentage of the initial added amount of monomeric PEO-350.

Table 4.2. Distribution of PEO-350 in the PS-B system

Location	Estimated amount of PEO-350 (%)
At the particle surface[a]	27
'Inside the particle'[b]	68
In the aqueous phase[c]	5

[a] From PS-B after filtration.
[b] From amount of PEO-350 added minus PS-B before filtration.
[c] From the permeate.

The PEO-balance amounts to practically 100%. Furthermore, the density of PEO-350 at the PS-B particle surface was calculated as 1 molecule of PEO-350 per 2.48 nm^2 ($d_{polystyrene}$ = 1.05 g cm^{-3}).

This result was also checked by ^1H NMR spectrometry (data not shown), using deuterated chloroform ($CDCl_3$) as the solvent for polystyrene. From the assignments in the PEO-350 spectrum and the integrated peak area of the PEO signal in the PS-B spectrum (the PEO signal was also found in the PS-C spectrum) and assuming that all the PEO present was located at the surface of the PS-B particle it was calculated that one PEO-molecule covers about 1.38 nm^2.

Taking into consideration the result from the molybdatophosphoric experiments that a part of the PEO (68%) would be inside the particle, the NMR value and the molybdatophosphoric acid value almost coincide. This result is somewhat flattered because a part of the PEO is removed by having the latex freed from the coagulum after polymerization. Although the experiments were not meant to yield quantitative statements about the surface coverage, it is gratifying that two totally different detection techniques yield more or less the same value.

4.5. Conclusions

From three different methods of characterization it is confirmed that copolymerization of PEO-350/methacrylate enables us to prepare a charge-stabilized latex with PEO moieties at the surface of a polystyrene particle.

Acknowledgements

We are indebted to Ans van Velthoven for the performance, reporting and discussions with regard to the colloidal stability experiments. We would like to thank Dr. J. L. Ammerdorfer (Laboratory of Polymer Chemistry, Eindhoven University of Technology, The Netherlands) for the helpful discussions on the preparation of the latices. Also Dr. B. Gebben (Akzo Research Laboratories, Arnhem, The Netherlands) is acknowledged for his useful suggestions. The NMR work was perfectly assisted by A. van Veldhuizen and R. Schrijvers (Dept. of Organic Chemistry, Wageningen Agricultural University).

References

1. Cowell, C., Lin-in-on, R. and Vincent, B., J. Chem. Soc., Faraday Trans. 74, 337-347 (1978).
2. Bromley, C.W.A., Colloids and Surfaces 17, 1-11 (1986).
3. Liang, W., Tadros, Th. F. and Luckham, P.F., J. Colloid Interface Sci. 153, 131-139 (1992).
4. Goodwin, J.W., Hearn, J. C., Ho, C. and Ottewill, R.H., Colloid Polym. Sci. 252, 464-471 (1974).
5. Einarson, M.B. and Berg, J.C., J. Colloid Interface Sci. 155, 165-172 (1993).
6. Ottewill, R.H. and Walker, T., Trans. Faraday Soc. 70, 917-926 (1974).
7. Nuysink, J. and Koopal, L.K., Talanta 29, 495-501 (1982).
8. Sakota, K. and Okaya, T., J. of Appl. Polym. Sci. 20, 1735-1744 (1976).
9. Hearn, J., Wilkinson, M.C. and Goodall, A.R., Adv. Colloid Interface Sci. 14, 173-236 (1981).
10. Hawkett, B., Napper, D.H. and Gilbert, R.G., J. Chem. Soc., Faraday Trans. 77, 2395-2404 (1981).
11. Furusawa, K., Norde, W. and Lyklema, J., Kolloid Z. u. Z. Polymere 250, 90- (1972).
12. Kolthoff, I.M. and Miller, I.K., J. Am. Chem. Soc. 73, 3055- (1951).
13. Labib, M.E. and Robertson, A.A., J. Colloid Interface Sci. 67, 543-547 (1978).
14. Pelssers, E.G.M., Cohen Stuart, M.A. and Fleer, G.J., J. Colloid Interface Sci. 137, 350- (1990).
15. Long, J.A., Osmond, D.W.J. and Vincent, B., J. Colloid Interface Sci. 42, 545-553 (1973).

Chapter 5

Proteolytic stability of Savinase in colloidal systems

Abstract

The aim of this chapter is to establish the relation between the inactivation of the proteolytic enzyme Savinase and its adsorption on different types of solid-liquid interfaces. The loss of activity has been determined both in solution and in the presence of colloidal particles, which provide a surface area for adsorption of 25% of the enzyme population. Analysis of the remaining solution at different periods of incubation of the various systems shows that the intact protein is converted into autolytic degradation products at the expense of biological activity. The different particles, however, deactivate the enzymes to a different extent. Under the experimental conditions the half-life of the enzymatic activity in solution is 3.5 h. In the presence of particles that have hydrophobic surface properties (teflon- or polystyrene latex) the half-life is reduced to 0.7 h. On the contrary, hydrophilic silica particles stabilize the enzyme against autodigestion as compared to the inactivation in solution. Polystyrene latex particles which are chemically grafted with short poly(ethylene oxide) chains ([EO]8) are, for steric reasons, also mild with respect to the reduction of enzymatic stability. It is thus concluded that the type of surface determines the mode in which the enzyme is adsorbed on a particle which, in turn, affects the autocatalytic rate.

This chapter has been published in Biochimica et Biophysica Acta.
Maste, M.C.L., Rinia, H.A., Brands, C.J.M., Egmond, M.R. and Norde, W., Biochim. Biophys. Acta 1252, 261-268 (1995).

5.1. Introduction

Enzymatic autolytic cleavage in solution is a phenomenon characteristic for proteases, particularly for those with broad substrate specificity. Although Subtilisin proteinases have these qualities [1-3], the enzyme has a preference for hydrophobic amino-acid residues in positions P_1 and P_4 [3] (Schechter and Berger notation [4]). The enzyme investigated in this study is wild-type Subtilisin 309 (Savinase™, ≈ 40% variance with Subtilisin BPN' in amino-acid sequence). The surface structure of Savinase [5] demonstrates that for autodigestion a conformational change of the protein structure is required to make it available for interaction with the attacking enzyme [6-10]. Once a primary cleavage site has been hydrolyzed, other internal residues will become exposed so to allow further degradation.

A change in structure is achieved by, for example, a change in temperature-, media or pH. Denaturation of protein molecules may also be realized by adsorption on interfaces [11, 12]. The extent of a conformational change on a surface is determined by the type of protein, the type of sorbent surface and the physicochemical conditions. Fig. 5.1 represents several models of the autolytic process induced by adsorption of the enzyme. Apart from mechanisms that may explain enhanced autodigestion on the basis of a conformational change (route a and b), activity may be lost by a change in structure, which is not restored when the molecule returns into the remaining solution (Fig. 5.1, route c) [13, 14]. The common element among the different routes is that the converted protein on the surface is always displaced by an intact enzyme from solution. As this enzyme undergoes, in principle, the same processes as the displaced protein, it would ultimately affect all the enzyme present.

Surface-enhanced autodigestion of other proteinases was discussed by Johnson and Whateley [15] and by Brode et al. [16]. For trypsin and chymotrypsin it was shown [15] that autolytic inactivation is enhanced by adsorption on silica particles, although attempts to collect degradation products were not made. In addition to silica surfaces, the effect of hydrophobic surfaces on the autolytic inactivation of Subtilisin BPN' has been investigated [16]. Although Brode et al. do not provide a systematic experimental basis for discussing a mechanism, they demonstrate that autodigestion is prevented by reducing the level of adsorption.

The present chapter extends the work on the autolytic inactivation of a protease to Savinase and also includes a number of different surfaces. It is investigated how the inactivation is modified by the various surfaces and whether or not autodigestion, as is illustrated in Fig. 5.1, is validated.

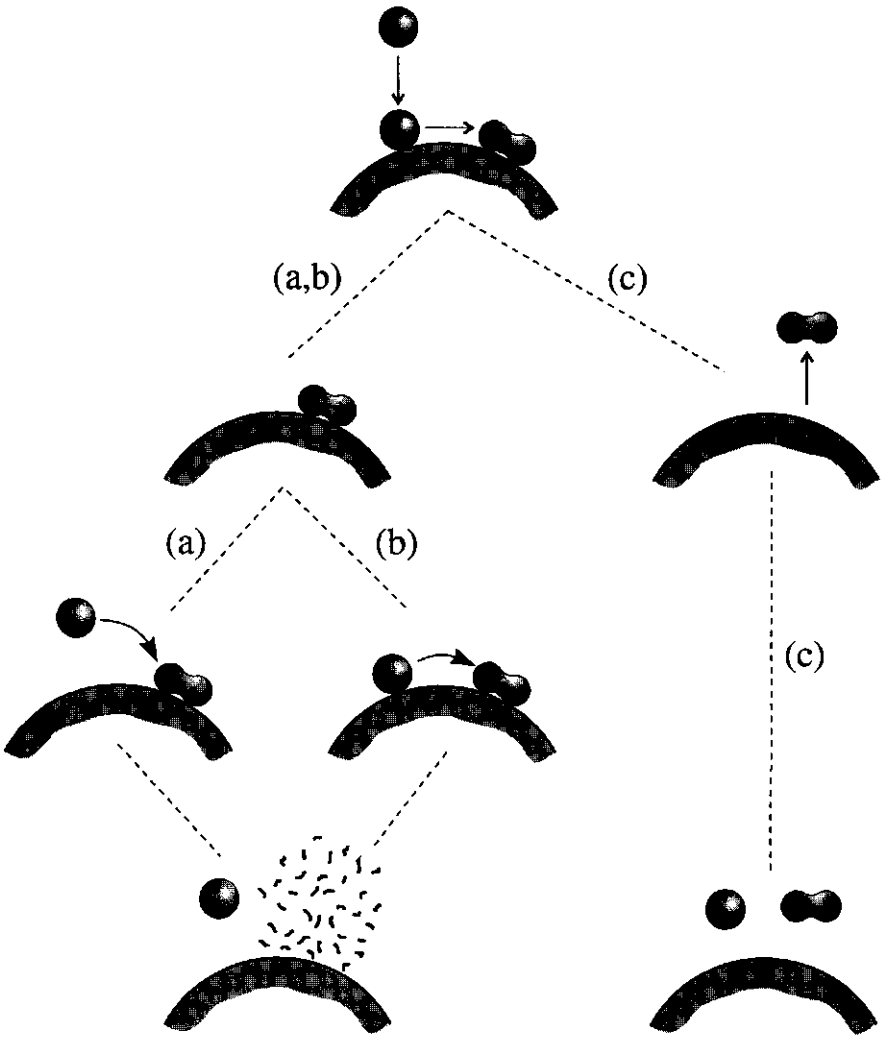

Fig. 5.1. Possible routes of inactivation of a proteinase in the presence of an interface. The straigt arrow denotes a change in state; the curved arrow denotes interaction. Route a: denaturation on the surface and attack by enzyme from solution. Route b: denaturation on the surface and attack by enzyme on the surface. Route c: denaturation on the the surface and displacement by native enzyme. Note that routes a and b result in degradation.

5.2. Experimental

5.2.1. Activity assay

The activity of Savinase was determined spectrophotometrically as the initial change in A_{405}, $(dA_{405}/dt)_{t=0}$, by using N-succinyl-Phe-Ala-Ala-Phe-p-nitroanilide (Bachem, Switzerland, further denoted FAAF) as a small chromogenic peptide substrate. Prior to use, FAAF was dissolved in DMSO. The concentration of Savinase is 0.33 μg ml^{-1} and [FAAF]=0.070 mM ($\approx 6.K_m$). The physicochemical conditions (pH, ionic strength and type of buffer) in the assay were adjusted to the incubation conditions of deactivation. The temperature in the assay was kept at 30.0°C. To determine K_m and k_{cat} of FAAF-hydrolysis the concentration-range of FAAF was varied between 0.004 and 0.14 mM. The data were fitted by assuming Michaelis-Menten kinetics, giving each data point a constant weight in a non-linear least squares method.

5.2.2. Kinetic parameters of active and inhibited enzyme

The kinetic characterization of WT-Savinase prior to use was done by determination of the K_m- and k_{cat}-values. The values for the active enzyme are $k_{cat} \approx 200$ ($\pm$ 20) s^{-1} and $K_m \approx$ 0.012 ($\pm$ 0.001) mM under the experimental conditions, while $k_{cat} \approx 0.1\%$ after inhibition with PMSF (see section 3.6.1).

5.2.3. Sorbent-surfaces

The adsorbents used were a perfluoroalkoxy (PFA-) teflon latex which was free of contaminants (diameter $d \approx 215$ nm; density ρ=2.0 g cm^{-3}), a silica suspension (Ludox HS40, $d \approx 18$ nm; ρ= 2.2 g cm^{-3}; the teflon- and silica suspensions were kindly donated by Dupont de Nemours) and two kinds of emulsifier-free polystyrene latices ($d \approx 480$ nm; ρ=1.05 g cm^{-3}), denioted PS-A and PS-B. The PS-B latex is different from PS-A by the presence of short polyethylene oxide (PEO) moieties (8 segments) that are covalently grafted on the particle surface [17]. The diameters of the different particles were measured by dynamic light scattering. Further, the colloidal suspensions are highly monodisperse as judged from electron microscopy (electron micrographs have been given in the appendix to this chapter). All adsorbents were negatively charged.
The hydrophobicity of a surface has proven to be an important parameter for the structural properties of proteins at interfaces [18]. The hydrophobicity of the surface has been inferred from the contact angle θ of a sessile water droplet on a tablet of the dried material. The tablet was prepared by bringing a volume of dry solids of the suspensions

under high pressure (8 bar). The surface of the constituted tablet was macroscopically smooth. A droplet of 15 μl of water was placed on the tablet surface while the advancing contact angle (through the water phase) was measured with the aid of a microscope with a goniometric device.

5.2.4. Adsorption isotherms

Adsorption isotherms for both PMS-Savinase and autolytic fragments were established by solution depletion at pH 8.0, T=20°C and I=10 mM in 1.5 ml of a $Na_2B_4O_7$-buffer. The buffer preparation was described in section 3.6. The isotherm was determined at constant protein concentration and a varying amount of sorbent surface area. The incubation time (30 min) was sufficiently long to attain plateau values of adsorption. The fragments were obtained from a temperature-enhanced (T≈50°C) autodigestion in solution (Fig. 5.5). The solution concentrations of intact protein and fragments after adsorption on teflon and silica were determined by measuring the absorbance at 214 nm. In the case of PS-A and PS-B a modified Lowry-procedure [19, 20] has been applied. The accompanying calibration curves for the intact and degraded enzyme are shown in Fig. 5.2a.

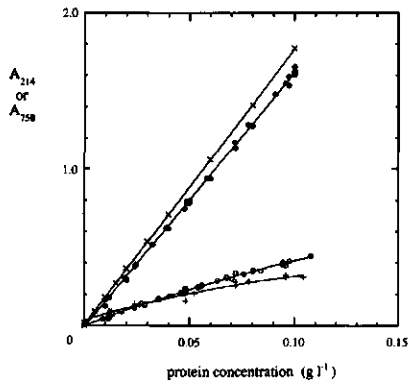

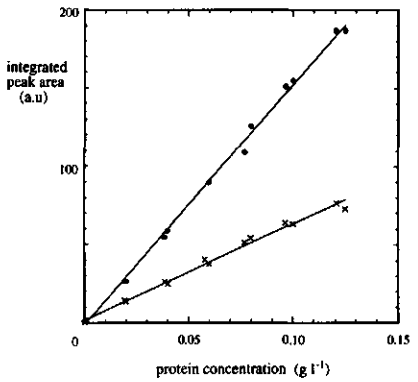

Fig. 5.2a (left). Optical density of PMS-Savinase at 214 nm (●) and at 750 nm (after Lowry colouring, ○) and heat-induced autolytic fragments of WT-Savinase at 214 nm (×) and at 750 nm (+), as a function of protein concentration in solution.

Fig. 5.2b (right). Integrated peak area in the HPLC-RP chromatogram as detected by A_{214}, as a function of the concentration of PMS-Savinase (●) and heat-induced autolytic fragments of WT-Savinase (×). For elution details see legend to Fig. 5.5.

5.2.5. Determination of proteolytic stability

A volume of 1.5 ml of enzyme solution was subjected to deactivation. The concentration of enzyme is 0.10 g l^{-1} (≈ 3.5 μM). The incubation was carried out in glass tubes (Ø 10 mm) at pH 8, T=20°C and I=10 mM (as described for the isotherms). The use of glass tubes is based on the fact that adsorption onto the wall of hydrophobic tubes may cause artifacts [13, 16], although solution inactivation of Savinase in polypropylene tubes was comparable to that in glass tubes (not shown). A spinbar (for cuvettes, height 8 mm, Ø 9.5 mm from Tamson, The Netherlands) was used for stirring while the magnetic stirrer (Variomag Multipoint HP15) was set at 850 rpm. The amount of particles added was such that, according to the plateau values of the corresponding isotherms, the fraction of enzyme molecules adsorbed was always 25%. At suitable time intervals during incubation aliquots (10 μl) were drawn for assay of the residual activity.

5.2.6. Supernatant analyis

In the course of inactivation the residual activity and the physical state (i.e. state of degradation) of the protein were quantified in the supernatant. The analysis of the supernatant is justified as the inactivated proteins cannot accumulate on the surface of the colloidal particles. If the enzymatic activity is significantly lost and the particle-surface accomodates 25% of the protein at the most, the major part of the inactivated protein must reside in the supernatant. Also, when fragments are produced (Fig. 5.1, routes a and b), the above statement holds as the fragments have no affinity for the surfaces under investigation (Fig. 5.3a).

Instead of sampling from one tube in course of time, a set of tubes with similar contents were used. For each point in time the contents of a tube (1.5 ml) were transferred to an eppendorf vial. For centrifugation of the aliquot the rotor was operated for 10 min at 8000 g. To prevent autodigestion during centrifugation as much as possible, the activity was decreased by an order of magnitude by lowering the temperature to 0°C. The effects of the temperature change on the adsorption equilibrium and hence the composition of the supernatant turned out to be of minor importance. After assaying the supernatant activity, the remainder of the supernatant was used for HPLC-analysis. In order to prevent further autodigestion TFA is added (trifluoroaceticacid from Baker: gradient grade, 0.06 % w/v in final protein solution).

In order to discriminate between route a and b (Fig. 5.1) an additional experiment was carried out. The surface areas of teflon and silica were varied at constant enzyme

concentration (0.1 g l^{-1}), leaving out the rising part of the adsorption isotherm. The supernatants of the teflon- and silica suspensions were analyzed after 1.5 and 6.5 h of incubation, respectively, of enzyme and sorbent. The amount of fragments was determined by following the procedure as mentioned in the above paragraph.
The analysis of the supernatant is carried out by HPLC-RP and subsequent detection at 214 nm. This spectrophotometric detection has proven to be more sensitive and more accurate as compared to colouring methods as Lowry's [20] (see Fig. 5.2a) or BCA [21] (not shown). A calibration was performed for heat-induced fragments and intact enzyme. The area of their respective peaks in the HPLC chromatogram is proportional to the known concentration (Fig. 5.2b). The dissimilar calibration factors for the two species as compared to those obtained with direct spectrophotometry at 214 nm (Fig. 5.2a) could be caused by the loss of small peptides that do not bind to the column. These peptides elute under the first peak in the chromatogram (Fig. 5.5) which, for practical reasons, was neglected in the calibration. Hence, for the first stage of degradation, when the small peptides are not abundantly present, the calibration factor ε (in $c_{protein} = A_{214}/\varepsilon$) for the fragments, is too low. It leads to overestimation of the amount of fragments. As degradation proceeds the estimate will be better.

5.3. Results and Discussion

From the water contact angle θ of a water droplet on a tablet of the dried material, it is concluded that teflon (θ=96°) and PS-A (θ=84°) are relatively hydrophobic colloids. The effect of the PEO-moieties on the hydrophobicity is not clear. A free PEO-polymer is characterized as hydrophilic and water-soluble [22] and it is generally assumed that PEO renders a surface more hydrophilic. A recent study on the effect of adsorbing block co-polymers consisting of PEO on the hydrophobicity of membranes has shown an opposite effect [23]. It is, however, commonly accepted that steric hindrance caused by the PEO-chains reduces the amount of protein adsorbed, which is in accordance with our results. The adsorbed amount of PMS-Savinase on PS-B is lower as compared to PS-A (Fig. 5.3b) although θ for PS-B (87°) is hardly different from θ for PS-A (84°). A similar feature was observed for a polystyrene latex which was sterically stabilized by covalently bound $[EO]_{45}$ moieties [17, 24] (θ=95°, the adsorbed amount was reduced to zero). Also the θ-value of teflon (96°) was not significantly altered by coating with Triton X-100 (containing a hydrophobic adsorbing tail and a small PEO-moiety).
While the teflon and polystyrene tablets were firm tablets, the silica tablet suffered from a lack of coherence. Though, upon placing a water droplet on the silica tablet surface, it

was observed that the droplet first spreads fully (implying θ=0°) and was next absorbed in the tablet by capillary action. Although the θ-value could not be measured, the silica surface was characterized as hydrophilic.

The affinity of PMS-Savinase for the various surfaces is relatively high as inferred from the initial slope of the adsorption isotherms (Figs. 5.3a and b). The plateau values for teflon, silica, PS-A and PS-B are estimated to be 2.2, 1.9, 2.3 and 1.5 mg m^{-2}, respectively. The variation in plateau values between the different adsorbents is due to differences in electrostatic- (protein-surface and protein-protein) and hydrophobic interactions and possibly the structure of the adsorbed protein as well [25]. An ordered monolayer of native enzyme molecules contains about 2.5 mg m^{-2} which means that in all cases the particle-surface is more or less below complete monolayer coverage.

It is important to notify that the adsorption characteristics of the enzyme on teflon and silica with respect to the affinity and the plateau value are more or less similar. For verifying a mechanism, it does not make sense to investigate the autolytic rate between two types of surfaces that have more variation than the hydrophobicity (as in [16], with respect to the surface occupation and the degree of depletion).

The inactivation of Savinase in solution and in the presence of the different adsorbents is depicted in Figs. 5.4a and b. Under the experimental conditions the half-life of the enzymatic activity of Savinase in solution is 3.5 h. In the presence of PS-A- or teflon particles, the half-life is reduced to 0.7 h. The fast initial drop in residual activity in the teflon and PS-A system is due to an apparently high adsorption-rate while the adsorbed enzymes do not retain their activity towards FAAF (data not shown).

In contrast with PS-A and teflon, silica particles have an unusual effect on the inactivation. In first instance, the activity decreases faster as compared to the activity in solution. At a later stage, i.e. after 3.0 h, the curves for solution and silica intersect. In other experiments with higher amounts of silica, the intersection is again found (not shown). The sharp initial drop as observed for PS-A and teflon is not found for silica. Although Savinase also has a high affinity for silica, the adsorbed species on silica have retained their activity (towards FAAF) to a considerable extent (data not shown).

The stability of Savinase in the PS-B system could not be measured accurately in the presence of the latex particles, but it is inferred from comparison of the supernatant data of PS-A and PS-B (Fig. 5.4b). Like for silica, the influence of PS-B on the enzymatic stability appears to be mild. The relatively high enzymatic stability in the presence of PS-B is attributed to the steric action of the PEO-layer, possibly preventing the enzyme from unfolding on the surface. Although the activity from the PS-B and silica system could not be measured in a similar way, it is possible that PS-B has the same stabilizing action as silica.

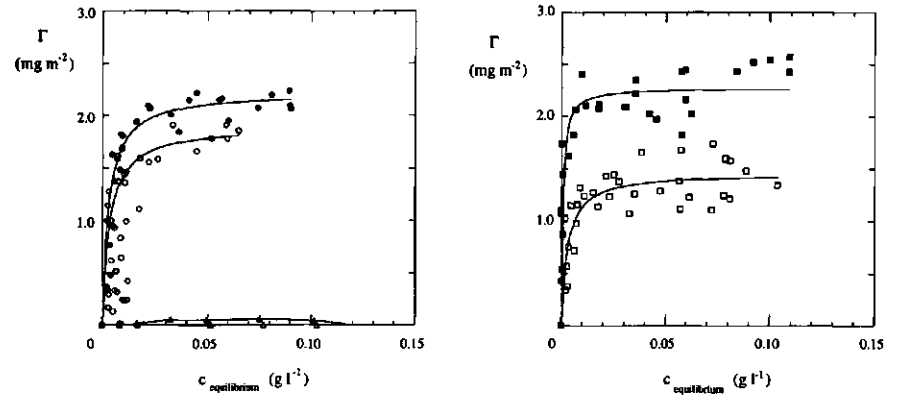

Fig. 5.3a (left). Adsorption isotherms of PMS-Savinase on teflon (●) and silica (○) and heat-induced autolytic fragments of WT-Savinase on teflon (▲) and silica (△).

Fig. 5.3b (right). Adsorption isotherms of PMS-Savinase on PS-A (■) and PS-B (❑).

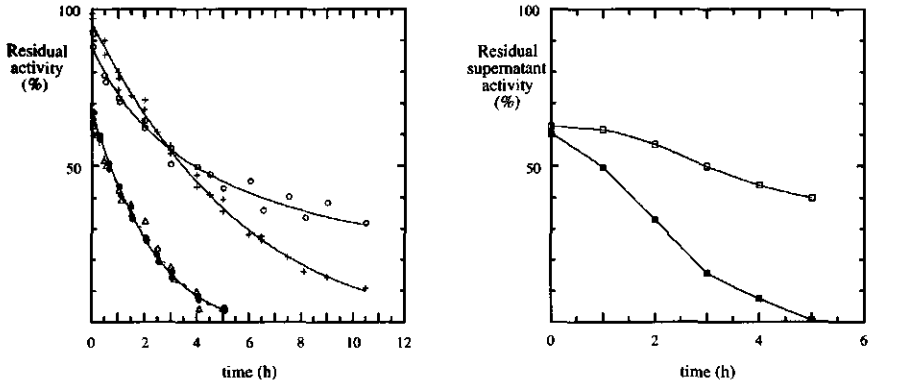

Fig. 5.4a. Inactivation of WT-Savinase in solution (+) and in the presence of silica (○), teflon (●) and PS-A (△).

Fig. 5.4b. Inactivation of WT-Savinase in the presence of PS-A (■) and PS-B (❑). The activity is measured from the supernatants.

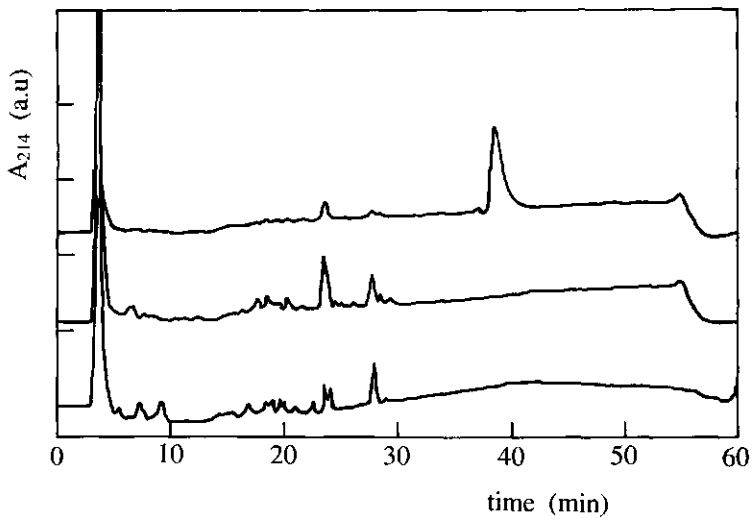

Fig. 5.5. HPLC-RP chromatogram of heat-induced autolytic fragments of WT-Savinase (lower) and the supernatant after 5 h of incubation of WT-Savinase with silica (upper) and with teflon (middle). The intact enzyme elutes at t=39 min. Detection at 214 nm. Column: Bakerbond 7116-00, Wide-Pore Butyl (C_4); 5 μm, 4.6*250 mm, $V_0 \approx 3$ ml. Eluent A: 0.06% w/v TFA (gradient grade) in water; eluent B: 0.06% w/v TFA in 80% acetonitril (gradient grade)/20% water (v/v), flowrate: 1 ml min^{-1}, sample loop: 100 μl. Gradient: 0-5 min: 100% A, 50 min:30% A-70% B, 55 min 100% B, 56 min: 100% A.

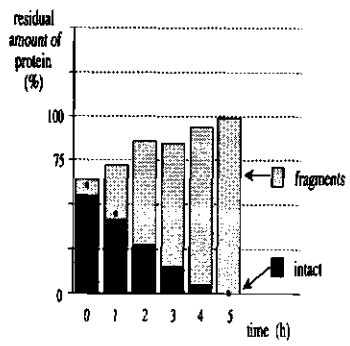

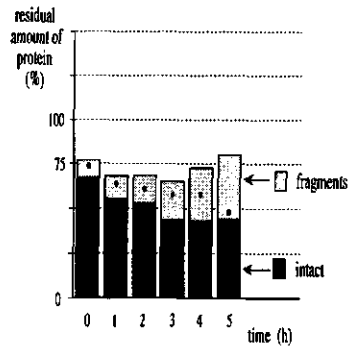

Fig. 5.6a (left). Amounts of intact and degraded enzyme during deactivation by teflon. The residual activity is indicated by (●).

Fig. 5.6b (right). Amounts of intact and degraded enzyme during deactivation by silica. The residual activity is indicated by (●).

Typically, Fig. 5.5 shows the HPLC-RP patterns of the silica- and teflon system after 5 h of incubation. As compared to the silica system the teflon system contains a larger amount of fragments at the expense of intact protein. It should be noted that there is a slight difference in the composition of the fragments as obtained by heat- and by surface inactivation (Fig. 5.5). From the area under their respective peaks and from the calibration factors of the curves in Fig. 5.2b the amounts of intact protein and degradation products are calculated independently for the different systems in the course of the inactivation process. The results for teflon and silica are shown in Figs. 5.6a and b. The residual activity in the supernatant is indicated by the black dot. The first sample taken a few minutes after mixing of enzyme and sorbent is indicated as t=0 h. As judged from Fig. 5.6, the supernatant contains around 75% of the protein at t=0, according to the imposed depletion of 25%. For all systems the extent of inactivation correlates with the amount of fragments produced (not shown for solution, PS-A and PS-B). If mere unfolding would be the inactivating mechanism (Fig. 5.1, route c), the residual activity should have been lower than the residual amount of intact protein. This conclusion for hydrophobic surfaces was also arrived at by Brode et al. [16].

An additional interesting feature is that the amount of fragments in the teflon-supernatant amounts to 100% after 5 h. Apparently, the surface of the teflon-particle becomes free of any protein- or peptide material when autodigestion proceeds. This is in agreement with the lack of affinity of fragments for teflon (Fig. 5.3a). When fragments desorb from the particle-surface, a new adsorption-equilibrium will be attained according to the adsorption isotherm. Thus, the change in the amount of protein adsorbed during inactivation can be inferred from the isotherms in Fig. 5.3, following the curve from the right- to the left hand side.

Alternatively, the enhanced autodigestion on the hydrophobic particles may be caused by enhanced lateral interactions on the particle surface (Fig. 5.1, route b). This may have been possible because the enzyme and substrate are in proximity when the molecules are concentrated on the surface. The experiments, however, do not support this speculation. If route b would have been the exclusive mechanism of inactivation, the inactivation should have been more or less the same for teflon and silica as judged from the more or less identical surface coverage. The occurrence of route b is further investigated by performing inactivation at varying concentrations of teflon and silica within a range where the surface is saturared with protein (see Fig. 5.3a). The degree of autodigestion was measured in the supernatant at a point in time where a sufficient amount of fragments have developed. From the results in Fig. 5.7 it is demonstrated that an optimum occurs when varying the teflon surface area, while a constant decrease is observed with silica upon increasing surface area. The results are presented such that

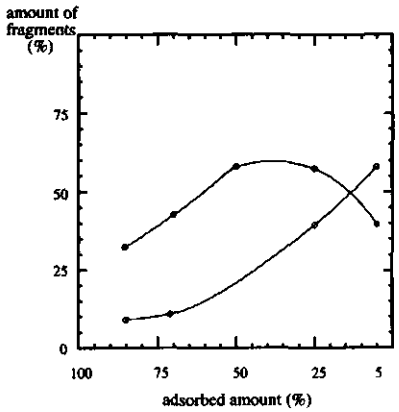

Fig. 5.7. Amount of fragments as a function of the initial adsorbed amount of Savinase. Protein concentration was set at 0.1 g l^{-1} and the surface area of teflon (●) or silica (○) was varied. Fragments were analyzed (HPLC-RP) in the supernatant after 1.5 h (teflon) or 6.5 h (silica) of incubation.

the ordinate corresponds with that of the adsorption isotherm (e.g., 25% adsorption means 0.075 g l^{-1} at equilibrium). Again, if route b would have been the sole pathway of inactivation for teflon, the amount of fragments would have increased continuously upon increasing the amount of surface area. The exclusion of route b from the mechanism is further substantiated by additional experiments in chapter 7. Summarizing the results with respect to the pathway of inactivation (Fig. 5.1), route b and c do not contribute to the mechanism. It appears that route a is the best option as a model for adsorption-enhanced autodigestion.

The result for silica from Fig. 5.7, shows that lateral interaction is not under discussion. On the contrary, the silica surface provides an environment for the enzyme where it behaves la-tently with respect to autodigestion. Obviously, from Fig. 5.4a, the enzymatic activity is regained substantially upon assaying. The effect of silica is remarkable and it has not been found in other investigations [15, 16]. The stabilization could be accounted for by an orientational effect of the enzyme. The enzyme may be adsorbed in such a way that the primary cleavage site is shielded from solution and is not available for interaction. An alternative explanation is a possible fixation of the native structure of Savinase on the silica surface which renders it more stable against unfolding and autodigestion as compared to the free enzymes in solution. The inactivation kinetics of Savinase in the presence of silica is found to be second-order but, to our opinion, the inactivation order is apparent and has as such no physical meaning.

From the inactivation kinetics presented here or elsewhere [15, 16] it is difficult to make explicit statements about denaturation of the enzyme on the hydrophobic surface as suggested in Fig. 5.1. The inactivation may just as well be promoted by orientational organization of the protein molecules on the surface. The protein may have the same conformational properties as in the dissolved state, but there may be more succesful encounters that lead to inactivation. Specifically, it is frequently found that the extent of unfolding depends on the extent of surface occupation by protein. A high surface coverage reduces the degree of unfolding of the enzyme [25]. Hence, a conformational change is allowed if the rate of unfolding is higher than the rate of supply to the surface. The inactivation kinetics, however, are thus determined by the kinetics of adsorption, which -obviously- does not permit assessment of a conformational change.
Though, in the limiting case of fast supply to and a slow (first-order) conformational change (e.g., a minor one) on the particle surface, a constant surface occupation of native enzyme molecules is reached. Consequently, this should give rise to zeroth order inactivation kinetics. The second-order inactivation behaviour as found by Brode et al. for a hydrophobic inactivation of Subtilisin BPN' [16] or first-order inactivation as found for trypsin and chymotrypsin on a hydrophilic surface by Whateley [15] do not illustrate the occurrence of a conformational change.
Altogether, it is clear that a thorough analysis of the inactivation kinetics (which include the different steps, i.e., transport towards the surface, attachment, denaturation and autodigestion) is necessary. Direct assessment of the structural properties of the adsorbed protein in situ —e.g., by spectroscopic methods— is helpful for the analysis. More detailed discussion on the role of structural changes in the adsorbed protein molecule and on the kinetics of inactivation will be presented in chapters 6 and 7.

5.4. Conclusions

Concluding the work of this chapter, we find that inactivation is always the result of autodigestion, irrespective of the type of system in which inactivation takes place. Inactivation, as suggested by route b or c in Fig. 5.1, does not occur. Clearly, the rate of autodigestion is dependent on the way (orientation and/or conformation) the enzyme is adsorbed on the surface. In the presence of hydrophobic latices the autolytic susceptibility is greatly enhanced, whereas adsorption on hydrophilic particles shield the enzyme from autodigestion. Additionally, particles which carry PEO-moieties are relatively mild with respect to the reduction in enzymatic stability.

Appendix

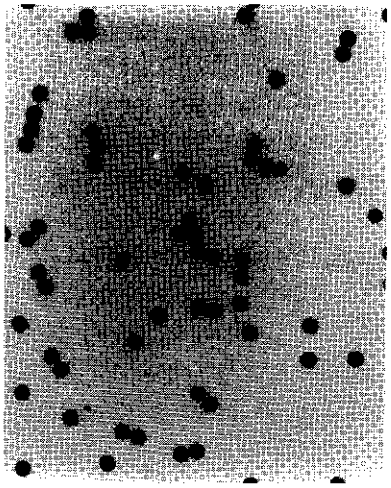

I. PS-A

II. PS-B

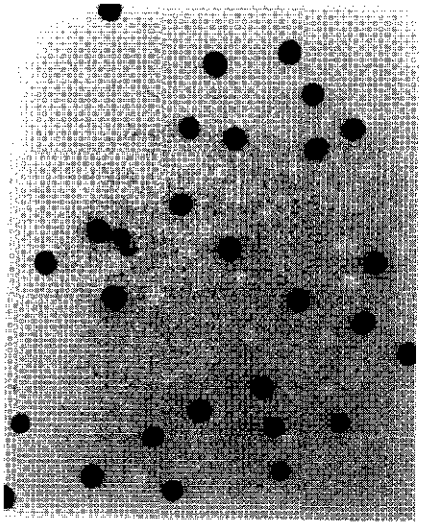

III. Teflon-PFA

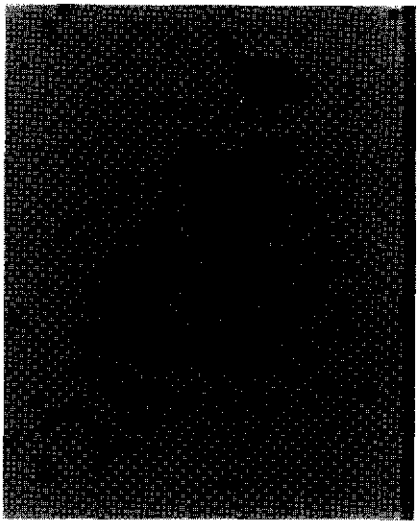

IV. Silica Ludox HS40

Legend to the figures: Electron micrographs of the the different sorbent particles (PS-A, PS-B, teflon and silica), using a Philips EM 400T electron microscope, are given in pictures I, II, III and IV, respectively. All samples showed monodisperse spherical particles. The diameters showed excellent agreement with those obtained from dynamic light scattering. The silica and teflon particles were probably exposed to the light beam too long, causing partial melting of the particles.

Acknowledgements

We are indebted to Hilde Rinia and Carline Brands for the performance, reporting and discussions on most of the experiments. The work on the contact angles was done by Alphonso Anusiem (University Port Harcourt, Nigeria). The teflon latex was kindly granted by D. Lévy from Dupont deNemours, Le-Grand Saconnex, Switzerland. The Ludox silica was also supplied by this company. The HPLC work was assisted by J. A. Boeren (Dept. of Biochemistry, WAU). The electron micrographs were taken by E. Bouw (RIKILT-DLO, Wageningen). Critical comments were from Maarten Egmond (Unilever Research Laboratory, Vlaardingen).

References

1. Keil, B., *Specificity of Proteolysis*, Springer-Verlag, Berlin-Heidelberg, 1992.
2. Bratovanova, E.K. and Petrov, D., Biochem. J. 248, 957-960 (1987).
3. Bech, L.M., Sorensen, S.B. and Breddam, K., Biochem. 32, 2845-2852 (1993).
4. Schechter, I. and Berger, A., Biochem. Biophys. Res. Commun. 27, 157-162 (1967).
5. Betzel, C., Klupsch, G., Papaendorf, G., Hastrup, S., Branner, S. and Wilson, W.S., J. Mol. Biol. 223, 427-445 (1992).
6. Antonov, V.K., *Chemistry of Proteolysis*, 2nd edn, Springer-Verlag, Berlin-Heidelberg, 1993.
7. Adler-Nissen, J., *Enzymic Hydrolysis of Food Proteins*, Elsevier Appl. Science Publ., London, 1986.
8. Eijsink, V.G.H., Dijkstra, B.W., Vriend, G., Zee, R. van der, Veltman, O.R., Vinne B. van der, Burg, B. van der, Kempe, S. and Venema, G., Protein Eng. 5, 421-426 (1992).
9. Kumar, S., Biochem. 9, 291-297 (1970).
10. Sakai, T., Suzumura, M. and Nohara, D., Chem. Pharma. Bull. 36, 2750-2758 (1988).
11. Andrade, J.D., in: *Surface and Interfacial Aspects of Biomedical Polymers* (J.D. Andrade, Ed), Vol. 2, Plenum Press, NY, 1985.
12. Norde, W., Adv. Colloid Interface Sci. 25, 267-340 (1986).
13. Sandwick, R.K. and Schray, K.J., J. Colloid Interface Sci. 121, 1-12 (1988).
14. Oshima, G., Int. J. Biol. Macromol. 11, 43-48 (1989).
15. Johnson, P. and Whateley, T.L., Biochem. J. 193, 285-294 (1981).
16. Brode, P.F. III, Erwin, C.R, Rauch, D.S., Lucas and Rubingh, D.N., J. Biol. Chem. 269, 23538-23543 (1994).
17. Maste, M.C.L., Velthoven, A.P.C.M. van, Norde, W. and Lyklema, J., Colloids Surfaces 83, 255-260 (1994).
18. Norde, W. and Lyklema, J., J. Biomater. Sci. Polymer Edn. 2, 183-202 (1991).
19. Duinhoven, S., *Enzyme Adsorption at Interfaces*, Ph.D thesis, Wageningen Agricultural University, The Netherlands, 1992.
20. Lowry, O.H., Rosebrough, N.J., Farr, A.L. and Randall, R.J., J. Biol. Chem. 193, 265-275 (1951).
21. Smith, P.K., Krohn, R.I., Hermanson, G.T., Mallia, A.K., Gartner, F.H., Provenzano, M.D., Fujimoto, E.K., Goeke, N.M., Olson, B.J. and Klenk, D.C., Anal. Biochem. 150, 76-85 (1985).
22. Bailey, F.E. and Koleske, J.V., *Poly(ethyleneoxide)*, Academic press, NY, 1976.
23. Schroën, C.P.G.H., Cohen Stuart, M.A., Padt, A. van der and Riet, K. van, Colloids Surfaces 90,235-249 (1994).
24. Liang, W., Tadros, Th.F. and Luckham P.F., J. Colloid Interface Sci. 153, 131-139 (1992).
25. Haynes, C.A. and Norde, W., Colloids and Surfaces (B) 2, 517-566 (1994).

Chapter 6

Conformational state of adsorbed Savinase

a tryptophan-fluorescence and circular dichroism study

Abstract

This chapter contributes to the understanding of the structural properties of Savinase on solid-liquid interfaces. The experimental approach consisted of time-resolved and steady-state fluorescence of tryptophan residues and of circular dichroism (CD) of the protein. These properties are measured for PMSF-inhibited Savinase *in situ* on a hydrophilic silica- and on a hydrophobic teflon surface. The results are compared with those obtained from the protein in solution. In the case of fluorescence it is reasoned that the average excited-state lifetime and short internal rotation correlation times are indicative parameters for structural changes in the protein. The internal rotation is superimposed on the rotation of the adsorbed protein which is immobile on the fluorescence timescale.

Fluorescence and CD both prove that Savinase alters its conformation when it adsorbs at low surface coverage on hydrophobic teflon particles. In that case the tryptophan fluorescence lifetime is decreased which is accompanied by an increase in the amount of α-helix. At monolayer coverage the protein maintains its original structure, although minor changes in fluorophore dynamics occur. On hydrophilic silica particles the results from both techniques do not point in the same direction. The fluorescence was not affected, irrespective of the surface occupation, while the CD experiments show a decrease in α-helix content at low surface coverage.

An adapted version of this chapter has been accepted for publication in the J. Colloid Interface Sci. M.C.L. Maste, E.H.W. Pap, A. van Hoek, W. Norde and A.J.W.G. Visser.

6.1. Introduction

In the work described in this chapter conformational changes of Savinase upon adsorption on hydrophilic- (silica) and hydrophobic particles has been probed with spectroscopic methods. The used hydrophobic sorbent particles that are used are from teflon latex (see chapter 5) which allow to obtain unambiguous spectroscopic results for the adsorbed protein. Teflon is a copolymer of tetrafluoroethylene and perfluorovinyl-ether. The polymeric particles consist of a perfluoroalkoxy (PFA) fluorocarbon resin (further denoted teflon) that does not contain any UV-absorbing double bonds and aromatic groups. Its refractive index (1.35) is close to that of water (1.33). Hence, it has the desired properties of negligible light absorption and very low light scattering.
The study has been carried out by means of both time resolved- and steady state fluorescence techniques. The use of extrinsic labels which may trigger conformational changes in the protein molecule has been avoided by taking advantage of the fluorescence of the naturally occurring tryptophans. The great advantage of fluorescence is its relatively high sensitivity to changes in the micro-environment of the fluorophores. In addition, circular dichroism (CD) is used as a tool to monitor changes in the secondary structure elements in the adsorbed state.
There exists an abundance of literature on the application of optical spectroscopic methods like fluorescence- and CD for determining the interaction between proteins and membrane-like structures, such as vesicles [1-10] or micelles [11, 12]. Much less spectroscopic information exists on the adsorption of proteins on solid particles. An experimental problem encountered in a number of spectroscopic studies is light scattering by e.g. vesicles or suspended solid particles. In case of fluorescence this phenomenon leads to aberrant values for the measured fluorescence anisotropy [13, 14]. In CD this problem has been circumvented by having the protein desorbed prior to the measurement [15-18]. However, the structure of the desorbed protein may well differ from that of the protein in the adsorbed state [19]. So far, successful CD measurements on adsorbed proteins have been reported using dilute dispersions of ultrafine silica particles for which absorption and light scattering are minimized [19, 20]. A few CD and fluorescence studies using hydrophobic surfaces have been reported [21-23]. However, these investigations were perturbed by considerable light absorption of the polymeric sorbents. Furthermore, in a few cases the particles used were also good scatterers.

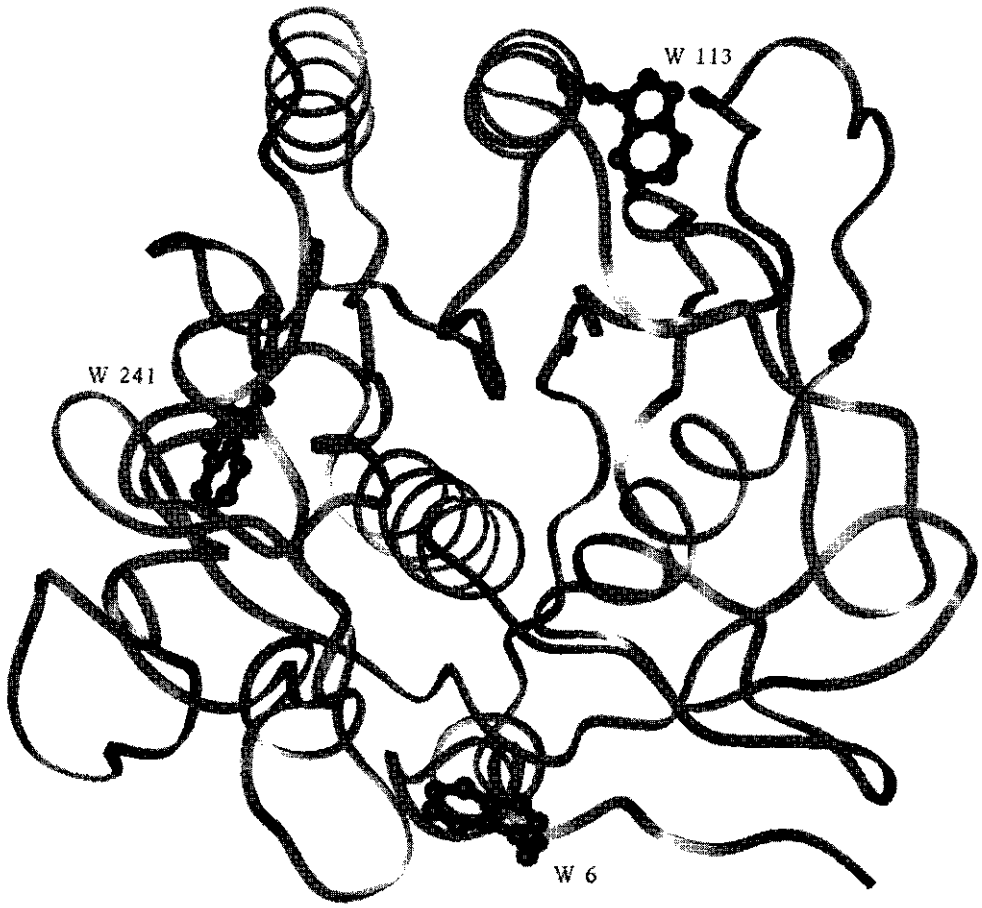

Fig. 6.1. Tertiary structure of Savinase. The three tryptophan residues are located on the exterior of the protein.

6.2. Molecular aspects

The secondary structure of Savinase [24] (section 2.4 and Fig. 2.1) demonstrates the presence of 9 α-helices (83 residues≈31%) and 9 β-pleated sheets (50 residues≈19%). Further, the three tryptophan residues (W or Trp in the one- or three letter code, respectively) in Savinase are located at positions 6, 113 and 241 in the primary structure of the enzyme. These numbers are assigned on the basis of homology with Subtilisin BPN' [25]. Molecular modelling reveals that these residues are situated near the surface of the molecule. Fig. 6.1 shows the three tryptophans in the Savinase molecule. The water-accessible surface area of the side chains are 0.36, 0.46 and 0.61 nm^2 for W6, W113 and W241, respectively, as compared to 1.81 nm^2 for a fully exposed side chain. This indicates that the Trp-residues in Savinase are embedded in the protein matrix allowing a modest water accessibility.

The three tryptophan residues all play a role in the fluorescent behaviour of the whole protein, as is illustrated in Fig. 6.2. An imaginary plane, that embodies the three residues, has been positioned normally to the plane of the paper. The rate of transfer of excitation light between the three tryptophans depends on the distance between the chromophores and the orientation factor. The distances between the residues (28 ± 2 Å) are beyond the critical energy transfer distance for tryptophans (≈15 Å) [26]. Moreover, the side chains lie more or less perpendicularly to each other. Hence, intramolecular energy transfer is unlikely and the observed protein fluorescence is a superposition of the fluorescence of the individual tryptophans.

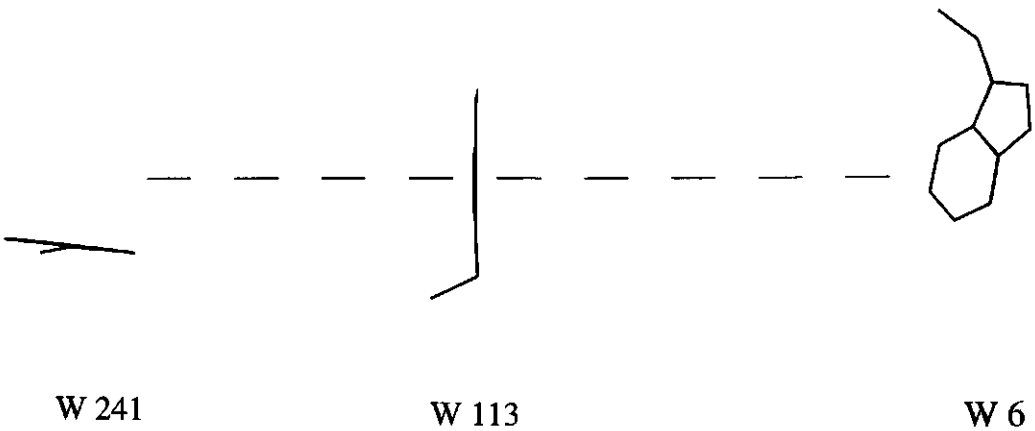

Fig. 6.2. The relative position of the aromatic side chains of the three tryptophans in Savinase. The plane through the tryptophans is perpendicular to the plane of the paper. In three dimensions, W113 is behind the paper. The inter-tryptophan distances are ≈28 ± 2 Å.

6.3. Principles of fluorescence

The sensitivity of fluorescence to dynamic processes inside proteins is a consequence of the relatively long lifetime of the first excited singlet state. During this 1-10 ns lifetime, a variety of processes can occur, including protonation or deprotonation, solvent relaxation, local conformational changes, and processes related to translational or rotational motion. This is in contrast with e.g. CD. On the time scale of CD (10^{-15} sec), the molecule and its environment are effectively static, allowing deduction of the *average* secondary structure.

The fluorescent Trp-residues can serve as a convenient and sensitive probe of the Trp-environment of the protein [27]. This is due to the sensitivity of the ^1L_a-excited state of the indole moiety of tryptophan to the mobility and polarity of its environment [28]. Apart from environmental factors, the complex fluorescence decay of Trp may be attributed to factors such as C_α-C_β bond rotamers [29] or superposition of Trp- and Trp-solvent-exciplex emissions [30].

The fluorescence of tryptophan residues in proteins has been first reviewed by Burstein et al. [31]. It has been shown that three discrete spectral classes of Trp-residues can be distinguished, one (class I) buried in nonpolar regions of the protein (spectral maximum position, λ_{em} = 330-332 nm, spectral band width at half maximum, $\Delta\lambda$=48-49 nm and average lifetime, τ=2.1 ns) and two on the surface. One of the latter is in limited contact with water (class II) which is probably immobilized by bonding to the macromolecular surface (λ_{em}=340-342 nm, $\Delta\lambda$=53-55 nm and τ=4.4 ns). The other (class III) is completely exposed to water (λ_{em}=350-353 nm; $\Delta\lambda$=59-61 nm and τ=5.4 ns). Intermediate values of $\Delta\lambda$ and λ_{em} give information about the presence of more than one Trp-class.

Since the Trp-environment in a protein is heterogeneous, the experimental fluorescence decay has been analyzed using a sum of exponential terms. The lifetimes and the relative amplitudes of each component could be associated with a particular protein conformation and with the relative population of each conformation, respectively.

When a protein in an aqueous environment changes its structure, it may, for example, involve a larger solvent exposure of a Trp-residue. This causes a larger extent of solvent-relaxation around the excited state which is observed as a red-shifted fluorescence [32-35]. In this way, the position and the shape of the emission spectrum and the sensitivity of the fluorescence to extrinsic quenchers give information about the physical exposure of Trp to the solvent [31, 33]. Depending on the degree of exposure, the fluorescence of Trp can be usually quenched by I^- or acrylamide. Any remaining fluorescence at high concentrations of quencher originates from Trp-residues which are not solvent-accessible. Hence, the fraction of buried and accessible residues can be deduced from a

so-called modified Stern-Volmer plot [34]. Furthermore, as the remaining fluorescence of a protein in the presence of a high amount of quencher originates from buried tryptophans, λ_{em} should be progressively shifted to lower values.

The fluorescence behaviour of tryptophan itself in aqueous solution [29, 30] and of Trp-residues in proteins [31, 35] are well described in the literature. An approach that is followed allows the resolution of the steady-state emission spectrum into components associated with a particular lifetime. It is found that short lifetime components emit fluorescence light at a low wavelength (i.e. the blue region) while the emission of longer lifetimes occurs in the red region of the spectrum. Hence, a larger exposure to the aqueous environment which favors the fractional contribution of the longer living components results in a red shift of the emission and an increased average lifetime. In addition, it is conceivable that the lifetime-values of the separate components show changes upon denaturation [36].

The photophysics of tryptophan itself [37], especially when embedded in a protein matrix [33], is intrinsically complex since the Trp-fluorescence is sensitive to a wide variety of environmental factors. The contacts between the indole moiety and water molecules, amino acid residues, peptide bonds or specific groups of the sorbent surface affect Trp-fluorescence. It is illustrative that the fluorescence of single-tryptophan containing proteins may decay multiexponentially. Because of all complexities involved, this study is not aimed at determining the precise conformation of the enzyme in the dissolved and the adsorbed state. Though, the strong sensitivity of fluorescence to the tryptophan environment enables us to conclude whether rearrangements in the protein structure upon adsorption occur or not.

6.4. Experimental

6.4.1. Protein

Apart from wild-type Savinase, a more structure labile T71A-mutant (T71 is an interior residue) was investigated. The mutation did not affect the direct environment of the three tryptophans. The denaturation temperature, which could be taken as a measure of the structural stability, is 65°C for the wild-type enzyme and 54°C for the mutant as inferred from differential scanning calorimetry at pH 8.5 [38]. Both the wild type and the T71A-mutant were inhibited with phenylmethanesulfonylfluoride (PMSF bound to Ser-221) to prevent autodigestion during the course of the experiment. The inhibition procedure and check on protein quality (purity and degree of inhibition) were described in section 3.6 and 5.2.

6.4.2. Sorbents and sample preparation

The sorbents used were a teflon latex (diameter d≈215 nm; density ρ=2.0 g cm^{-3}) and a silica suspension (Ludox HS40, d≈18 nm; ρ=2.2 g cm^{-3}) as described in section 5.2.3. The adsorption isotherms and the spectroscopic measurements were established at pH 8.0, T=20°C and I=10 mM in $Na_2B_4O_7$-buffer. The buffer preparation was described in section 3.6. The adsorption isotherms for PMS-Savinase on teflon and silica were demonstrated in Fig. 5.3a. The plateau values for teflon and silica are estimated to be 2.2 and 1.9 mg m^{-2}, respectively. Because of the small difference between those values, both plateau values are said to be 2 mg m^{-2}, which approximates surface saturation.
For the spectroscopic measurements the coverage Γ of the teflon surface by PMS-Savinase (and also by T71A) was adjusted while the total protein concentration was maintained at 0.10 g l^{-1}. To this end, the amount of teflon particles was varied between 0.25% w/w for Γ≈2 mg m^{-2} (=$\Gamma_{plateau}$ in the isotherm) and 1.40% for Γ=0.5 mg m^{-2}, according to the position on the adsorption isotherm. An analogous procedure was applied for the protein on silica. The equilibrium concentration of protein in solution (after 10 min contact time) at Γ≈2 mg m^{-2} was 0.025 g l^{-1} (75% of the protein adsorbed) while for Γ=0.5 mg m^{-2} practically all protein was adsorbed. The final buffer composition was the same as described for the adsorption isotherms. Sample volumes were 0.4 ml and 1 cm lightpath-cuvettes were used. The properties of the adsorbed protein are compared with those of the protein in aqueous solution.

6.4.3. Fluorescence quenching.

Quenching experiments were carried out using acrylamide as an uncharged quenching probe [36]. Quenching of the free protein was performed at concentrations of acrylamide (further denoted [Q]) between 0.015 and 0.70 M. The experiment was not carried out for the adsorbed protein as the adsorption equilibrium is likely altered upon acrylamide addition.

6.4.4. Steady-state fluorescence.

Emission spectra were recorded between 310 and 450 nm by an SLM-Aminco DMX-1000 spectrofluorimeter. The excitation wavelength was set at 300.0 nm in order to prevent excitation of tyrosine. Both excitation and emission slits were set at 4 nm bandwidth. The absorption- and emission spectrum of PMS-Savinase are sketched in Fig. 6.3.

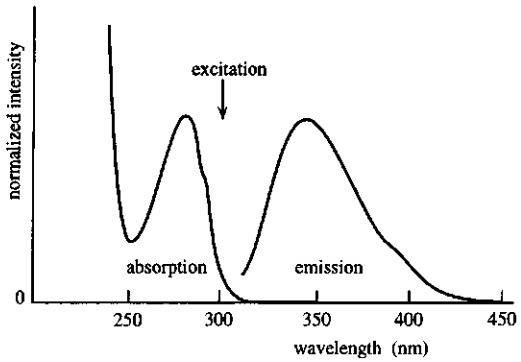

Fig. 6.3. Absorption- and emission spectrum of PMS-Savinase. Tryptophan was excited at 300 nm.

6.4.5. Time-resolved fluorescence

Measurements were carried out using a time-correlated photon counting set-up as described previously [10, 39], although a few exceptions were made. The reference compound to yield the dynamic instrumental response function of the set-up was para-terphenyl (PTF), dissolved in a mixture of 30% carbon tetrachloride and 70% cyclohexane, which was characterized by a 16 ps single exponential decay [40]. The excitation wavelength was set at 300.0 nm, while detection of emission light was at 348.8 nm. Per experimental decay 1024 channels of the multichannel analyzer were used with a time spacing of 25 ps per channel.

6.4.6. Analysis of time-resolved fluorescence data

The fluorescence decays (including the leading edge, i.e. the initial part of the curve ahead of the maximum) were analyzed with an exponential series using the commercially available maximum entropy method (MEM, Maximum Entropy Data Consultants, Cambridge, UK). The principle of MEM is described elsewhere [39, 41]. For the analysis of the total fluorescence decay into a distribution of lifetimes τ_i with amplitudes α_i, 100 equally spaced values on a $\log(\tau)$ scale between 0.1 and 10 ns were used. The initial distribution of $\alpha(\tau)$ versus τ was flat. The (second-order) average fluorescence lifetime, $<\tau_2>$, was calculated from the lifetime distribution according to:

$$<\tau_2> = \sum_{i=1}^{N} \alpha_i \tau_i^2 \Big/ \sum_{i=1}^{N} \alpha_i \tau_i \qquad (6.1)$$

where N is the number of exponential components in the distribution and the subscript 2 in τ_2 denotes the second-order character of the lifetime. It has been demonstrated that τ_2 reflects the true average time a fluorophore remains in the excited state [34]. The average lifetime $<\tau_2>$ will be further denoted τ.

In the anisotropy analysis one obtains a spectrum of amplitudes β against correlation times ϕ. In this case, the final image $\alpha(\tau)$ of the fluorescence decay was introduced as a fixed image in the analysis of the anisotropy decay. The recovery of $\beta(\phi)$ was obtained by starting with a flat distribution in log (ϕ) space between 0.1 and 100 ns. The integrated amplitude $\beta(\phi)$ corresponds with the initial anisotropy, R_0.

6.4.7. Circular Dichroism

CD spectra were recorded between 195 and 240 nm on a Jobin-Yvon Mark V dichrograph in cuvettes of 1 mm pathlength and analyzed for secondary structure using the Contin computer program supplied by S.W. Provencher (Max Planck Institute, Göttingen, Germany) [42]. The data in the region between 190 and 195 nm were given less weight in the analysis.

6.5. Results and Discussion

6.5.1. Solvent exposure in aqueous solution

The first target of the work was to obtain information about the water accessibility of the Trp-residues in Savinase. This was done since the water accessibility of these residues could be an important parameter for the structure of the protein. Molecular graphics studies showed that the three Trp-residues are lying underneath the protein surface and have a moderate water accessible surface area. This observation has now been tested by additional experiments.

The emission spectrum in Fig. 6.4, which has been corrected for Raman scattering of water, is characterized by a centre of gravity at λ_{em}=344 nm and a full width at half maximum $\Delta\lambda$=55 nm. The position and shape of the emission spectrum of PMS-Savinase suggest that the three tryptophans in the protein are all of the class II type and hence partly solvent-accessible. The value for λ_{em} at full exposure of the Trp-residues to

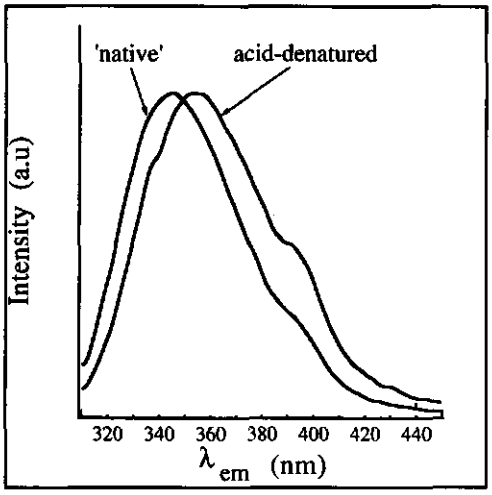

Fig. 6.4. Tryptophan-fluorescence emission spectrum of 'native' (i.e. at pH 8.0, I=0.01 M and T=20°C) and acid-denatured (pH 2) PMS-Savinase. The spectra have been normalized. Experimental conditions, see section 6.4.

the solvent may be inferred from the spectrum of acid denatured PMS-Savinase (Fig. 6.4). In aqueous solution of pH=2 (acidified with HCl) λ_{em}=356 nm which more or less agrees with the value given by Burstein [31] for completely exposed residues.

The solvent accessibility of the residues can be further determined by fluorescence quenching. The simple case is considered where two types of tryptophans are present in the protein, those on the protein molecular surface (with fractional contribution f_a) and those buried inside the protein matrix (with fractional contribution f_b; f_a+f_b=1). To elucidate the fraction of quencher-accessible tryptophans it is convenient to use a modification of the classical Stern-Volmer equation for dynamic collisional quenching [28].

$$\frac{\tau_0}{\tau_0 - \tau} = \frac{1}{f_a K[Q]} + \frac{1}{f_a} \qquad (6.3)$$

where τ_0 and τ are the average fluorescence lifetimes in the absence and the presence of quencher respectively, f_a the contribution to total fluorescence which is quenched and K the Stern-Volmer quenching constant. At very high infinite quencher concentration the excited surface residues are depopulated instantaneously and only the buried ones will be fluorescent.

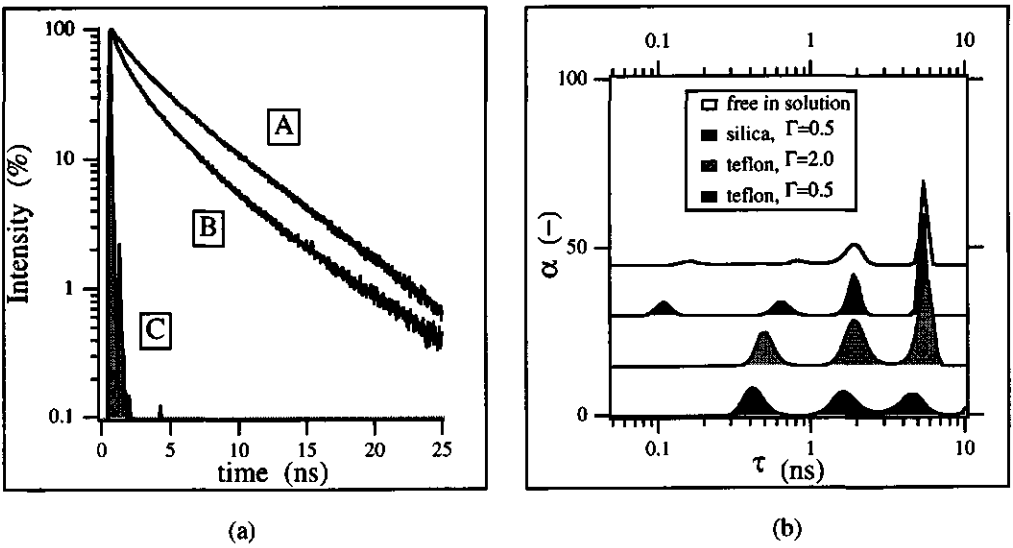

Fig. 6.5. (a) Fluorescence decay of PMS-Savinase, free in solution [A] and adsorbed on teflon (Γ=0.5 mg m^{-2}, [B]). Curve [C] is from the fast-decaying reference compound. (b) Fluorescence lifetime distribution of PMS-Savinase, in solution (χ^2=1.12), adsorbed on silica (Γ=0.5 mg m^{-2}, χ^2=0.98) and on teflon (at Γ=0.5 mg m^{-2}, χ^2=0.94 and at 2 mg m^{-2}, χ^2=1.00). Experimental conditions, see section 6.4.

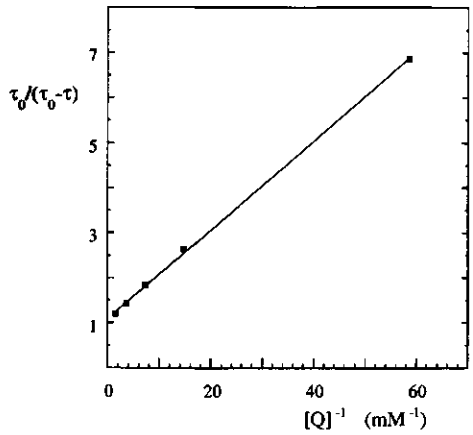

Fig. 6.6. Relationship between the fluorescence-lifetime τ of PMS-Savinase in solution and the concentration of acrylamide quencher [Q] as depicted in a modified Stern-Volmer plot. The lifetime without quencher is denoted τ_0. The tryptophan accessibility is calculated from the reciprocal intercept on the lifetime-axis. Experimental conditions, see section 6.4.

Hence, a plot of $\tau_0/(\tau_0-\tau)$ versus $[Q]^{-1}$ yields f_a from the reciprocal intercept. The experimental fluorescence decay of PMS-Savinase at pH 8.0 in aqueous buffer and its lifetime distribution are shown in Fig. 6.5a (curve A) and Fig. 6.5b, respectively. The distribution consists of four exponentials at 0.2, 0.8, 1.8 and 5.3 ns. The most important contribution (around 85 %) stem from the two longest lifetime components. The average lifetime τ of PMS-Savinase free in solution is 4.6 ns (σ_{n-1}=0.05; n=3). Fig. 6.6 shows a Stern-Volmer plot for PMS-Savinase in aqueous solution. From the intercept it follows that f_a=0.9. From a modified Stern-Volmer plot of the *individual* lifetime components, it follows that the reduction in fluorescence is due to the quenching of the two longest lifetime components.

As from above, the amount of quenched fluorescence does not correlate with a specific amount of exposed tryptophan-residues. This feature is particularly demonstrated in a protein like lysozyme. The molecule contains six Trp-residues, although the fluorescence originates for 80% from two residues [44]. In conclusion, it appears that all three tryptophan residues of PMS-Savinase are moderately solvent-accessible and the accessible surface area varies to some extent between the residues.

6.5.2. Average fluorescence lifetime

The fluorescence lifetime, τ is a valuable and reliable parameter for the environmental characteristics of the protein adsorbed on the particles. For the higher surface coverages ($\Gamma \geq 1.5$ mg m^{-2}) where the adsorbed amount is in equilibrium with a substantial amount of protein in solution, the fluorescence orginates from two distinct populations of protein molecules. The fluorescence lifetime of the adsorbed population has been calculated by subtracting the fluorescence contribution of the free population (i.e., 10% and 25% at Γ=1.5 mg m^{-2} and 2 mg m^{-2}, respectively) from total fluorescence (method not shown).

Fig. 6.7 illustrates τ for PMS-Savinase adsorbed at a varying surface occupation on both silica and teflon. The data at Γ=2 mg m^{-2} demonstrate that fluorescence of the adsorbed protein is not quenched by the silica- or teflon particles. Hence, the fluorescence quenching which is observed at Γ-values lower than 2 mg m^{-2} on teflon is attributed to another origin, probably related to structural rearrangements in the adsorbed protein molecules at the lower surface coverage. The average value of τ at Γ=2 mg m^{-2} is 4.5 ns (σ_{n-1}=0.01; n=2) which decreases to 4.0 ns (σ_{n-1}=0.12; n=3) at Γ=0.5 mg m^{-2} (→ curve B in Fig.6.5a). The average lifetime of the enzyme adsorbed on silica is more or less invariant with the surface occupation (τ=4.5 ns, σ_{n-1}=0.09; n=3).

The lifetime distribution of the adsorbed species on silica and on teflon are given in Fig. 6.5b. Apparently, there is a fixed distribution of protein conformers. At Γ=2 mg m^{-2} on

teflon the fractional contributions to the different conformations are more or less the same as for the protein in solution. At a lower surface occupation, the longer lifetime components become less populated at the benefit of conformations for which non-radiative processes are more efficient. Accordingly, a lower τ is obtained. Moreover, at Γ= 0.5 mg m^{-2} the conformational states are quenched to some extent. The picture of a fixed set of conformations may be oversimplified. For example, other conformations that start to prevail upon adsorption may give rise to similar values for the lifetime components. This statement holds as the fluorescence decay of the multiple-tryptophan containing lysozyme is resolved into only a double exponential [43]. Nevertheless, in view of the above, it appears that the enzyme molecule undergoes a conformational change on the teflon particle at a sufficiently low surface occupation.

6.5.3. Fluorescence anistropy

The anisotropy decays of PMS-Savinase both in aqueous solution and adsorbed on the various surfaces (at Γ=0.5 mg m^{-2}) are shown in Fig. 6.8. From the MEM-analysis of the anisotropy decay, a single correlation time of 11.4 ns (σ_{n-1}=0.3; n=4) for PMS-Savinase in solution has been applied. The single, long correlation time implies that the tryptophans rotate with the whole protein; there is no internal motion. By applying the Stokes-Einstein relation for the rotation of a spherical particle, the rotational correlation time ϕ is related to the protein hydrodynamic radius R_h:

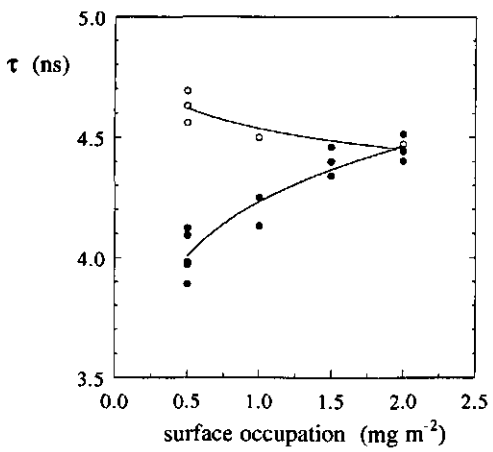

Fig. 6.7. Fluorescence lifetime τ of PMS-Savinase adsorbed on silica (○) and on teflon (●) as a function of the sorbent surface occupation of the protein. The fluorescence lifetime of dissolved PMS-Savinase is 4.6 ns. Experimental conditions, see section 6.4.

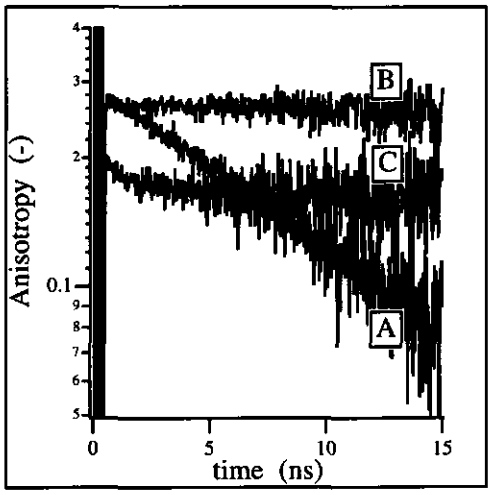

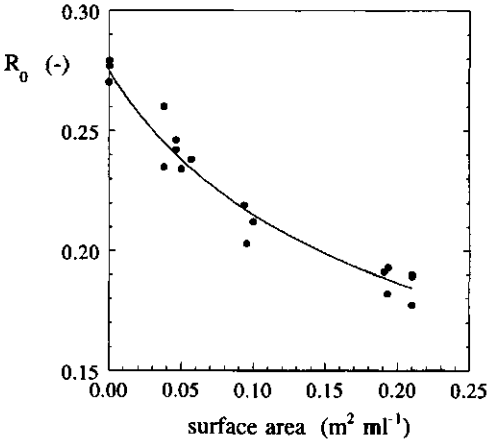

Fig. 6.8 (left). Fluorescence anisotropy decay of PMS-Savinase in solution [A], adsorbed on silica (Γ=0.5 mg m^{-2}, [B]) and on teflon (Γ=0.5 mg m^{-2}, [C]). Experimental conditions, see section 6.4.

Fig. 6.9 (right). Initial fluorescence anisotropy, R_0, as a function of the teflon surface area. The R_0 of PMS-Savinase free in solution is indicated as zero surface area. Experimental conditions, see section 6.4.

$$\phi_{protein} = 4\,\pi R_h^3\,\eta/(3\,k\,T) \qquad (6.4)$$

where k is the Boltzmann constant, T the temperature in Kelvin and η is the viscosity of the aqueous medium (0.890 mPa.s at T=298 K). Hence, the estimated R_h amounts to 2.3 nm which is in line with the reported value for the dehydrated molecule (radius, 2.1 nm). The finite value of the anisotropy at infinite observation time, R_∞, reflects the immobilized state of the protein on teflon and on silica. In all cases, where silica or teflon was present, $0.10 \leq R_\infty \leq 0.25$.

Further, from Fig. 6.8, it is observed that the initial anisotropy, R_0, for PMS-Savinase adsorbed on teflon (R_0=0.19) is lower as compared to that of PMS-Savinase adsorbed on silica or free in solution (R_0=0.27). The decreased R_0 on teflon could be attributed to several effects which may have been induced by a conformational change of the protein in the adsorbed state.

In Fig. 6.9, R_0 is plotted against the surface area of particles (=proportional to amount of particles) because the observed trend indicated that the decrease in R_0 is related to scattering of the fluorescence emission by the teflon particles [13, 14, 34]. It is observed that the initial anisotropy increases at an increasing amount of particles (at constant

protein concentration), which is expected on the basis of light scattering.

This view is supported by two other observations. First, R_0 at Γ=0.5 mg m^{-2} on teflon increases from 0.19 to 0.24 upon diluting the system by a factor 3. While the surface occupation remains more or less 0.5 mg m^{-2} upon dilution (due to the irreversibility of the adsorption), the amount of particles is three times as low. Thus, comparing with Fig. 6.9, the increase in R_0 is rationalized. The second observation is a decrease of R_0 from 0.27 to 0.25 when the surface occupation on silica ranges from 0.5 to 2 mg m^{-2} (data not shown). For silica, it is observed that light scattering increases significantly in the range where the surface occupation runs from 0.5 to 1.0 mg m^{-2}. Specifically, the negatively charged silica particle is electrostatically neutralized by adsorption of a sufficient amount of positively charged protein which induces iso-electric aggregation of the protein-covered silica. Hence, a lower R_0-value is found at higher surface concentration of proteins on silica. Adsorption-induced aggregation also holds for teflon but it already occurs at the low surface occupation as the particles have a low negative charge density. Moreover, the increase in scattering with teflon is much less because the particles have a relatively large size.

In conclusion, the initial anisotropy is modified by light scattering. Perhaps, R_0 also contains depolarizing contributions stemming from a conformational change, i.e. a changed intra- or intermolecular energy transfer or altered dynamics of the protein fluorophores. Yet, the occurrence of a conformational change has to be distinguished from other fluorescence characteristics.

The distribution of correlation times as obtained from the MEM-analysis of the experimental anisotropy decay (Fig. 6.8) is depicted in Fig. 6.10. The cases are considered for free PMS-Savinase (graph A, ϕ≈11.4 ns), for adsorbed enzyme on silica at Γ=0.5 mg m^{-2} (graph B) and on teflon at Γ=0.5 mg m^{-2} (graph C) and at 2 mg m^{-2} (graph D). It is observed that a significant amount of free protein is present at the high occupation (2 mg m^{-2}) on teflon. Qualitatively, this is in line with the equilibrium situation as inferred from the isotherm (Fig. 5.3a). A remarkable feature is the occurrence of shorter correlation times around 1 ns when the protein is adsorbed on teflon, irrespective of the surface occupation. For the protein adsorbed on teflon at low occupation (0.5 mg m^{-2}) this effect can also be observed qualitatively from the initial, relatively rapid anisotropy decay in Fig. 6.8 (curve [C]). Obviously, the tryptophans in the protein on teflon have a strong internal mobility.

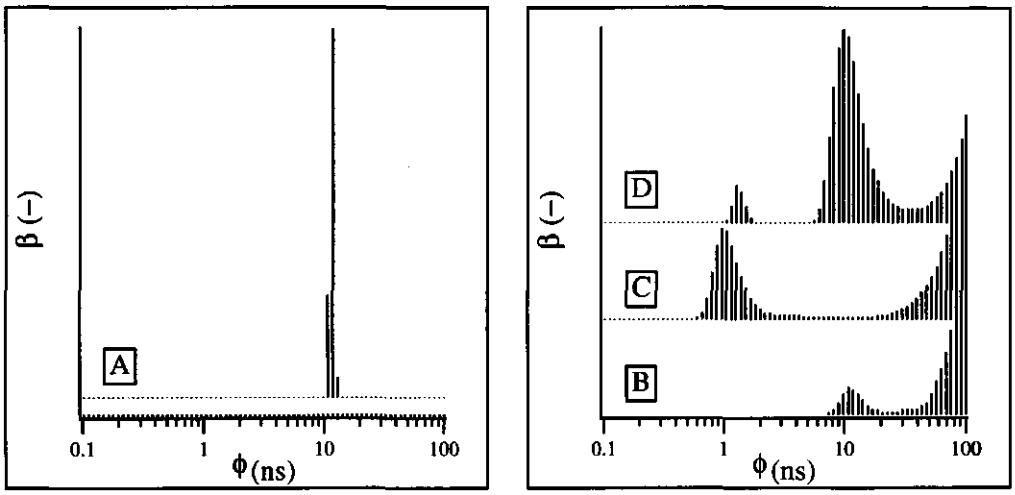

Fig. 6.10. Fluorescence anisotropy distribution. (a) PMS-Savinase free in solution ([A], χ^2=1.15). (b) PMS-Savinase adsorbed on silica (Γ=0.5 mg m^{-2} [B], χ^2=1.06) and on teflon (at Γ=0.5 mg m^{-2} [C], χ^2=0.98 and at Γ=2 mg m^{-2} [D], χ^2=1.05). Experimental conditions, see section 6.4.

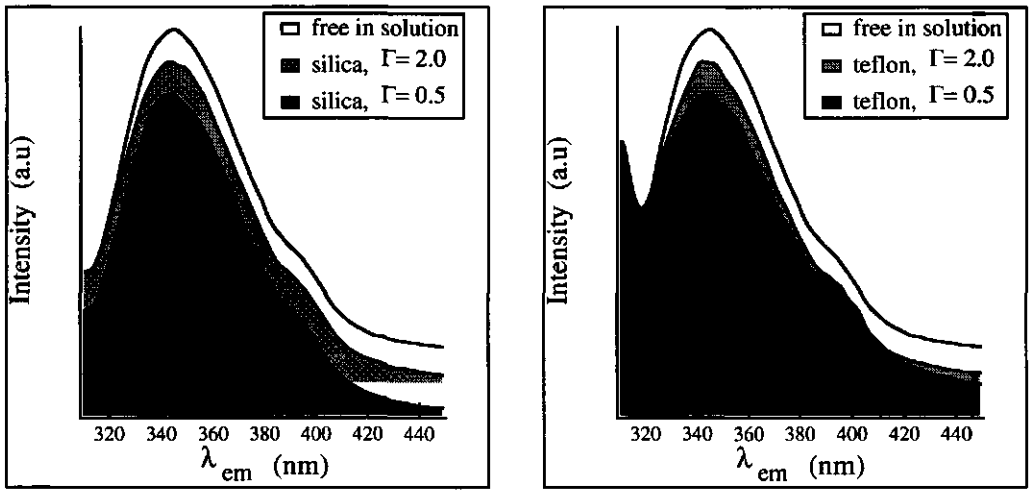

Fig. 6.11. (a) Emission spectra of PMS-Savinase in solution and adsorbed on silica at Γ=0.5 and 2 mg m^{-2}. (b) As (a), for teflon. Experimental conditions, see section 6.4.

The enzyme Savinase is recognized as a protein which has a relatively large structural stability [17, 38]. The classification of proteins as being "hard" or "soft" with respect to the structural stability on an interface [44] is fairly sound when the structural properties are measured on a hydrophilic surface, because soft proteins change their structure upon attachment at this type of surface. However, 'hard' proteins may change their structure considerably on hydrophobic surfaces as well [19, 44, 45]. Given the fluorescence lifetimes it appears from this study that PMS-Savinase remains intact upon adsorption on silica, but changes its structure upon adsorption on a hydrophobic teflon surface. However, at high protein occupation on teflon, PMS-Savinase has maintained its integrity, as inferred from the unchanged lifetime-value as compared to that in solution. It is probable that for high occupation on teflon the shorter internal rotational correlation time does not reflect extensive structural changes. Following this concept, the fluorescence properties of a more structure-labile mutant (T71A) have also been measured in solution and on silica at low occupation. The average lifetime of T71A in solution is 4.58 ns (σ_{n-1}=0.06; n=2) while the value for the adsorbed state is 4.63 ns (σ_{n-1}=0.09; n=2). It appears that the structural stability of T71A is not low enough to be disrupted by the silica surface. Moreover, the values of τ for T71A and the wild-type at the different surface occupations on teflon were similar. Hence, restricting ourselves to the rough classification of proteins as being either 'hard' or 'soft', both the wild-type and mutant are 'hard'. This may be valid as the denaturation temperature does not necessarily correlate with the sensitivity to surface denaturation. Nevertheless, the supposed discriminative action of a silica surface could just as well be put in perspective. Instead, it could be stated that both the structural stability of proteins and the denaturing force of the colloidal particle surface follow a gradual scale.

6.5.4. Steady-state fluorescence of adsorbed Savinase

The steady-state fluorescence characteristics of the adsorbed enzyme are briefly summarized in Fig. 6.11. Because of scattering of the tryptophan fluorescence by the suspended particles the measured intensities were different between the various experiments. Therefore, the fluorescence intensity has been normalized. It appears that the centre of gravity of the fluorescence emission (λ_{em}) is independent of the type of particle used and also independent of the surface coverage. Obviously, adsorption of the protein does not change the polarity of the tryptophan environment.

Altogether, the fluorescence data as described in 6.5.1. through 6.5.4. demonstrate the occurrence of a conformational change of PMS-Savinase at low surface coverage on

teflon. The conformational change does not involve a change in the polarity of the environment of the tryptophan residues, as inferred from the unaltered value for λ_{em}. The quenched excited state suggests that the residues have changed their interactions with the protein matrix.

6.5.5. Circular dichroism

CD experiments have been performed in order to establish the overall secondary structure of PMS-Savinase in solution and adsorbed on the different surfaces. Except for silica, the spectra (without protein) are virtually zero. The silica particles have a significant amount of CD in the far UV region, but this background effect has been subtracted as well as possible. Fig. 6.12 presents typical fitted CD spectra as well as the weighted residuals between experimental and fitted curves. The results of the calculation of the α-helix and β-sheet content are given in Table 6.1.

In solution the measured amount of α-helix and β-sheet is roughly according to the crystallographic data (31% and 19%, respectively). At high occupation on teflon, the structure is not altered while the protein increases its amount of α-helix at a lower Γ (amount of β-sheet not changed). The same trends are observed for T71A-S (data not shown). It should be noted that the use of teflon particles is a fundamental improvement since the secondary structure of proteins adsorbed on hydrophobic interfaces can now be unambiguously established. In earlier studies this was not possible. On silica the α-helix content is decreased at a lower Γ while the amount of β-sheet has increased. The determined structure at low surface occupation on silica contradicts the observations made in chapter 3 for PMS-Savinase on silica. It could be argued whether the effect is significant or whether it is due to some artifact, caused by the CD of the silica particles themselves. Although it has not been measured, it is likely that the determined structure of PMS-Savinase at high occupation on silica (at low amount of silica) is identical to that in solution.

The increased α-helix content on hydrophobic surfaces sheds new light on the conformational state of the adsorbed protein [17] and possibly on that of other proteins as well. A decrease in the α-helix content is generally found for proteins adsorbing on a hydrophilic silica surface. It also contradicts the general assumption that denaturation of proteins on interfaces implies unfolding. In earlier literature it was reported that α-helix structures from synthetic polypeptides are stable when they reside in the air-water interface [46]. A number of inner membrane proteins also contain a large amount of α-helix in the parts that reside in the hydrophobic layers of membrane. For example,

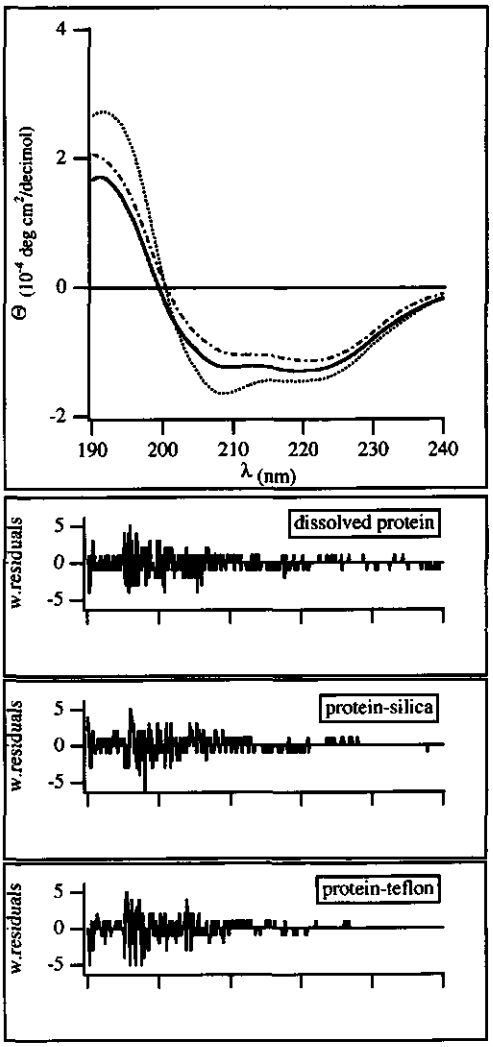

Fig. 6.12. (a) Molar residual ellipticity Θ of PMS-Savinase free in solution (solid line), adsorbed on silica (Γ=0.5 mg m^{-2}, ----------) and on teflon (Γ=0.5 mg m^{-2}, ··········) and weighted residuals (indicating a very low noise). (b) Blank curves (without protein) for the samples of (a), i.e. buffer, buffer+silica, buffer+teflon (=lower curve).

Table 6.1.
Secondary structure content from CD spectra of PMS-Savinase free in solution and adsorbed on different sorbent surfaces at a varying surface occupation.

	FREE		TEFLON		SILICA	
	α-helix	β-sheet	α-helix	β-sheet	α-helix	β-sheet
	35	26				
Γ						
2			36	24	-	-
1.0			47	28	27	33
0.5			50	26	20	47

bacteriorhodopsin that uses the energy of light to pump protons across the membrane of *Halobacterium halobium*, contains seven transmembrane α-helices [47]. Another example is Colicin A which is a protein that kills *E. coli* cells. When the protein comes into contact with the host cell it spontaneously forms ten α-helices in the cell membrane which are believed to be functional with respect to the antibiotic action [6, 48]. From so called hydropathy plots it is inferred that the α-helices in membranes have a relatively large amount of hydrophobic amino acid residues. This was also inferred for the α-helices in native Savinase (section 2.4). It appears that the formation of α-helices is due to an optimization of the interaction of the hydrophobic side chains and the hydrophobic environment. Thus, the increase in α-helix content of PMS-Savinase onto a teflon particle may be rationalized by the formation of these secondary structures close to the hydrophobic surface.

In other work [17] it is claimed that PMS-Savinase does not undergo structural changes upon adsorption on a hydrophobic surface, irrespective of the adsorption conditions. The results of the CD- and fluorescence measurements as described in this chapter strongly oppose this statement. Additionally, it is important to define denaturation or, for that matter, to define structure. Each technique such as calorimetry, proton titration, infrared, CD, fluorescence, NMR, etcetera, measures specific aspects of the protein structure. Hence, it depends on the applied technique and its sensitivity in relation to the investigator's definition whether or not structural rearrangements are inferred.

6.6. Conclusions

In the case of fluorescence it has been reasoned that the average excited-state lifetime and short internal rotational correlation times are indicative parameters for structural changes in PMS-Savinase. The lifetime of the excited state of PMS-Savinase at monolayer coverage on teflon and at all surface occupations on silica equals that of the enzyme in solution. The lifetime decreases upon a decreasing coverage on the teflon surface. A short internal rotational correlation time is found for PMS-Savinase on teflon, irrespective of the surface coverage. The far UV CD spectrum of the protein at full surface occupation on teflon was not influenced by adsorption. At a decreasing surface coverage the α-helix content of the protein increases on teflon.

Acknowledgements

The facilities are kindly offered by the Dept. of Molecular Physics and the Dept. of Biochemistry of the Wageningen Agricultural University. The co-authors of the paper are gratefully acknowledged for the many valuable discussions.

References

1. Rietveld, A., Ponjee, G.A.E., Schiffers, P. Jordi, W., van de Coolwijk, P.J.F.M., Demel, R.A., Marsh, D. and de Kruijff, B., Biochim. Biophys. Acta 818, 398-409 (1985).
2. Sidorowicz, A. and Michalak, K., Studia Biophys. 108, 133-139 (1985).
3. John, E. and Jähnig, F., Biophys. J. 54, 817-827 (1988).
4. Peng, K., Visser, A.J.W.G., van Hoek, A., Wolfs, C.J.A.M. and Hemminga, M.A., Eur. Biophys. J. 18, 285-293 (1990).
5. Jongh, de H.H.J. and de Kruijff, B., Biochim. Biophys. Acta 1029, 105-112 (1990).
6. Suga, H., Shirabe, K., Yamamoto, T., Tasumi, M., Umeda, M., Nishimura, C., Nakazawa, A., Nakanishi, M. and Arata, Y., J. Biol. Chem. 266, 13537-13543 (1990).
7. Vincent, M. and Gallay, J., Eur. Biophys. J. 20, 183-191 (1991).
8. González-Mañas, J.M., Lakey, J.H. and Pattus, F., Biochemistry 31, 7294-7300 (1992).
9. Mosmuller, E.W.J., Pap, E.H.W., Visser, A.J.W.G. and Engbersen, J.F.J., Biochim. Biophys. Acta 1189, 45-51 (1994).
10. Pap, E.H.W., Bastiaens, P.I.H., Borst, J.W., van den Berg, P.A.W., van Hoek, A., Snoek, G.T., Wirtz, K.W.A. and Visser, A.J.W.G., Biochemistry 32, 13310-13317 (1993).
11. Vincent, M., Deveer, A, de Haas, G.H., Verheij, H.M. and Gallay, J., Eur. J. Biochem. 215, 531-539 (1993).
12. Visser, A.J.W.G., van Engelen, J., Visser, N.V., van Hoek, A., Hilhorst, R. and Freedman, R.B., Biochim. Biophys. Acta 1204, 225-234 (1994).
13. Teale, F.W.J., Photochem. Photobiol. 10, 363-374 (1969).
14. Lentz, B.R., Moore, B.M. and Barrow, D.A., Biophys. J. 25, 489-494 (1979).
15. Soderquist, M.E. and Walton, A.G., J. Colloid Interface Sci. 75, 386-397 (1980).

16. Norde, W., MacRitchie, F., Nowicka, G. and Lyklema, J., J. Colloid Interface Sci. 112, 447-456 (1986).
17. Duinhoven, S., Poort, R., Van der Voet, G., Agterof, W.G.M., Norde, W. and Lyklema, J., J. Colloid Interface Sci. 170, 340-350 (1995).
18. Sato, H., Tomiyama, T., Morimoto, H. and Nakajima, A., in: *Proteins at Interfaces*, ACS Symposium Series 343 (J.L. Brash and T.A. Horbett, Eds), Washington D.C., p. 76-87, 1987.
19. Norde, W. and Favier, J.P., Colloids and Surfaces 64, 87-93 (1992).
20. Kondo, A., Oku, S., Murakami, F. and Higashitani, K., Colloids and Surfaces (B) 1, 197-201 (1993).
21. Walton, A.G. and Maenpa, F.C., J. Colloid Interface Sci. 72, 265-278 (1979).
22. Tan, J.S. and Martic, P.A., J. Colloid Interface Sci. 136, 415-431 (1986).
23. Kondo, A., Oku, S., Murakami, F. and Higashitani, K., Biotechn. Bioeng. 40, 889-894 (1992).
24. Betzel, C., Klupsch, G., Papaendorf, G., Hastrup, S., Branner, S. and Wilson, W.S., J. Mol. Biol. 223, 427-445 (1992).
25. Siezen, R.J., Vos, W.M. de, Leunissen, J.A.M. and Dijkstra, B.W., Protein Engineering 4, 719-737 (1991).
26. Steinberg, I.Z., Ann. Rev. Biochem. 40, 83-114 (1971).
27. Prendergast, F.G., Bajzer, Z., Axelsen, P.H. and Haydock, C., in: *Proteins* (V. Renugoplakrishnan, Ed.), p. 208-219, ESCON, Leiden, The Netherlands.
28. Demchenko, A.P., *Ultraviolet Spectroscopy of Proteins*, Springer-Verlag Berlin Heidelberg, p.166, 1986.
29. Szabo, A.G. and Rayner, D.M., J. Am. Chem. Soc. 102, 554-563 (1980).
30. Vekshin, N., Vincent, M. and Gallay, J., Chem. Phys. Letters 199, 459-464 (1992).
31. Burstein, E.A., Vedenkina, N.S. and Ivkova, M.N., Photochem. Photobiol. 18, 263 (1973).
32. Gabel, D., Steinberg, I.Z. and Katchalski, E., Biochemistry 10, 4661-4669 (1971).
33. Eftink, M.R. and Ghiron, C.A., Biochemistry 15, 672-680 (1976).
34. Lakowicz, J.R., *Principles of Fluorescence Spectroscopy*, Plenum Press New York and London, p.134, 1983.
35. Beechem, J.M. and Brand, L., Ann. Rev. Biochem. 54, 43-71 (1985).
36. Kieleczawa, J., France, L.L., Sutherland, J.C. and Hind, G., Arch. Biochem. Biophys. 298, 63-69 (1992).
37. Creed, D., Photochem. Photobiol. 39, 537-562 (1984).
38. Pedersen, J.T., Olsen, O.H., Betzel, C., Eschenburg, S., Branner, S. and Hastrup, S., J. Mol. Biol. 242, 193-202 (1994).
39. Bastiaens, P.I.H., van Hoek, A., Benen, J.A.E., Brochon, J.C. and Visser, A.J.W.G., Biophys. J. 31, 839-853 (1992).
40. Visser, N.V., Visser, A.J.W.G., Konc, T., Kroh, P.V. and van Hoek, A., in: *Time-resolved laser spectroscopy in biochemistry IV* (J.R. Lakowicz, Ed.), Proc. SPIE (Intern. Soc. Opt. Eng.), Bellingham, Washington Vol. 2137, 618-626,1994.
41. Livesey, A.K. and Brochon, J.C., Biophys. J. 52, 693-706 (1987).
42. Provencher, S.W. and Glockner, J., Biochemistry 20, 33-337 (1981).
43. Imoto, T., Forster, L.S., Rupley, J.A. and Tanaka, F., Proc. Natl. Acad. Sci. USA 69, 1151-1155 (1971).
44. Norde, W. and Lyklema, J., J. Biomater. Sci. Polymer Edn. 2, 183-202 (1991).
45. Haynes, C.A. and Norde, W., J. Colloid Interface Sci. 169, 313-328 (1995).
46. Malcolm, B.R., Adv. Chem. Ser. 145, 338-359 (1975).
47. Kyte, J. and Doolittle, R.F., J. Mol. Biol. 157, 105-132 (1990).
48. Parker, M.W., Pattus, F., Tucker, A.D. and Tsernoglou, D. Nature 337, 93-96 (1989).

Chapter 7

Kinetic analysis of surface-enhanced autodigestion

Abstract

The experimental data on solution- and hydrophobic inactivation described in chapter 5 are subjected to kinetic analysis aiming at the possible occurrence of a conformational change. The experimental inactivation data of Savinase have been extended to two other types of teflon latices besides the one discussed in chapters 5 and 6. The latices behave differently with respect to the plateau value of protein adsorption.

A model for surface-enhanced autodigestion has been developed and involves transport and attachment of the enzyme to the particle surface as well as processes that describe the chemical conversion of the molecule. By analytical or numerical simulation, the effect of each step in the model is investigated. The order of the inactivation reaction with respect to time is a useful parameter to assess any conformational change. Following this method and considering the distinction in deactivation behaviour between the different latices it is concluded that the hydrophobic inactivation data carry the information of a rate-increasing conformational change.

7.1. Introduction

In chapter 5 it has been deduced that inactivation of Savinase is due to autodigestion irrespective of the type of the system in which inactivation takes place. However, the rate at which the autodigestion occurs does depend on the nature of the system. For instance, it has been demonstrated that silica and PS-B protect the enzyme from inactivation as compared to that in solution. On the other hand, rapid deactivation is observed in systems containing particles that have hydrophobic surface properties, such as polystyrene- or teflon latex (Fig. 5.4a). The intention of the analysis in this chapter is to obtain a better understanding of the kinetics of the rapid inactivation on hydrophobic particles.

From earlier results it has been inferred that adsorption on a hydrophobic surface renders the adsorbed protease susceptible to proteolytic attack by the remaining non-adsorbed fraction of the enzyme (route a, Fig. 5.1). A provisional explanation is that autolytic susceptibility is induced by a conformational change incurred by the protein upon adsorption on the hydrophobic surface. The occurrence of such a conformational change is now tested by analyzing the kinetics of inactivation. To this end, a model for the inactivation of a proteolytic enzyme is proposed taking into account a conformational change.

In earlier literature on surface-enhanced autodigestion the observed inactivation has been ordinarily fitted to a first- or second order decay with respect to time [1, 2]. Then, the order of the inactivation was supposed to originate from a rate-controlling conformational change or complexation. The possibility of mixed kinetics (by processes which are separated in space or which occur subsequently in time or which have a similar rate) has not been considered. Neither was the idea considered that the rate of inactivation could be determined by the rate of transport towards the surface. In the model, to be presented, each individual step will be carefully examined.

Information on the rate of a conformational change in autodigestion can only be obtained when the conformational change is the rate-limiting step in the autodigestion. As the rate parameters of the various transitions are not known (if they were, the answer to the question would already been given) it is important that the conformational change is characterized by a unique order. Yet, if the order would show similarity to that of any of the other steps in the process and also to the obtained experimental order, the information would be ambiguous. A few additional experiments on hydrophobic inactivation will be introduced which will also be analyzed on the basis of the adopted model.

7.2. A model for autodigestion

Several stages may be distinguished in surface-enhanced autodigestion. The first stages involve the supply of native enzyme E to the surface, i.e. transport and attachment. The transport occurs via diffusion and convection to the interfacial layer, where the enzyme is denoted E_i in Fig. 7.1. The attachment is characterized by the adsorption equilibrium between E_i and the adsorbed species E^*. The subsequent stages include conversion processes on the surface of the particle, i.e. denaturation of E^* into a structurally changed form D, the association of the proteolytically susceptible species D with E_i and finally disintegration of the protein.

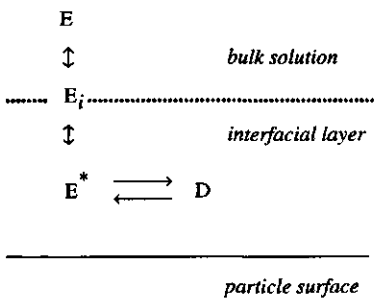

Fig. 7.1. Schematic picture of transport, attachment and denaturation of a protein in a colloidal system, see text for explanation.

In the transport-limiting situation, the rate of autodigestion would be governed by diffusion and convection. In a stationary state of inactivation the flux $J_e(R)$ of enzyme towards the surface of a colloidal particle (i.e., at $r=R$; r is distance from the centre of the particle and R is its radius) equals the flux from bulk solution, $J_e(b)$ (Eq. 7.1).

$$J_e(R) = J_e(b) \tag{7.1}$$

The bulk solution is depleted according to:

$$J_e(b) = \frac{V}{A}\frac{dc}{dt} \tag{7.2}$$

where V is the volume, A the total surface area in the system and t is time. The symbol c denotes the enzyme concentration. The flux towards the surface $J_e(R)$ is described by Fick's first law:

$$J_e(R) = - D \frac{\partial c}{\partial r} \qquad (7.3)$$

where $c = c(r,t)$ and D is a constant diffusion coefficient.

Eq. 7.3 should be put in perspective since J_e is defined as a flux with respect to a *plane of reference*, e.g. the wall of the particle. However, the diffusion coefficient of a molecule is per definition mutual, i.e. its magnitude depends on the backdiffusion of the molecules that are displaced. Hence, transport of a protein to the particle surface during autodigestion is not necessarily characterized by a displacement of water molecules. Specifically, fragments are produced on the particle surface as a result of autodigestion. If the fragments adsorb on the surface immediately after hydrolysis and if they cannot be released from the surface through displacement by enzymes, the process of inactivation will be hindered. Obviously, this is not the case, as inactivation was found to be complete within the timescale of the experiment (Fig. 5.6a).

In order to investigate the validity of Eq. 7.3 for this case, the quantity j_e is introduced which is the flux with respect to the *centre of gravity* of diffusing molecules. Hence, in a stationary state, the flux of enzymes towards the surface, j_e, must be equated to the backflux of desorbed fragments (j_f). Accordingly, it is stated that $j_e+j_f=0$ which enables us to find a new expression for $J_e(R)$. For that, the following relations are applied:

$$j_e = (\upsilon_e - \bar{\upsilon}).c_e \qquad J_e(R) = \upsilon_e.c_e \qquad J_f(R) = \upsilon_f.c_f$$

$$J_f(R) = -n.J_e(R) \qquad c_e = c.x_e \qquad c = c_e + c_f$$

$$\bar{\upsilon} \equiv (\upsilon_e c_e + \upsilon_f c_f) / (c_e + c_f) \qquad (7.4)$$

where υ is the diffusional velocity of matter, $\bar{\upsilon}$ is the drift of the ensemble of molecules, c is the concentration of diffusing molecules, x is the molar fraction, n is the stoichiometric coefficient for the overall chemical conversion $E \rightarrow n.F_i$ (E and F_i as well as the subscripts e and f denote enzyme and fragments, respectively). According to definition:

$$j_e = - D \frac{\partial c_e}{\partial r} \qquad (7.5)$$

The more general expression for $J_e(R)$ can thus be derived from Eqs. 7.4 and 7.5:

$$J_e(R) = - D\left[\frac{1}{1+(n-1)x_e}\right]\frac{\partial c_e}{\partial r} \qquad (7.6)$$

Thus, for n=1, i.e. considering diffusion on a weight basis, Eq. 7.6 is reduced to Eq. 7.3, although the value of D for the arriving enzymes could be lower than that in pure aqueous solution. The flux $J_e(R)$ in Eq. 7.3 is obtained by applying the diffusion equation for spherical diffusion [3]:

$$\frac{\partial c}{\partial t} = -\frac{\partial J_e}{\partial r} = D\left[\frac{\partial^2 c}{\partial r^2} + \frac{2}{r}\frac{\partial c}{\partial r}\right] \qquad (7.7)$$

Using χ=$c.r$, an equation mathematically equivalent to that for linear flow is obtained. Surface-enhanced autodigestion is a result of a heterogeneous reaction for which a well chosen boundary condition leads to the solution to the transport-limited case. In a transport-limited situation, the protein molecules have relatively short time of contact with the surface. The products of the chemical reaction, i.e. the fragments, are rapidly released. Hence, the boundary condition in the system is: c=0 at r=R (t>0). Using Laplace transformation of Eqs. 7.3 and 7.7 and considering a finite value of the bulk concentration c at t=0, the solution of J_e (R) becomes:

$$J_e(R) = D\,c\left(\frac{1}{[\pi.D.t]^{1/2}} + \frac{1}{R}\right) \qquad (7.8)$$

which for $t >> R^2/(\pi D)$ (D≈10^{-10} m^2 s^{-1} in aqueous solution and $R \approx 10^{-7}$ m) is reduced to:

$$J_e(R) = \frac{D}{R}.c = m_d.c \qquad (7.9)$$

The quantity m_d (=D/R) can be seen as the time-independent mass transfer coefficient for spherical diffusion. Substitution of Eqs. 7.2 and 7.9 in Eq. 7.1 and subsequent integration gives:

$$c = c_0\, e^{-b\,t} \qquad (7.10)$$

where c_0 is the initial bulk concentration and b=$m_d A/V$. Thus, for *transport-limited autodigestion* the inactivation reaction appears to be *first-order* with respect to time.

For linear transport, i.e. when $t >> R^2/(\pi D)$ in Eq. 7.8, it has been demonstrated that the flux becomes independent of time when natural or forced convection is considered [4]. Physically, this means that a constant supply of molecules prevents the diffusion layer from growing in time. Therefore, $J_e(R)$ should also be time-independent for spherical transport. Further, when considering convection, a mass transfer coefficient m should replace m_d in the expression for b in Eq. 7.10. The quantity m can be estimated from the Sherwood number (Sh). The Sh number is the ratio of diffusional resistance to total transport resistance:

$$Sh = \frac{1/m_d}{1/m} = \frac{m}{m_d} = \frac{m}{(D/R)} \tag{7.11}$$

Usually, Sh is calculated from the dimensionless Reynolds- (Re) and Schmidt (Sc) numbers. In systems where the flow conditions are not well-defined, empirical relations can be used. For convection around solid spheres an acceptable empirical expression is [5]:

$$Sh = 1 + p.Re^q Sc^r \tag{7.12}$$

With empirically determined values for p, q and r, the mass transfer coefficient m can be established from Eqs. 7.11 and 7.12. It suffices to state here that for convection $m > m_d$ ($Sh > 1$) which renders mass transport more efficient. The order of the transport is not affected.

Next, the equations that describe adsorption (Eq. 7.13), denaturation (Eq. 7.14) and autodigestion (Eq. 7.15) are given.

$$E \underset{k_d}{\overset{k_a}{\rightleftharpoons}} E^* \tag{7.13}$$

$$E^* \underset{k_{-0}}{\overset{k_{+0}}{\rightleftharpoons}} D \tag{7.14}$$

$$E + D \underset{k_{-1}}{\overset{k_{+1}}{\rightleftharpoons}} ED \xrightarrow{k_{+2}} E + 2F_i \tag{7.15}$$

where k_a, k_d, k_{+0}, k_{-0}, k_{+1}, k_{-1} and k_{+2} are the rate constants for adsorption, desorption, denaturation, renaturation, association, dissociation and disintegration, respectively.

Equation 7.15 corresponds with the Michaelis Menten model for enzyme kinetics. At each time the activity is interpreted as stemming from E and ED. The ED-complex is assumed to dissociate upon assaying (either to the right or to the left in Eq. 7.15), producing one active E species.

A simple model of adsorption would be to assume that the rate of attachment is a second-order process. Thus, the rate of adsorption is proportional to the concentration of free enzymes near the interface, $[E_i]$, and to the concentration of surface sites which are available for adsorption $\{N-([E^*]+[D]+[ED])\}$. The symbol N stands for the total surface area relative to the total amount of protein molecules minus the surface area that is occupied by the proteins (hence, $0<N<1$). The rate of desorption is supposed to be proportional to the concentration of $[E^*]$ instead of the total amount of adsorbed species. Specifically, structural changes usually render the adsorption irreversible [6].

The model has Langmuir characteristics and it also includes additional features. The Langmuir premises involve the absence of an activation energy when the surface is replenished with adsorbate. Furthermore, each collision between an arriving molecule and the bare surface leads to adsorption. It is assumed that the energy of adsorption is independent of the surface occupation and that the adsorbed molecules are in dynamic equilibrium with the molecules in solution. In addition to Langmuir, it is implicitly stated that the occupied surface area of E^*, D and ED are similar. This assumption is reasonable when conformational changes are minor. Further, the model implicitly states that once the fragments are formed they are desorbed from the surface. This may not necessarily be true for large initial fragments, but it is certainly the case for the final autolysate (Fig. 5.6a).

In spite of the above-mentioned physical restrictions, the chosen model for adsorption is useful to describe the rate of immobilization. Likewise, using this type of description, the boundary of the maximal amount of adsorbed protein, which was experimentally imposed (section 5.2.6, $N=0.25$), is mathematically realized. When $[E^*]+[D]+[ED]$ has reached the maximum value of 0.25, further adsorption is impeded. Hence, the rate equations for the concentrations of E, E^*, D and ED become:

$$\frac{d[E]}{dt} = -k_a[E]\{N - ([E^*] + [D] + [ED])\} + k_d[E^*] - k_{+1}[E][D] + (k_{-1} + k_{+2})[ED] \quad (7.16)$$

$$\frac{d[E^*]}{dt} = +k_a[E]\{N - ([E^*] + [D] + [ED])\} - (k_d + k_{+0})[E^*] + k_{-0}[D] \quad (7.17)$$

$$\frac{d[D]}{dt} = + k_{+0}[E^*] - k_{-0}[D] - k_{+1}[E][D] + k_{-1}[ED] \quad (7.18)$$

$$\frac{d[ED]}{dt} = + k_{+1}[E][D] - (k_{-1} + k_{+2})[ED] \quad (7.19)$$

The loss of intact protein molecules into the smaller fragments F_i (Eq. 7.20) is obtained by summing of Eqs. 7.16 through 7.19.

$$\frac{d[E]}{dt} + \frac{d[E^*]}{dt} + \frac{d[D]}{dt} + 2 \cdot \frac{d[ED]}{dt} = -k_{+2}[ED] \quad (7.20)$$

Given the value for k_{+2}, the rate of autodigestion is determined by [ED]. The rate of activity loss, however, is determined by the extent to which the adsorption is out of 'equilibrium' (Eq. 7.21).

$$\frac{d[E]}{dt} + \frac{d[ED]}{dt} = -k_a[E]\{N - ([E^*] + [D] + [ED])\} + k_d[E^*] \quad (7.21)$$

Autodigestion in bulk solution is described analogous to Eqs. 7.14 and 7.15 when E^* is replaced by E. From the set of equations that can easily be derived, it appears that autodigestion is also determined by the magnitude of [ED], while the rate of activity loss is determined by the relaxation of the conformational transition.

7.3. Experimental intermezzo

In addition to the experiments described in chapter 5, the surface occupation is introduced as an experimental variable. Apart from the original teflon latex (see chapter 5), two other types of teflon latices have become available by dialysis of the original one. It was observed that after dialysis the amount of protein adsorbed was reduced

(Fig. 7.2). The reduced plateau value of protein adsorption is assumed to be caused by the removal of carboxylated stabilizers that were non-covalently bound to the original particles. As a result the negative surface charge was reduced, thereby decreasing electrostatic attraction between the protein and the teflon surface (pH < IEP). Teflon latices which are obtained in this way are denoted teflon H(igh), M(edium) and L(ow) according to the comparative level of protein adsorption (Γ= 2.1, 1.5 and 1.1 mg m^{-2}, respectively). Hence, the variation in plateau value is recognized as an important parameter in the analysis of the kinetic data. Specifically, it has been demonstrated in chapter 6 that the level of adsorption correlates with the degree of structural rearrangements of the adsorbed protein. At lower surface occupations, the structural change is more pronounced. If the observed structural change at the lower occupations makes the protein more susceptible to autodigestion, this should be observed by increased inactivation.

Adsorption- and inactivation experiments have been performed according to procedures that are described in sections 5.2.4 and 5.2.5. In order to maintain a constant degree of depletion from bulk solution (25%) at the beginning of inactivation the amount of particles added is adjusted. The results on hydrophobic inactivation (together with inactivation for PS-A and in solution) are given in Fig. 7.3. At first sight there seems to be significant differences in the half-life of the enzymatic activity between the hydrophobic systems, although this effect could be due to variations in the "initial" activity (<75%). The data will be subjected to a more detailed analysis in the next section.

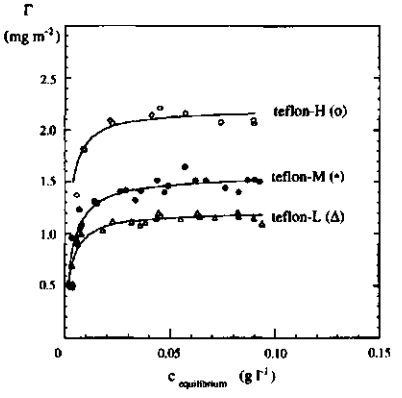

Fig. 7.2. Adsorption of PMS-Savinase on Teflon H, M and L at pH 8, I=0.01, T=20°C.

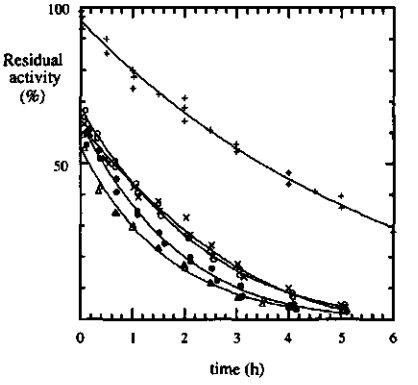

Fig. 7.3. Solution- (+) and hydrophobic [PS.A (x), teflon H (○), M (●)and L (Δ)] inactivation of WT-Savinase at pH 8, I=0.01, T=20°C.

7.4. Kinetic analysis

7.4.1. Hydrophobic inactivation

It turns out impossible to arrive at analytical solutions of Eq. 7.20 or 7.21, unless we make steady-state assumptions of the protein species 'a priori'. Hence, the simulation will be performed by numerical integration [7]. The values for the parameters have been chosen on the basis of standard enzyme kinetics, although arbitrary values could be chosen as well for the purpose of this chapter. For the simple case of adsorption (N=0.25, k_a=50, k_d=1) and subsequent denaturation (k_{+0}=0.2, k_{-0}=0), Figs. 7.4a (k_{+1}=0) and 7.4b (k_{-0}=2000, k_{+1}=1.10^6, k_{+2}=50) show numerical results for the decrease of ([E]+[ED]), i.e. the decrease of activity. When k_{+1}=0 it is observed that the amount of E* increases to almost full surface coverage and then decreases to produce D. When D is converted into fragments as soon as it is formed (Fig. 7.4b), E* arrives in a stationary state. Apparently, surface area which has become available for adsorption is instantaneously replenished with new enzyme from solution. As such this is not surprising, though it is important to recognize that the slow conformational change gives thus rise to zero order kinetics of inactivation with respect to time (neglecting the fast initial drop in activity). This behaviour becomes more manifest from a semilogarithmic plot of the residual activity. Obviously, the rate is determined by k_{+0}[E*]. As [E*] is constant, pseudo-zero order kinetics are observed.

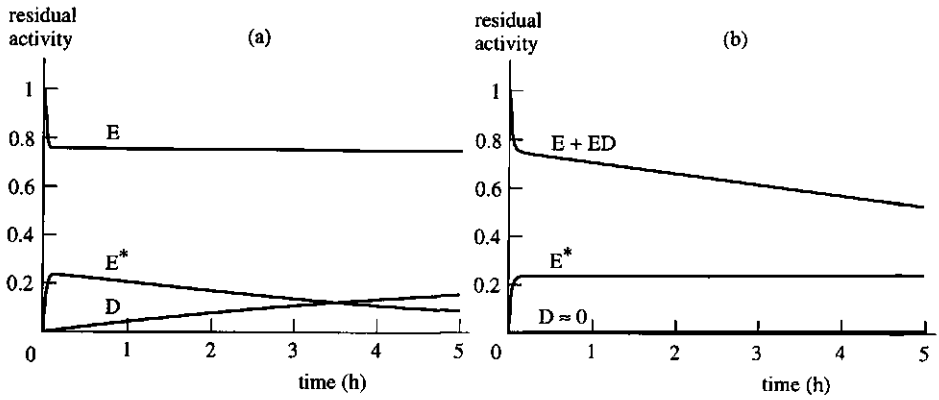

Fig. 7.4. Numerical solution of surface-enhanced inactivation for heterogeneous reaction (N=0.25, k_a=50, k_d=1, k_{+0}=0.2). Activity (E+ED) and concentration of E* and D versus time: (a) k_{-0}=0, k_{+1}=0 (hence, [ED]=0), (b) k_{-0}=2000, k_{+1}=10^6, k_{+2}=50.

Following this procedure, the order of the inactivation with respect to time is investigated for the cases that other steps are rate-limiting. Appropriate values for all rate parameters have been chosen. Provisionally, it is supposed that the chemical reaction is fully heterogeneous, i.e., the conversion only occurs on the surface and not in solution. In Table 7.1 the results, including the result that was obtained for transport towards the surface, are given.

Table 7.1 Order of the inactivation of individual steps of processes involving solution- and hydrophobic inactivation.

	solution	particles
(analytical)		
Transport by diffusion and convection	—	1
(numerical)		
Adsorption/attachment	—	1
Denaturation/conformational change	1	0
Complexation/association	2	1
Decomposition/disintegration	1	0

From Table 7.1 it appears that the order of the inactivation process is decreased by one unit when the homogeneous reaction in solution becomes heterogeneous. When transport or attachment becomes rate-determining the inactivation shows first-order characteristics. Unfortunately, the zero-order character of a rate-determining conformational change is also obtained when decomposition would be a relatively slow process. So, on this basis no discrimination is feasible.

The solution- and hydrophobic inactivation data which are obtained in chapter 5 are now analyzed in more detail. Apparently, from the inactivation data in Fig. 7.3, transport and attachment are fast reactions responsible for the initial loss of 25% of the activity. Fast transport is supported by the fact that hydrophobic inactivation is not dependent on the rate of stirring. Inactivation at 150 rpm is exactly identical to that at 850 rpm (data not shown). Furthermore, from the numerical analysis the initial loss in activity is only obtained for a high value of k_a as compared to k_d ($k_a \geq 50.k_d$). It is clear that supply to the surface is definitely not determining the rate of the overall inactivation.

The data for solution (at $t \geq 0$) and for the different latices (at $t > 0$) are now subjected to a differential fitting procedure. The fitting is carried out by non-linear regression where χ^2 (sum of squares of residuals) is minimized. The general expression for the rate of a reaction is:

$$\frac{dc}{dt} = - k c^{P} \qquad (7.22)$$

where k and P refer to the rate constant and the order of the reaction, respectively. Except for first-order reactions the solution for $c=c_0$ at $t=0$ is:

$$c = \{c_0^{(1-P)} - (1-P)\,k\,t\}^{1/(1-P)} \qquad (7.23)$$

The parameter P, obtained in this way, is the order of the reaction with respect to time. The fitting data from Fig. 7.3 are given in Table 7.2 (as an indication of the quality of the fit, $\chi^2 << 1.2$ in all cases when the data would have been weighted).

Table 7.2 Experimental decay parameters for solution- and hydrophobic inactivation

	solution	PS.A	Teflon H	Teflon M	Teflon L
Γ (mg m^{-2})	—	2.3	2.1	1.5	1.1
c_0 (%)	96	63	68	66	55
P	0.81	0.55	0.79	0.90	0.93
k (h^{-1})	0.41	2.10	1.02	0.88	0.80

It is observed that the order of solution inactivation is equal to 0.8 which does not satisfy the value $P=1$ given in Table 7.1. This deviation is mainly due to the tail of the curve, i.e at longer times. The reaction proceeds at a slightly higher rate than expected on the basis of $P=1$. There is no reasonable explanation for this effect. Taking the data until $t=5$ h, the best fit obtained has a first-order character ($P=1.01$), while P for hydrophobic inactivation is not changed. The order for hydrophobic inactivation, especially for PS-A, is lower than 1, which may lend support to the idea of a slow conformational change on the surface. The values of c_0 for hydrophobic inactivation should have been 75%, according to the imposed depletion of 25%. For solution inactivation the c_0-value nearly satisfies the expected 100%. The fitted data are plotted in Figs. 7.5a (linear) and 7.5b (semilogarithmic), where c_0 has been normalized.

The fitted curves in Fig. 7.5 have important characteristics. It is observed that hydrophobic inactivation becomes less when the surface occupation increases. From chapter 5 (Fig. 5.7) there were already strong indications that route b (Fig. 5.1) is an unlikely mechanism. On the basis of Fig. 7.5, we can now definitely exclude route b. Hence, the assumption that E^* is not autolytically active in the chosen model was justified.

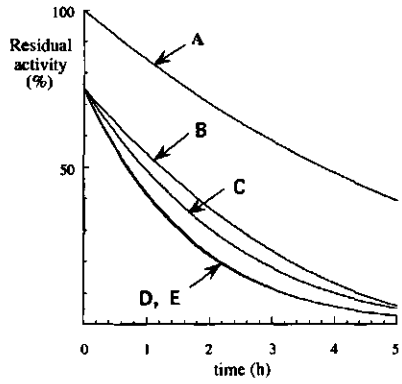

Fig. 7.5a Linear inactivation plot; fit of Eq. 7.23 to data from Fig. 7.3; (A) Solution, (B) PS-A, (C) teflon-H, (D) Teflon-M, (E) Teflon-L.

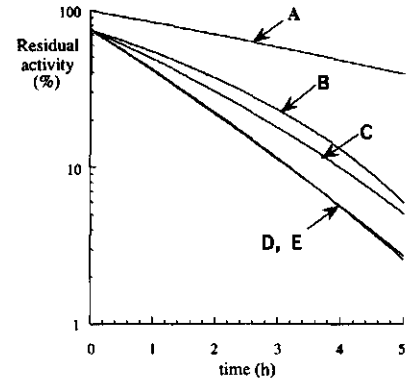

Fig. 7.5b Semilogarithmic inactivation plot; fit of Eq. 7.23 to data from Fig. 7.3; Symbols as in Fig. 7.5a.

With regard to the curves in Fig. 7.5, it may furthermore be noted that the mixed order of the reaction, observed in hydrophobic inactivation, could be due to a combination of homogeneous (=solution) and heterogeneous (=surface) kinetics. Alternatively, it is possible that for heterogeneous inactivation the rate of denaturation on the surface is larger than was numerically simulated. This would slowly deplete the surface during inactivation so that pseudo-zero order kinetics would become more first-order. A strong experimental indication for the change in $[E^*]$ was given in chapter 5. The amount of fragments in the remaining solution has been independently measured during inactivation. It has been demonstrated that the amount progressively increases from 0 to 100%, which implies that the particle gradually becomes depleted during inactivation (by following the adsorption isotherm —Fig. 5.3 and 7.2— from the right- to the left hand side).

It is demonstrated in Fig 7.6 that the experimental curves in Fig. 7.5 for hydrophobic inactivation (curve A) are better fitted when homogeneous inactivation in the remaining solution is taken into account (curve B). The numerically obtained fit is further refined, with respect to both rate and order of inactivation, when the rate of denaturation on the surface is chosen higher than in the remaining solution. The result (Fig 7.6, curve C) approximately explains the inactivation for PS-A. For teflon M and L the inactivation has a more first-order character. The numerical method qualitatively demonstrates this by an increased rate of denaturation on these surfaces. We shall not attempt to exactly match the parameters of Eqs. 7.16 through 7.19 to the data, because there are too many

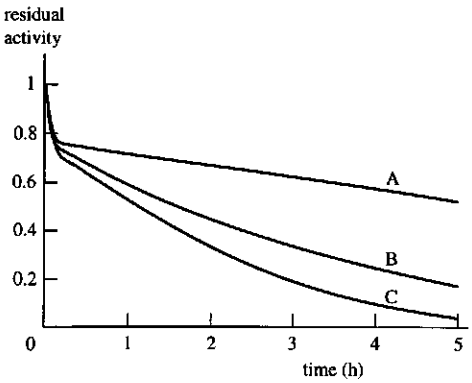

Fig. 7.6. Numerical solution of surface enhanced inactivation. Residual activity (=[E]+[ED]) versus time: (A) k_{+0}=0.2, heterogeneous reaction; (B) k_{+0}=0.2 for both homogeneous and heterogeneous reaction; (C) k_{+0}=0.2 for homogeneous and k_{+0}=0.5 for heterogeneous reaction.

parameters to be fitted, producing a variety of solutions. A visual inspection had been intentionally preferred to indicate general trends.

7.4.2. Evaluation of the order of inactivation

So far, the order with respect to time has been used for interpretation of the results. This method has the disadvantage that secondary processes that occur during inactivation may affect the value obtained. As far as inactivation in solution is concerned, there is evidence that the enzyme protects itself against autodigestion at high concentrations of enzyme. This is demonstrated in Fig. 7.7, where the residual activity as a function of time is plotted for various initial enzyme concentrations.

The 100% value on the abscissa is the initial activity at c=0.1 g l^{-1}. The initial activity at the lower concentrations are correspondingly lower. The curve for 0.1 g l^{-1} does not correspond with that in Fig. 5.4a, probably because the stirring conditions were different. It is not clear why stirring would affect the rate of inactivation in solution. However, assuming first-order kinetics of inactivation in solution, the rate constants are: -0.296, -0.093, -0.063, -0.034 and -0.019 h^{-1} at c=0.025, 0.045, 0.060, 0.075 and 0.100 g l^{-1}, respectively. Hence, the initial rate of inactivation of enzymes in solution (which is the product of the initial enzyme concentration and the first-order rate

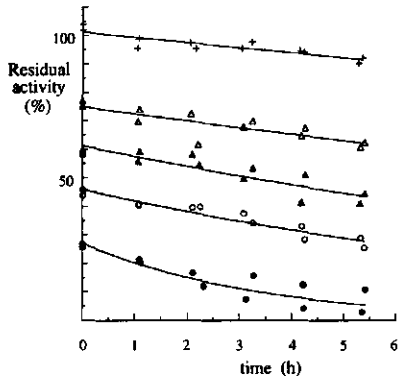

Fig. 7.7. Residual activity versus time of WT-Savinase at c=0.025 (●), 0.045 (○), 0.060 (▲), 0.075 (△) and 0.100 g l^{-1} (+) at pH 8.0, I=0.01 M and T=20°C.

constant) *decreases* upon increasing enzyme concentration. This is a striking observation, since an increase was expected according to standard reaction kinetics. A possible explanation is that fragments that are released as hydrolysis products retard further degradation of whole enzymes [8, 9]. Since hydrophobic inactivation also involves inactivation in the remaining solution, product inhibition in the solution may also play a certain role.

The alternative to the use of the time-order is the concentration-order which is derived from a logarithmic plot of *initial* decay rates as a function of concentration (see Eq. 7.22) [10]. However, since the contribution of inactivation in the remaining solution cannot be neglected in hydrophobic inactivation, this method would yield negative values for the order, as it appears from Fig. 7.7. Hence, the time-order is preferred to the concentration-order.

As it appears from Fig. 7.7 it could be argued that hydrophobic inactivation is solely due to the removal of 25% of the enzyme by adsorption and a relatively increased inactivation of the 75% population in the remaining solution. However, this hypothesis is rejected by the experimental results as this effect should also occur for silica, whereas the curves for silica on the one hand and the hydrophobic particles on the other diverge as time proceeds (Fig. 5.4a). In addition, when the adsorbed fraction on the hydrophobic particle would be *equally* susceptible to autodigestion as the enzymes in solution, the amount of fragments which are produced during solution inactivation and hydrophobic inactivation, should be similar. Except for a lower value of c_0, the rate-

and order of hydrophobic inactivation should then equal those for solution inactivation. As this is not the case (Fig. 7.5b), hydrophobic inactivation is a real phenomenon. Irrespective of the validity of the model and the accuracy of the analysis, the variation in inactivation characteristics for the different hydrophobic latices is decisive. It informs us that inactivation correlates well with the degree of occupation of a hydrophobic surface (see Table 7.2). In turn, the occupation by proteins correlates with the conformational state, as was visualized by time-resolved fluorescence in chapter 6. Reasoning along these lines proteolytic susceptibility correlates with the conformational state of the adsorbed protein.

7.5. Conclusions

In conclusion, the mathematical analysis does not prove the occurrence of conformational changes, but neither is it rejected. Nevertheless, the *experimental* results on hydrophobic inactivation in combination with the fluorescence results of chapter 6 strongly indicate that surface-enhanced autodigestion is triggered by conformational changes of the adsorbed protein.

Acknowledgements

We thank Maarten Egmond (Unilever Research Laboratory, Vlaardingen), Herman van Leeuwen (Dept. of Physical and Colloid Chemistry, WAU) and Tiny van Boekel (Dept. of Food Science, section Dairying and Physics, WAU) for their critical comments.

List of Symbols

A	surface area	[m^2]
b	rate of transport	[s^{-1}]
c	concentration	[mol m^{-3}]
Γ	adsorbed amount	[mg m^{-2}]
D	diffusion coefficient	[m^2 s^{-1}]
$J_e(r)$	flux of enzyme towards the particle surface with respect to a plane of reference	[mol m^{-2} s^{-1}]
$J_e(b)$	flux of enzyme from bulk solution	[mol m^{-2} s^{-1}]
j_e	flux of enzyme towards the particle surface with respect to the centre of gravity of diffusing molecules	[mol m^{-2} s^{-1}]
j_f	flux of fragments from the particle surface with respect to the centre of gravity of diffusing molecules	[mol m^{-2} s^{-1}]
k	rate constant	
k_a	rate of adsorption	[m^3 mol^{-1} s^{-1}]
k_d	rate of desorption	[s^{-1}]
k_{+0}	rate of denaturation	[s^{-1}]
k_{-0}	rate of renaturation	[s^{-1}]
k_{+1}	rate of association	[m^3 mol^{-1} s^{-1}]
k_{-1}	rate of dissociation	[s^{-1}]
k_{+2}	rate of decomposition	[s^{-1}]
m_d	mass transfer coefficient for spherical diffusion	[m s^{-1}]
m	mass transfer coefficient for spherical diffusion + convection	[m s^{-1}]
n	stoichiometric coefficient	
N	initial fraction of adsorbed enzyme	[-]
v	diffusional velocity of matter	[m s^{-1}]
$\bar{v}$	drift of the ensemble of molecules	[m s^{-1}]
P	order of the inactivation	
r	distance from the centre of a colloidal particle	[m]
R	radius of a colloidal particle	[m]
Re	Reynolds number	[-]
Sc	Schmidt number	[-]
Sh	Sherwood number	[-]
t	time	[s]
V	volume	[m^3]
x	molar fraction	[-]

References

1. Johnson, P., Whateley, T.L., Biochem. J. 193, 285-294 (1981).
2. Brode, P.F. III, Erwin, C.R, Rauch, D.S., Lucas, Rubingh, D.N., J. Biol. Chem. 269, 23538-23543 (1994).
3. Lyklema, J., *Fundamentals of Interface and Collod Science*, Vol. 1, p.6.67, Ac. Press Ltd., London, 1991.
4. Leeuwen, H.P. van, in: *Environmental Particles*, J. Buffle and H.P van Leeuwen, Eds., IUPAC Environmental Analytical and Physical Chemistry Series, Vol. 1 (Lewis Publishers), 1992.
5. Wijffels, R.H., *Nitrification by Immobilized Cells*, Ph.D thesis, Wageningen Agricultural University, The Netherlands, 1994.
6. Norde, W., Adv. Colloid Interface Sci. 25, 267-340 (1986).
7. Wolfram, S., *Mathematics: a system for doing mathematics by computer*, 2nd ed., Addison-Wesley Company, p. 108 and 696, 1992.
8. Determann, H., Jaworek, D., Kotitscke, R. and A. Walch, Hoppe-Seyler's Z. Physiol. Chem., 350, 379-388 (1969).
9. Adler-Nissen, J., *Enzymic Hydrolysis of Food Proteins*, Elsevier Appl. Science Publ., London, 1986.
10. Laidler, K.J., in: *Chemical Kinetics*, 3rd ed., Harper and Row, New York, 1987.

Summary

Proteolytic enzymes in liquid detergents suffer from lack of stability in the sense that activity diminishes with time. Although the phenomenon could be attributed to several factors, the influence of colloidal surfaces on the enzymatic stability was investigated. Besides the types of surfaces that are present in the usual detergent systems, other surfaces have been also studied. The enzyme under investigation was wild-type Savinase^{TM}, which belongs to the class of microbial alkaline serine proteinases. This thesis contains a set of experiments and discussions on the interactions, viz. adsorption and inactivation, between Savinase and several types of surfaces.

In order to understand the mechanism of adsorption of Savinase from aqueous solution, adsorption from solution was achieved by stagnation point flow towards an oxidized silicon strip. The adsorbed amount was monitored continuously as a function of time by reflectometry. In order to prevent autodigestion during the experiments, the enzyme was irreversibly inhibited by reaction of the active site with a small inhibitor. The adsorbed amount was monitored as a function of time. The experimental variables were the amphipathicity of the solid surface, the pH, the ionic strength, the type of monovalent ions used and the protein concentration. It was concluded that electrostatic interactions dominate the adsorption of Savinase on a hydrophilic surface and that unfolding of the protein molecule does not take place. On the other hand, for a hydrophobic surface, adsorption is dictated by unfolding of the protein structure and/or hydrophobic dehydration.

Another type of surface that was relevant for this study, was a negatively charged model surface, carrying chemically grafted short poly(ethylene) oxide chains. To that end, a method was developed to prepare charge-stabilized polystyrene latex particles, carrying these moieties. The latices had a surface charge and possessed on the surface a PEO-350/methacrylate molecule, where the number refers to the molecular weight of the ethylene(oxide) part. The surface properties of this latex (PS-B) were compared to those of a similar latex but without the PEO-surface group (PS-A). The presence of the PEO-moiety on the PS-B particles could be established by the colloidal stability against salt, complexation with molybdatophosphoric acid and proton NMR.

The loss of activity of wild-type Savinase was determined both in solution and in the presence of colloidal particles, which provided a surface area for adsorption of 25% of the enzyme population. It was demonstrated that the intact protein was always converted into autolytic degradation products at the expense of biological activity. The different particles, however, deactivated the enzymes to different extents. In the presence of particles that have hydrophobic surface properties (PS-A or teflon latex) autodigestion was substantially enhanced as compared to that in solution. It was inferred that hydrophobic inactivation was due to an increased sensitivity of the adsorbed enzyme towards digestion by the enzyme remaining in solution. On the other hand, PS-B and hydrophilic silica rendered the enzyme more stable against autodigestion than in solution. It is thus concluded that the type of surface determines the mode (conformation/ orientation) in which the enzyme is adsorbed on a particle which, in turn, affects the autocatalytic rate. As the colloidal interfaces present in the usual liquid detergents, i.e. the zeolite-water and vesicle-water interfaces, are modelled by those of silica and PS-B, respectively, the surfaces in the detergents probably *increase* the enzymatic stability as well.

The rapid hydrophobic inactivation was rationalized by a conformational change of the adsorbed protein which increases its autolytic susceptibility. The experimental approach to verify structural changes consisted of time-resolved and steady-state fluorescence of tryptophan residues and of circular dichroism (CD) of the protein. These properties were measured for inhibited Savinase in situ at the hydrophobic teflon latex. The results are compared with those obtained from the protein at the hydrophilic silica suspension and in solution. In the case of fluorescence it is reasoned that the average excited-state lifetime and short internal rotation correlation times are parameters indicative of structural changes in the protein.

Fluorescence and CD both proved that Savinase altered its conformation when it adsorbed at low surface coverage on hydrophobic teflon particles. In that case, the tryptophan fluorescence lifetime was decreased which was accompanied by an increase in the amount of α-helix. The fluorescence of the protein on silica was not affected, irrespective of the surface occupation. At monolayer coverage on teflon, the protein maintained its original structure although significant changes in fluorophore dynamics occurred.

Hence, as hydrophobic inactivation of the wild-type enzyme occurred at full surface occupation, the altered dynamics may render the adsorbed protein more liable to proteolytic attack. This assumption should be qualified, since the conformational change that is required for autodigestion may not be the same as that involved in tryptophan dynamics.

Therefore, the experimental data on solution- and hydrophobic inactivation were subjected to kinetic analysis regarding the possible occurrence of a critical conformational change. In addition, the inactivation data of Savinase were extended to two other types of teflon latices which were different with respect to the plateau value of protein adsorption.
A mathematical model for autodigestion was developed. It involved transport and attachment to the particle surface as well as processes that describe the chemical conversion of the molecules. By analytical or numerical simulation, the effect of each step in the model was investigated. The order of the inactivation reaction with respect to time was used for the detection of a conformational change, although this was not a rigourous procedure. Following this method and considering the distinctly different deactivation behaviour of the various hydrophobic latices it was concluded that the model for surface-enhanced autodigestion, including a conformational change of the enzyme at the surface, has good validity.

Samenvatting

Sinds de jaren tachtig zijn, uit oogpunt van marketing, wasmiddelen niet alleen als droge poeders, maar ook in *vloeibare* vorm op de markt gebracht. Met weglating van enkele ingrediënten is een vloeibaar wasmiddel niets anders dan een waspoeder dat in een weinig water opgelost is. In tegenstelling tot waspoeders zijn vloeibare wasmiddelen echter nog niet zo populair, omdat zij de was minder schoon blijken te maken*. Voor een belangrijk deel heeft dit te maken met een verschil in de kwaliteit van het enzymsysteem.

Enzymen zijn biologisch aktieve moleculen die bepaalde soorten vuil en vlekken snel af kunnen breken. Het voordeel van het gebruik van enzymen in wasmiddelen is dat er minder wasmiddel nodig is, de was schoner wordt en bij lagere temperatuur gewassen kan worden. In een wasmiddel komen verschillende soorten enzymen voor, zoals enzymen tegen vetvlekken, zetmeelresten en eiwitvlekken. Het onderzoek dat beschreven is in dit proefschrift betreft de groep eiwit-afbrekende enzymen, oftewel *proteinasen.* Onder invloed van deze enzymen worden bijvoorbeeld hardnekkige bloed-, gras- en vele voedselvlekken tot kleinere delen afgebroken. De brokstukken worden verwijderd doordat ze makkelijk oplossen in het waswater.

Omdat enzymen zelf ook eiwitachtige stoffen zijn, is de afbrekende werking van proteinasen in een vloeibare omgeving onbedoeld mede gericht tegen moleculen van de eigen soort. Deze vorm van kannibalisme treedt dus op ín de verpakking tijdens de langdurige opslag in de fabriek, in de winkel of naast de wasmachine. Tegen de tijd dat het produkt in de wasmachine terechtkomt, heeft het produkt verloren aan waskracht.

Omdat de enzymen zich in een vloeibare omgeving gemakkelijk kunnen verplaatsen, is het goed voorstelbaar dat zij ook in aanraking komen met ándere componenten in het medium. Hierdoor kan de achteruitgang van de *enzymatische stabiliteit* sterk beinvloed worden. Eén van die componenten is zeep. De zeepmoleculen in een vloeibaar wasmiddel zijn geordend in zogenaamde vesikels die eenvoudigweg voor te stellen zijn als kleine druppeltjes die in de vloeistof zweven. Ook zijn in het wasmiddel zogenaamde zeolieten aanwezig; deze onopgeloste deeltjes dienen voor het ontharden van water. Door de kleine afmetingen van zowel vesikels als zeoliet, heeft een vloeibaar wasmiddel een enorm groot inwendig oppervlak waarmee het (nog kleinere) enzym een binding zou kunnen aangaan.

Het doel van dit onderzoek is om te doorgronden of er een relatie bestaat (en zo ja, welke) tussen de achteruitgang in enzymatische stabiliteit van de proteasen en een eventuele binding van deze enzymen aan de vesikel-water en zeoliet-water grensvlakken. Met de uitkomsten van het onderzoek kan de wasmiddelindustrie wellicht het vloeibare produkt verbeteren, bijvoorbeeld door aanpassing van de samenstelling.

Het enzym dat wordt bestudeerd, draagt de naam Savinase. Van oorsprong wordt dit enzym, een serine proteinase dat werkzaam is in alkalisch milieu, uitgescheiden door een bacterie. Van de vele proteolytische enzymen die bekend zijn, heeft dit enzym de weg naar de toepassing van wasmiddelen gevonden door zijn sterke katalytische eigenschappen onder de extreme omstandigheden tijdens het wasproces.

Het onderzoek dat beschreven is in dit proefschrift, is modelmatig van opzet. Behalve de invloed van de kolloidale oppervlakken die vóórkomen in de vloeibare wasmiddelen, is ook het effect van anderssoortige oppervlakken op de enzymatische stabiliteit onderzocht. De adsorptie en inaktivatie van het enzym is bestudeerd in een relatief eenvoudige waterige oplossing en in waterige suspensies van verschillende typen modelkolloiden.

Om het mechanisme van adsorptie beter te kunnen begrijpen, is een onderzoek gedaan naar de adsorptie van Savinase met behulp van een gecontroleerde stagnatiepuntstroming naar een geoxideerd silicium plaatje. Om autodigestie tijdens de metingen te voorkomen, werd het enzym geremd met een kleine competitieve remmer. De geadsorbeerde massa eiwit werd continu gemeten als functie van de tijd met behulp van de optische techniek reflectometrie. De aangelegde variabelen waren de amphipathiciteit (hydrofiele/hydrofobe karakter) van het oppervlak, pH, ionensterkte, type ionen en eiwitconcentratie. De conclusie was dat de adsorptie van Savinase op hydrofiele grensvlakken gedreven wordt door elektrostatische wisselwerkingen tussen het eiwit en het oppervlak. Structuurveranderingen van het eiwit vinden daarbij niet plaats. Daarentegen wordt op hydrofobe grensvlakken de adsorptie gedomineerd door wisselwerkingen die gepaard gaan met structuurveranderingen van het eiwit en dehydratatie van hydrofobe delen van het eiwit- en sorbensoppervlak. Elektrostatische interacties spelen hierbij een ondergeschikte rol.

Met deze resultaten is een beter inzicht verkregen in hoe een eiwit als Savinase zich gedraagt als het in aanraking komt met verschillende oppervlakken. Echter, zoals in het hiernavolgende duidelijk gemaakt zal worden, was er ook behoefte om de wisselwerking te bestuderen tussen Savinase en een oppervlak dat bedekt is met korte poly(ethyleen) oxide ketens. In een van de hoofdstukken (H. 4) is daarom een methode beschreven voor de bereiding van kolloidale polystyreendeeltjes met deze oppervlakte-eigenschap. Ook is een aantal karakteriseringsmethoden toegepast om de aanwezigheid van deze ketens aan te tonen.

In de volgende stap van het onderzoek is de enzymatische stabiliteit van natief Savinase bestudeerd in uiteenlopende kolloidale suspensies. Het verlies van enzymaktiviteit blijkt, zonder of met kolloïdale deeltjes, altijd het gevolg te zijn van autodigestie. Het is opmerkelijk dat hydrofobe oppervlakken (polystyreen- of teflonlatex) autolyse doen versnellen, terwijl andere typen adsorberende oppervlakken (hydrofiel silica of de polystyreenlatex bedekt met polyethyleenoxide-ketens) autolyse juist vertragen. Omdat de oppervlakken van respectievelijk zeoliet en vesicles tot de laatste categorie gerekend mogen worden voldoen, zullen zij dus de enzymstabiliteit in een vloeibaar wasmiddel verhógen. De vraag blijft dus waar de terugloop van aktiviteit in een vloeibaar wasmiddel vandaan komt.

Het verdere onderzoek heeft zich voornamelijk gericht op de effecten van hydrofobe oppervlakken op de enzymatische stabiliteit. Het beeld dat uit inactivatie-experimenten naar voren komt, is dat het enzym door adsorptie extra gevoelig wordt voor autolyse en dan als substraat dient voor een vrij enzym. De verhoogde autolysegevoeligheid kan het gevolg zijn van een *structuurverandering* van het substraat-eiwit aan het grensvlak. Aldus redenerend heeft de verhoogde stabiliteit op de genoemde anderssoortige oppervlakken waarschijnlijk te maken met het feit dat het geadsorbeerde enzym een specifieke oriëntatie aanneemt of een verhoogde structuurstabiliteit kent waardoor deze minder gevoelig is voor proteolytische aanval.

De hypothese dat op een hydrofoob oppervlak structuurveranderingen zouden kunnen plaatsvinden, wordt ondersteund door de resultaten die behaald zijn met reflectometrie. Echter, omdat een meer directe methode voor het bepalen van structuurveranderingen gewenst was en omdat het eiwit zich op een kolloidaal grensvlak zich misschien anders

gedraagt dan op een macroscopisch oppervlak, zijn fluorescentiemethoden en circulair dichroisme toegepast. De 'structuur' van het eiwit is zodoende bepaald in de opgeloste toestand en *in situ* op het hydrofobe teflonlatex. De uitkomst is dat de structuur van het eiwit in belangrijke mate afhangt van de bezettingsgraad van het eiwit op het oppervlak. Bij lage bezettingsgraad, verandert het eiwit zijn structuur, terwijl deze bij hoge bezettingsgraad nagenoeg intact blijft. De fijngevoelige fluorescentiemethode was echter in staat om te bepalen dat bij de hoge bezettingsgraad desalniettemin kleine veranderingen ten gevolge van adsorptie optraden in de beweeglijkheid van delen van het eiwit.
Het kan dus verondersteld worden dat de gevoeligheid voor autodigestie is toegenomen door de toegenomen beweeglijkheid van delen van het geadsorbeerde eiwit. Deze aanname moet gerelativeerd worden, omdat de structuurverandering die nodig zou zijn voor autodigestie niet dezelfde hoeft te zijn als die gemeten is met fluorescentie.

Om deze reden is een kinetische analyse uitgevoerd van de experimentele gegevens. Hiertoe is een model opgesteld voor het gehele inaktivatieproces (inclusief transport naar het oppervlak, adsorptie, structuurverandering en enzymatische omzetting). Ook zijn aanvullende inactivatie-experimenten uitgevoerd met hydrofobe oppervlakken die onderling verschillen met betrekking tot de bezettingsgraad van het eiwit. Aldus worden de resultaten van de laatste drie hoofdstukken tegen elkaar aangezet en wordt geconcludeerd dat het model voor autodigestie, waar conformatieveranderingen zijn inbegrepen, het verlies aan stabiliteit kunnen verklaren.

<u>De algemene conclusie van het proefschrift luidt dus:</u>

Hydrofobe oppervlakken verlagen de stabiliteit van Savinase tegen autodigestie in een waterig medium. De gevoeligheid voor autodigestie door adsorptie op het hydrofobe oppervlak kan verklaard worden door een gewijzigde eiwitstructuur aan het oppervlak in vergelijking met de eiwitstructuur in oplossing. De kolloidale oppervlakken in vloeibare wasmiddelen zijn van een andere aard en verhógen juist de stabiliteit tegen autodigestie.

* Consumentengids, Juni 1989, 'Vloeibaar valt tegen', blz. 340-345

Curriculum Vitae

Marc Cornelis Ludolf Maste is op 22 oktober 1965 te Amsterdam geboren. In de periode 1977-1983 volgde hij voorbereidend wetenschappelijk onderwijs aan het Gemeentelijk Gymnasium te Hilversum. Daaropvolgend, in september 1983, heeft hij gekozen voor de studie Levensmiddelentechnologie aan de Landbouwhogeschool (thans Landbouwuniversiteit) te Wageningen. Naast de hoofdrichting Levensmiddelennatuurkunde zijn Kolloid- en Grensvlakchemie, Zuivelkunde en Proceskunde als bijvakken opgenomen. Voor de hoofdrichting Levensmiddelennatuurkunde is in 1988 een stageperiode gevolgd bij het Unilever Research Laboratorium, Colworth House in Engeland. De studie is in juni 1989 afgesloten.

Daarna trad hij in dienst bij de afdeling research & development van de Divisie Industriële Produkten van het toenmalige DMV Campina (thans Campina Melkunie) te Veghel. In december 1990 is hij aan een promotieonderzoek begonnen bij de vakgroep Fysische en Kolloidchemie aan de Landbouwuniversiteit. Het onderzoek is uitgevoerd in samenwerking met het Unilever Research Laboratorium te Vlaardingen, waarvan dit proefschrift het resultaat is.

Per november 1995 is hij als wetenschappelijk onderzoeker (fysische-/biochemie) in dienst getreden bij het instituut voor Agrotechnologisch Onderzoek, Dienst Landbouwkundig onderzoek (ATO-DLO) van het Ministerie van Landbouw, Natuurbeheer en Visserij te Wageningen.